

NOTES ON QUANTUM COMPUTATION AND INFORMATION

Raghav G. Jha 

*Thomas Jefferson National Accelerator Facility, Newport News, VA 23606, USA
Perimeter Institute for Theoretical Physics, Waterloo, Ontario N2L 2Y5*

Abstract

We discuss basic fundamentals of quantum computing and information - quantum gates, circuits, algorithms, theorems, error correction, methods for unitary time-evolution and provide a collection of QISKIT¹ programs and exercises for the interested reader.

Note: Some of the material is based on lectures given at Rensselaer Polytechnic Institute (RPI) Summer School in June 2022, Hampton University Graduate Studies (HUGS) program and Quantum Computing Bootcamp at Jefferson Lab in June 2023. I thank the organisers of those programs for inviting me to teach and learn about this research area. Please send suggestions/corrections to raghav.govind.jha@gmail.com

Contents

1	Introduction	1
2	Notation and all that	7

¹It is an open source software development kit (SDK) for working with OpenQASM and the IBM Q quantum processors. Various IBM quantum simulators can be found [here](#).

3	States, quantum gates, density matrices, and rules	10
3.1	States on the Bloch sphere and gates	11
3.2	General quantum operations	23
3.3	Entanglement	25
3.3.1	Partial trace method	27
3.3.2	Entangled mixed states	28
3.4	Quantum Fourier Transform (QFT)	29
3.5	Quantum rules and limitations	30
4	Towards Quantum algorithms	32
4.1	Full-adder	32
4.2	Phase kickback	33
4.3	Deutsch-Jozsa Algorithm	33
4.4	Bernstein-Vazirani algorithm	35
4.5	Grover's algorithm	36
4.6	Quantum phase estimation (QPE) algorithm	36
4.7	Shor's factoring algorithm	38
5	Variational Quantum Eigensolver (VQE)	39
5.1	Quantum Anharmonic Oscillator	42
5.2	$O(3)$ non-linear sigma model	44
6	Quantum Error Correction (QEC)	46
6.1	Bit-flip error	47
6.2	Phase-flip error	49
6.3	Shor's nine qubit code	49
7	Looking at NISQ and beyond	52
7.1	Hamiltonian Simulation	54
8	Future	60
9	Acknowledgements	60
A	Continuous variable quantum computing	61
A.1	CV gates	63
A.2	CV states	65
A.3	Measurements	65
B	Fun with commutator algebra	66

C	Sample programs using Qiskit	72
C.1	Installing package and quantum hello world	74
C.2	Some basic operations using qubits and gates	75
C.3	Quantum full-adder	78
C.4	Grover’s algorithm with general diffuser routine	79
C.5	Implementing QFT	81
C.6	Bit-flip code, Phase kickback	83
C.7	VQE solution to anharmonic quantum oscillator for three qubits	84
C.8	Phase estimation	88
C.9	Decomposing any unitary in single-qubit and CNOT gates	89
C.10	Sample MATHEMATICA code for to compute vN entropy	90
	References	92

Introduction

One of the quotes that profoundly expresses the present state of the development in quantum computation and information is by Wheeler. In his colorful language, he said - ‘I think of my lifetime in Physics as divided into three periods. In the first period, I was in the the grip of the idea that everything is particles. I call my second period, everything is fields, and now I am in the grip of a new vision that everything is information’. In fact, we can safely add ‘quantum’ to this since it appears that everything is ‘quantum information’. There are several physicists who have explored this line of thought, see for example Refs. [1–3] and references therein to start a trail.²

The goal of theoretical physics is to understand the principles that govern the universe at different length scales. It is a challenging problem since the associated scales vary over a wide range (about thirty orders of magnitude) from inside the nucleus (10^{-15} m) to the size of typical galaxies (10^{15} m). We have two extremely accurate theories that govern each of them separately. The incredible progress made in the last 125 years has given us the basic principles of quantum mechanics and the special theory of relativity which when combined into the framework of ‘quantum field theory’ (QFT) holds the key to explaining a major portion of all physical phenomena occurring in nature at sub-nuclear scales and culminating in the Standard Model of particle physics. Some jewels of this framework are - calculating the magnetic moment of the electron to about ten decimal places, and the discovery of the Higgs boson at the Large Hadron Collider (LHC) at CERN. On the other hand, at the other extreme of the spectrum, we have the highly successful theory of general relativity which describes classical gravity, predicts the existence of black holes and has been tested to great accuracy culminating with the discovery of gravitational waves.

Another topic close to physicists is that of computing and since computing is a physical process it is governed by the laws of Physics. Computers³ have changed and affected every facet of life around us. From handling complex machines like airplanes to the RSA (Rivest–Shamir–Adleman)

²The quintessential example of how crucial information is can be understood from a well-known paradox due to Maxwell (1867). This is known as ‘Maxwell’s demon’. This thought experiment is an apparent violation of the second law of thermodynamics. Szilard wrote an interesting paper in 1929 which took a big step towards the resolution, but it did not ‘totally’ explain the paradox. It was Landauer’s work [4] and Bennett’s follow-up [5] that was resolved after 115 years and was one of the major problems that raged physicists throughout the century. The solution lies in the fact that information is physical, just like the entropy or energy in thermodynamics. Additionally, it is interesting to note that von Neumann in his letter to Teller on April 8, 1947 wrote - “I have some definite ideas concerning automata, memory, clearing, and irreversibility and entropy, somewhat connected to Szilard’s treatment of Maxwell’s demon and my old treatment of entropy and observability in quantum mechanics” [p. 245, John von Neumann Selected Letters, American Mathematical Society (October 1, 2005)] but we believe it was never written up by either of the Martians. The statement appears to the author to be closely related to the idea of erasure and non-violation of the second law as established by Landauer et al.

³Computer is a machine that maps an array of bits (0 and 1) from one configuration to another. If it manipulates quantum bits, it is called a quantum computer.

key protocol, which forms the basis of all Internet transactions. But there are certain classes of problems where even the fastest supercomputers of today's era fail. They fail because we have to wait for thousands of years to solve a problem using classical ideas of bits, on which they are based. Though classical computation has rapidly progressed to the extent that we can now have a billion transistors in a single laptop, it is probably not possible that the size of these transistors can be made smaller than the size of say hydrogen atom which is about 10^{-10} m or the frequency of the clock speed can be increased more than 1 PHz (10^{15} Hz) which is roughly the frequency of atomic transitions. So, it is clear that supercomputers will soon exhaust their capability, and problems with exponential complexity won't be solved using them. This leads to a paradigm shift in our idea of computing. Along this direction, already in the 1970s, Benioff started thinking about the theoretical feasibility of quantum computing and his paper [6, 7] which described a quantum mechanical model of Turing Machines was one of the first papers in the field of quantum computing. This work was based on a classical description in 1973 of reversible Turing machines from Ref. [8]. In the same year, there was another work [9] by Russian mathematician Manin who argued that the superposition and entanglement features of quantum mechanics would make for a substantial speedup compared to classical methods. Soon after, Feynman [10] argued that quantum computers will be better suited to these tasks than any classical computer we can ever build because they can store much more information compared to classical computers. He pointed out that - 'Let the computer itself be built of quantum mechanical elements which obey quantum mechanical laws'. In the early days of quantum computing, Poplavskii argued [11] - "The quantum-mechanical computation of one molecule of methane requires about 10^{42} grid points. Assuming that at each point we have to perform only 10 elementary operations, and assume that those calculations are performed at temperatures of 0.003 Kelvin, we would still have to use all the energy produced on Earth during the last century". This makes it clear that a full-fledged computation of quantum dynamics is beyond the reach of any classical computer. Nature is quantum mechanical and hence we have to make use of it. These problems and ideas gave rise to the field of quantum computation. In summary, quantum computation addresses one of the two issues that limit any classical computation: space (memory) and time. In quantum computers, we can store exponentially large information, so it is memory-wise way more efficient than its classical counterpart. We provide the first twelve years of the timeline of quantum computing in Fig. 1.

The usefulness of classical computers has been a monumental achievement of human mankind in the past century. The basic fundamental idea of classical computers (or computing) is the binary two-state signal: 0 and 1. It is practically the only thing a computer understands at its most fundamental level. A computer practically does two things: 1) it stores information as a string of 0s and 1s (also known as classical bits), and 2) Transform them based on the instructions given. It achieves the second task by using gates which perform simple logic operations to transform bits. Some examples of such gates are AND, NOT, OR gates. However, we know that at the microscopic level, the laws of Physics and hence nature is purely quantum-mechanical. It marks a paradigm

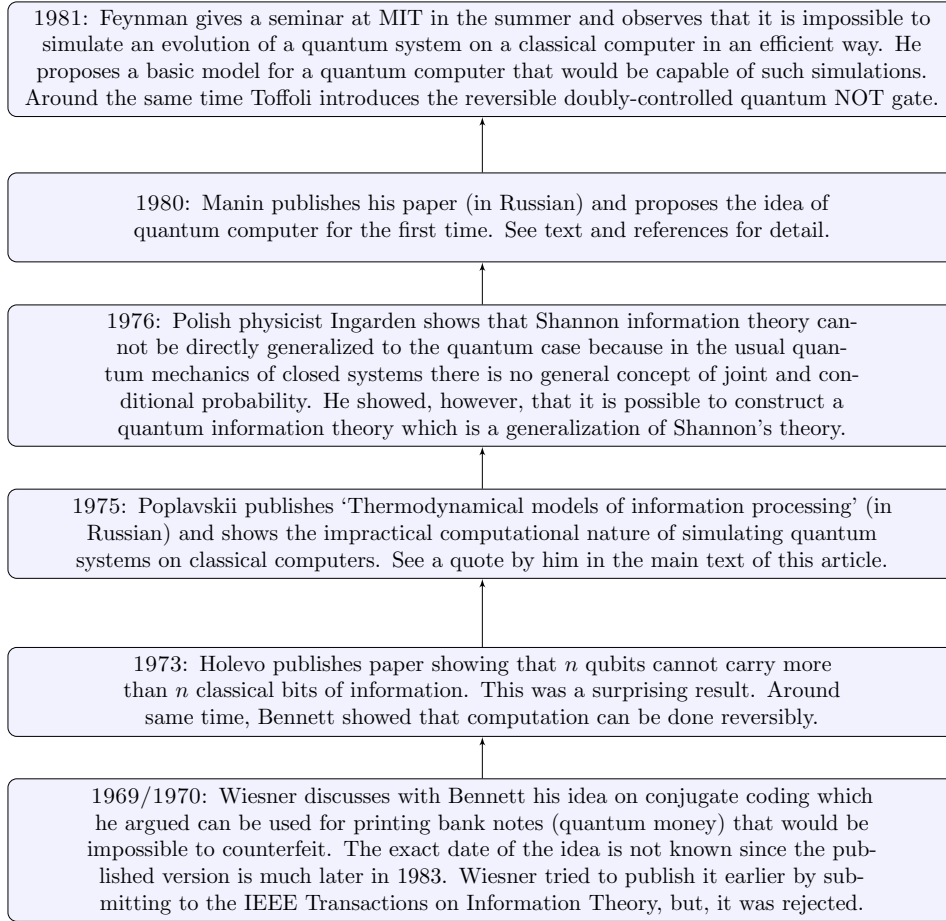


Figure 1. The brief history of quantum computation.

shift in our understanding compared to the classical world, which is deterministic. In simple terms, this means that while a classical bit can at a given time be either 0 or 1, a quantum bit (known as ‘qubit’)⁴ can be in a superposition of these two options and hence we can never conclude exactly which one until we measure it. The existing quantum devices contain $\mathcal{O}(100)$ qubits but they are noisy, so actual efficiency might be a small fraction of it. They are sometimes referred to as ‘Noisy Intermediate-Scale Quantum (NISQ)’ devices are also sometimes referred to as ‘NISQ era’.

To understand the power of principles of quantum mechanics, consider the amount of digital data in the world. It is estimated that the total digital data in the world by 2025 will be close to 175 ZB (1 ZB = 10^{21} bytes). This data can be contained in total if we have about 78 fully efficient qubits. This is the power of qubits (growth of ‘power of 2’).⁵ However, such power often

⁴If the vector space dimensions is $d > 2$, then it is called qudits. If we have qudits with $d \rightarrow \infty$, then we refer to it as ‘qumodes’ or a continuous variable (CV) system. A quantum harmonic oscillator is one example.

⁵Once a king offered any reward to a man who had done good for the kingdom. The man asked that a single

comes with its own set of troubles and limitations. For a review of quantum algorithms and other details, see Ref. [12]. As of today, there exists only a handful of useful⁶ quantum algorithms, and it is not yet known how many classes of problems will eventually benefit by exploiting the quantum features. One of the major applications of quantum computing is in the field of quantum many-body systems. The mightiest of computers today in the world cannot deal fully (without approximation and problems) with even a quantum system of highly interacting 100 electrons! Therefore, solving this is one of the major challenges in theoretical and computational Physics. Even though we only have a relatively small (< 100) number of non-error corrected qubits and the implementation faces several problems, it is expected that in the coming 2-3 decades the situation will change drastically. Even 100-200 error-corrected qubits in the future can completely revolutionize the nuclear computations and the whole of quantum chemistry and several areas of Physics.

Though we will mostly restrict to the theoretical side of quantum computing in these notes, it is good to point out some basic ideas about the experimental side of this story. The act of fabricating a proper logical qubit is a challenging task. In order to actually realize a quantum computer, we need to have qubits that can retain their properties and those which can be made to evolve/change as computationally desired. We must also prepare qubits in some initial state and measure them conveniently. In order to construct a computer as envisaged by Manin and others with these properties, DiVincenzo in 2000 [13] listed some conditions necessary to achieve this based on his attempts to construct a quantum computer (a machine that can efficiently simulate quantum systems such as solving the quantum many-body problems). These conditions are now known as ‘DiVincenzo criteria’ and are mentioned below:

- A scalable physical system with well-characterized qubits.
- The ability to initialize to some fiducial state such as $|000000 \dots 00\rangle$.
- Long decoherence time compared to gate operation time ($\tau_{\text{deco.}} \gg \tau_{\text{op.}}$).
- A universal set of quantum gates.
- A qubit-specific measurement capability.

These conditions are for quantum computation, such as superconducting quantum computing or trapped ion approaches. There are two more conditions that apply to quantum communication.

grain of rice be placed on the first square of the chessboard. Then two grains on the second square, four grains on the third, and so on, and doubling each time. The king was taken aback by such a small request and agreed. He ordered the treasurer to pay the sum agreed upon. After a few days, the treasurer explained that the sum could not be paid since by the time he got halfway through the board, the amount of grain required was more than the entire kingdom possessed. This is the exponential growth known to kings several thousand years before. I first heard this story from my grandfather when I was 8, however, this is now easily found online and also appears in some popular science books.

⁶Polynomial or exponential speedup compared to best-known classical algorithms

In order to understand these two conditions, we have to explain stationary and flying qubits. Stationary qubits are those which are in the computer and on which we apply gates while flying qubits are ones that move (say, like photons). With these definitions, the last two conditions are:

- The ability to interchange between stationary and flying qubits⁷.
- The ability to faithfully transmit flying qubits between specified locations.

The experimental challenge is that these conditions can often only be partially met. Single photons have two polarization states and are almost ideal qubits, but the optical material required to make them interact is difficult in practice without loss of coherence. One can represent spin-1/2 particles as qubits as is often done theoretically and experimentally for the trapped ion method to quantum computing, but the phonons that are used to mediate the interactions have short coherence time. Another approach is to use electric charge as a qubit representation and use excellent techniques from modern electronics, but even here lies the problem of decoherence. One advanced approach is to use charge carriers in not a usual metal but in a superconductor. The superconductor qubit representation is favored due to the robustness of the Cooper pairs involved. In fact, there are now some advancements achieved over this as well. As of today's technology, we have some major categories for these constructions. The *first* is the 'superconducting qubits' (SC). It was first observed that Josephson junction (JJ)⁸ is the element that provides the condition to turn a superconducting circuit into a qubit. One example is Google's Sycamore 53-qubit chip, which belongs to this category. In fact, these quantum processors use an advanced version of this which has more than one JJ and is known as 'transmons' which is the shortened name for 'transmission line shunted plasma oscillation qubit'. Both IBM and Google quantum processors use this modified qubit approach. It is closely related to the charge qubit (cooper pair box) but has better effectiveness due to improvement in decoherence time. There is *another* approach known as 'topological qubits' (Microsoft, Bell Labs) which underlies the application of Majorana fermions to create qubit states. There are other technologies based on trapped ions, silicon dots (Intel), and diamond vacancies. We will not discuss these here, since it would really digress us from the goal of this article.

In these notes, the emphasis is to introduce the idea of quantum computing inspired by the connection to classical computing and then use some SDKs to perform some simple computations on IBM's backend machines. These are not meant to be exhaustive, and the purpose is not to solve some model in Physics which cannot be solved in a reasonable time using computers we have today, but to introduce the elements which might in coming decades be part of advanced quantum algorithms and computation that can achieve those dreams. However, we want to make

⁷Flying qubits have restricted use compared to stationary qubits. They are only used to pass the information over some distance, whereas stationary qubits have a two-fold task: store information and perform calculations.

⁸A Josephson junction is made of a non-superconducting material between two layers of superconducting electrodes. A Cooper pair of electrons can tunnel through the non-superconducting barrier from one superconductor to another.

it clear to the reader that even with quantum computing and reliable error correction some physical problems might still not be solved in polynomial time. In order to understand this issue, one must talk in terms of complexity classes i.e., the problem of how the computational resources scale with increasing system size. This is one of the main problems in computer science. We say that \mathbf{P} is the set of problems where time scales as polynomial in system size on a deterministic Turing machine. This is also sometimes referred to as a problem that can be solved⁹ efficiently. The classical complexity classes introduced for Turing machines of both kinds (deterministic or probabilistic) have since then been extended to admit quantum complexity classes. For example, **BQP** stands for bounded-error quantum polynomial time and is referred to as the class of decision problems solvable by a quantum computer in polynomial time. It is the quantum analog of the complexity class **BPP**¹⁰. But since a quantum circuit can simulate a classical one, both \mathbf{P} , and its probabilistic analog, **BPP**, are contained in **BQP**. From a perspective of a physicist, it is important to know which problems belong to this complexity class since that would potentially benefit the most from the quantum computers in the future. For instance, the preparation of ground state of Hubbard model is not in **BQP** but the time evolution is. It is also known that the scattering problem in interacting QFT lies in **BQP**. In fact, not all physical problems lie in **BPP** or **BQP**, some of them belong to **NP** which stands for *non-deterministic polynomial time* requiring more than polynomial resources assuming that $\mathbf{P} \neq \mathbf{NP}$ ¹¹ but whose solution can be verified in polynomial time. The quantum analog of **NP** with polynomial intractable problems is denoted by **QMA**¹², and problems that belong to this class are *unlikely* to be solved efficiently even with a quantum computer assuming **BQP** \neq **QMA**. **QMA**-hard (defined similarly to **NP**-hard), is a class of problems if every problem in **QMA** can be reduced to it. A problem is said to be **QMA**-complete if it is **QMA**-hard and in **QMA**. One of the motivations for quantum computers is the potential to solve interesting problems which are **NP** hard like the model with sign problems. These cannot be efficiently solved on classical computers. However, some of these might still not belong to **BQP** and therefore might still be inaccessible with quantum resources. For example, it was shown in Ref. [14] that scattering in scalar QFT is **BQP**-complete, indicating that all problems in **BQP** can be mapped to scattering in scalar QFT with polynomial scaling time to solution, and further that the scattering problem itself is in **BQP** and thus can be efficiently simulated quantum mechanically. We say a problem is **BQP**-complete when it is both **BQP** and

⁹It is interesting to note that Gödel's letter to von Neumann in 1956 (when the latter was in the hospital) discussed a function ϕ which has some relation to complexity classes. It is probably the first written instance of \mathbf{P} versus **NP** issue. However, since von Neumann died early 1957, his answer to this letter was never known.

¹⁰**BPP** is class of decision problems or languages that can be solved in polynomial time by probabilistic Turing machines with error probability bounded by 1/3

¹¹ $\mathbf{P} \neq \mathbf{NP}$ has enormous practical and economic importance because modern cryptography is based on assumption that they are not equal. This means that there exist problems that are impossible for computers to solve, but for which the solutions are easily checked (polynomial). A failure of this could create havoc in modern cryptography resulting in breakdown of secure transactions all over the world.

¹²QMA is an acronym for Quantum Merlin Arthur

BQP-hard. Similarly, for the classical version, this means that a problem is said to be **NP**-hard if everything in **NP** can be transformed in polynomial time into it even though it may not be in **NP**. Conversely, a problem is **NP**-complete if it is both in **NP** and **NP**-hard.

We now give an outline of the notes. In Sec. 2, we explain the notation and basic fundamentals. In the next section, we introduce the idea of quantum states, quantum logic gates, density matrices, and the important quantum Fourier transform method. In Sec. 4, we mention several quantum algorithms such as phase kickback, Deutsch algorithm, Grover’s search algorithm, Kitaev’s phase estimation, and Shor’s algorithm. In Sec. 5, we discuss the variational quantum eigensolver (VQE) method to solve some simple problems. In Sec. 6, we mention an important feature of quantum computing i.e., quantum error correction and explain bit and phase flip and universal code to correct arbitrary (phase or flip) single-qubit errors. In the Appendix, i.e., Sec. C, we provide codes and instructions on how the user can run some simple simulations on a web browser (Google Collaboratory).

SECTION 2

Notation and all that

Before we delve into describing the notations and discussing basic ideas, we emphasize and point out the differences between digital classical and quantum computing in Table 1. We will restrict

Elements	Classical	Quantum
Algebra	Boolean	Linear
Basic Unit	Bit	Qubit
Gates	Logic gates	Unitary gates
Reversibility of gates	Sometimes	Always
Example of universal gate set	{NAND}	{H, T, CNOT}
Correction of errors	Repetition	Shor-like code

Table 1. Comparison between classical and quantum digital computing.

to the well-known Dirac’s¹³ bra-ket notation[17] which deals with states in Hilbert space based on von Neumann abstract and mathematical precise formulation of quantum mechanics written down around 1932¹⁴. We will briefly review this for interested readers. Suppose we have a column and

¹³Probably inspired by Grassmann’s similar notation used several decades before

¹⁴It might be surprising that just about three years later in 1935, he wrote to Birkhoff from 1935 – ‘I would like to make a confession which may seem immoral: I do not believe in Hilbert space anymore’. We encourage the interested reader to explore this direction if interested.

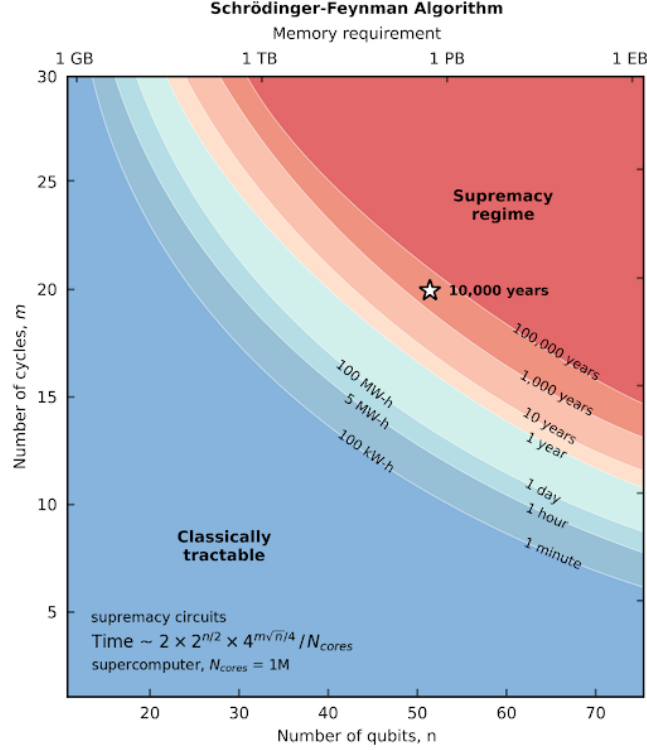


Figure 2. Estimate of the equivalent classical computation time assuming 1M CPU cores for quantum supremacy circuits as a function of the number of qubits and a number of cycles for the Schrödinger-Feynman algorithm. The star shows the estimated computation time for the largest experimental circuits. To know more about Schrödinger-Feynman (SF) algorithm, please see Ref. [15] and references therein. In short, Schrödinger’s method takes about m^{2n} time and about $2n$ memory, while Feynman’s method takes about 4^m time and about $m + n$ memory. Feynman’s algorithm saves memory because it calculates an amplitude instead of keeping track of the state vector throughout like in the Schrödinger approach. However, the fact that more intermediate steps are to be done means more time. There are some methods that combine features of both, and those belonging to the class of SF algorithms. This figure is taken from Ref. [16]. This diagram is only meant to provide a basic idea and should not be taken at face value.

row vector as given below:

$$|B\rangle = \begin{pmatrix} B_1 \\ \vdots \\ B_N \end{pmatrix}, \quad \langle A| = \begin{pmatrix} A_1^* & \cdots & A_N^* \end{pmatrix} \quad (2.1)$$

We can do two operations using them by computing the inner product, i.e., $\langle A|B\rangle$ or the outer product denoted by $|A\rangle\langle B|$. The first returns a number, while the latter gives a matrix. The row vector is called ‘bra’ while the column vector is called ‘ket’ and they are both dual to each other (in the vector space sense). This state denoted as ‘ket’ is postulated to contain all the information

about the physical state which we wish to know. We have the following relations: $\langle A |^\dagger = |A\rangle$, and $|A\rangle^\dagger = \langle A|$. In quantum mechanics, the state of a system is described by a ray $|\psi\rangle$ in Hilbert space, \mathcal{H} where the ray has unit norm. If we have, $\lambda = e^{i\phi}$ then we see that $|\psi\rangle$ and $\lambda|\psi\rangle$ both have the same norm because λ is just a phase, and they represent the same physical state. The phase of the ray is not an observable. The rays of Hilbert space \mathcal{H} are the equivalence class of unit vector that only differ by a phase. Two states can be added together as: $|\alpha\rangle + |\beta\rangle = |\gamma\rangle$. In fact, if $|\psi_0\rangle$ and $|\psi_1\rangle$ are two orthogonal states, then their linear superposition ($c_1|\psi_0\rangle + c_2|\psi_1\rangle$) is also a well-defined state but must satisfy $|c_1|^2 + |c_2|^2 = 1$. We refer to c_1 and c_2 as ‘amplitudes’ corresponding to $|\psi_0\rangle$ and $|\psi_1\rangle$ respectively. We can multiply a ket by a complex number c as: $|\alpha\rangle = c|\psi\rangle$ or $|\psi\rangle c$, however, physically speaking there is no difference between $|\alpha\rangle$ and $|\psi\rangle$ as discussed above. When we want to measure an observable, we apply the corresponding operator from the left on the ket as: $A \cdot |\psi\rangle$ or $\hat{A}|\psi\rangle$. Two kets denoted by α and β are said to be orthogonal if: $\langle\alpha|\beta\rangle = \langle\alpha|\beta\rangle = \langle\beta|\alpha\rangle^* = 0$. There are also some operations that are not allowed. The operator must be either on the left of ket or on the right of a bra, i.e., $|\psi\rangle A$, $A\langle\psi|$ are both incorrect for an operator A . Some products like $|\alpha\rangle|\beta\rangle$ are not allowed if the ket vectors belong to the same vector space. Note that when we write $|01\rangle = |0\rangle|1\rangle$ later on, we mean vector spaces of two distinct qubits so it is allowed. The expectation value of any observable corresponding to the Hermitian operator A is given by: $\langle A \rangle = \langle\alpha|\hat{A}|\alpha\rangle$. In fact, we can also write this as:

$$\langle A \rangle = \sum_{a', a''} \langle\alpha|a''\rangle \langle a''|A|a'\rangle \langle a'|\alpha\rangle = \sum_{a'} a' |\langle a'|\alpha\rangle|^2$$

Consider a spin-1/2 particle with spin-up $|\uparrow\rangle$ or down $|\downarrow\rangle$. The Hilbert space in this case is two-dimensional with two orthonormal basis which we denote as $|0\rangle$ and $|1\rangle$. This is an example of a quantum bit (‘qubit’). One often refers to the orthonormal basis $\{|0\rangle, |1\rangle\}$ as computational basis. Any state $|\alpha\rangle$ can be decomposed as a convex combination of projectors onto pure states¹⁵ i.e., $|\alpha\rangle = \sum_i p_i |\psi_i\rangle \langle\psi_i|\alpha\rangle$. In quantum computation, we have the following standard definitions:

$$|0\rangle = \begin{pmatrix} 1 \\ 0 \end{pmatrix}, \quad |1\rangle = \begin{pmatrix} 0 \\ 1 \end{pmatrix}. \quad (2.2)$$

These are one-qubit state. We can have two-qubit states as well, and then we use shorthand like

$$|00\rangle = |0\rangle|0\rangle = |0\rangle \otimes |0\rangle, |10\rangle = |1\rangle|0\rangle \text{ and so on. Therefore we have, } |10\rangle = \begin{pmatrix} 0 \\ 0 \\ 1 \\ 0 \end{pmatrix}, |11\rangle = \begin{pmatrix} 0 \\ 0 \\ 0 \\ 1 \end{pmatrix} \text{ and}$$

so on. We refer to a state as ‘normalized’ if $\langle\psi|\psi\rangle = 1$. This is called the inner product of a ‘bra’ and ‘ket’. For readers comfortable with this notation, nothing remains to be said, but for those who are new, we give a small example of ‘bra-ket’ gymnastics now. Suppose we have a system in state $|i\rangle$ and another in $|j\rangle$, then the composite state is written as $|ij\rangle = |i\rangle|j\rangle$. For example,

¹⁵Often mentioned as ‘inserting an identity’

$\langle j | \langle i | | k \rangle | l \rangle = |ij\rangle^\dagger |kl\rangle = \langle j | \langle i | k \rangle | l \rangle = \langle i | k \rangle \langle j | l \rangle$. One can also define an ‘outer product’ as, $|\psi\rangle \langle \phi|$ which is a matrix. Suppose we take $|0\rangle, |1\rangle$ and construct $\rho = 1/2(|0\rangle \langle 0| - |0\rangle \langle 1| - |1\rangle \langle 0| + |1\rangle \langle 1|)$. The matrix ρ is given by:

$$\rho = \frac{1}{2} \begin{pmatrix} 1 & -1 \\ -1 & 1 \end{pmatrix}.$$

More systematically, we define the outer product as:

$$|\psi\rangle \langle \phi| = \begin{pmatrix} \alpha \\ \beta \end{pmatrix} \begin{pmatrix} \gamma^* & \delta^* \end{pmatrix} = \begin{pmatrix} \alpha\gamma^* & \alpha\delta^* \\ \beta\gamma^* & \beta\delta^* \end{pmatrix}. \quad (2.3)$$

In fact, any square matrix can be written as a linear combination of outer products. The simplest example is to write any 2×2 matrix in this form given by:

$$A = A_{00} |0\rangle \langle 0| + A_{01} |0\rangle \langle 1| + A_{10} |1\rangle \langle 0| + A_{11} |1\rangle \langle 1| \quad (2.4)$$

This representation of a matrix in terms of ‘ket-bra’ also provides a simple interpretation of some quantum gates. For example, $|00\rangle \langle 00| + |01\rangle \langle 01| + |10\rangle \langle 11| + |11\rangle \langle 10|$ gives a representation of CNOT gate¹⁶ and implies the corresponding transformation.

EXAMPLE 1: Consider $|\psi\rangle = |a\rangle \otimes |b\rangle$, $A|a\rangle = a|a\rangle$, and $B|b\rangle = b|b\rangle$. Compute $A \otimes B|\psi\rangle$.

Proof. We can write $A \otimes B|\psi\rangle$ as $A \otimes B|ab\rangle = (A \otimes B)|a\rangle \otimes |b\rangle$ and then by distributing the operators write this as $A|a\rangle \otimes B|b\rangle = ab|\psi\rangle$. \square

SECTION 3

States, quantum gates, density matrices, and rules

In classical logic gates, the input signal can be a string of either 1 or 0 and there is a single output signal. The classical gates can be reversible or non-reversible. The NOT gate is an example of a reversible gate. For example, to see this clearly, consider the truth table representing the action of a XOR gate for two input classical bits, A and B. The output is given by $A \oplus B$. We mention this along with other two logic gates in the table below.

A	B	AND ($A \cdot B$)	OR ($A + B$)	XOR($A \oplus B$)
0	0	0	0	0
0	1	0	1	1
1	0	0	1	1
1	1	1	1	0

¹⁶We will soon learn about this gate in the next sections

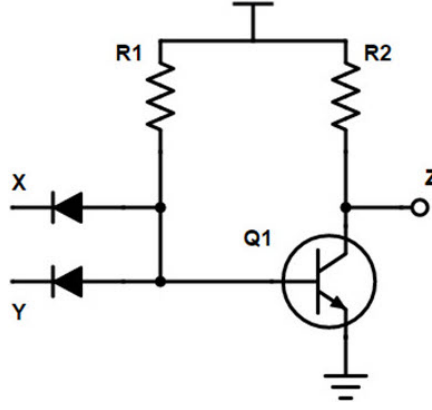


Figure 3. The construction of NAND gate using transistor and diodes. The Z is the output and the T-shaped sign signals the input $+V$ voltage. We say the input is high (1) if it is $+V$ while it is 0 if grounded.

This can be extended easily to have three input lines, the output is given by $A \oplus B \oplus C$ and will be high (1) if the number of highs in the input is an odd number. The fact that there is a single output line clearly implies that we can never run this operation backward. Given an output, we can never know what was the actual input. So XOR seems like a non-reversible gate. However, if we allow a garbage output (say A), then XOR can be made reversible. The AND gate is not reversible (even if we allow an extra output bit). NAND and NOR are the universal gate set for classical computers (which means that any gates can be constructed from them). The representation of a NAND gate made up of two transistors is shown below.

3.1 States on the Bloch sphere and gates

The inputs for the quantum case are known as ‘states’. They can either be $|0\rangle$, $|1\rangle$ or in a superposition of these two states or in some entangled state of these qubits. We will see this in more detail later on. The classical logic gate XOR we considered above, or any other logic gate behaves very differently compared to a quantum logic gate. In quantum circuits, the data (or states) are represented by ‘qubits’, the operations are described by unitary quantum logic gates and the results are obtained by doing measurements. The first point of difference is that in this case, the number of inputs is the same as the number of outputs. The circuit can be run backward, and we can reproduce input if we want. One striking property of quantum logic gates is that they can change the inputs in ways that cannot be done classically. One example of this is to look at Hadamard gate (H). If we take an input qubit to be $|0\rangle$ and then act on it with H gate, we have:

$$H|0\rangle \equiv |+\rangle = \frac{1}{\sqrt{2}}(|0\rangle + |1\rangle),$$

$$H|1\rangle \equiv |-\rangle = \frac{1}{\sqrt{2}}(|0\rangle - |1\rangle),$$

which is now in a superposition state. The Hadamard gate can also be expressed as a $\pi/2$ rotation around the Y-axis, followed by a 180° rotation around the X-axis i.e. $H = \sqrt{XY}$. We can represent

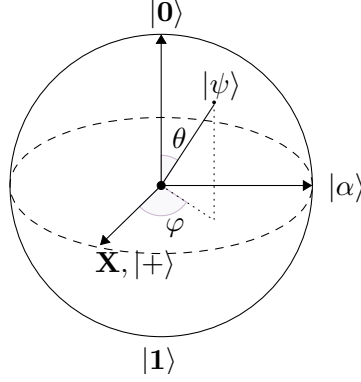


Figure 4. The representation of the possible states of single qubit on the Bloch sphere. We have $|\alpha\rangle = \frac{1}{\sqrt{2}}(|0\rangle + i|1\rangle)$ and $|\psi\rangle = \cos(\theta/2)|0\rangle + e^{i\varphi}\sin(\theta/2)|1\rangle$ which is just $P(\phi)R_y(\theta)|0\rangle$. The Z -basis is the ‘computational basis’.

this gate by the following matrix:

$$H = \frac{1}{\sqrt{2}} \begin{pmatrix} 1 & 1 \\ 1 & -1 \end{pmatrix} = \frac{|0\rangle + |1\rangle}{\sqrt{2}}\langle 0| + \frac{|0\rangle - |1\rangle}{\sqrt{2}}\langle 1| \quad (3.1)$$

A natural way of representing the qubit state is by using the Bloch sphere¹⁷ representation as shown in Fig. 4. The Hadamard transformation (also known as ‘Walsh-Hadamard’) is a special case of the more general Fourier transform (FT) which plays a major role in quantum algorithms. One special property of this gate is that $H = H^{-1}$ and therefore:

$$H\left(\frac{1}{\sqrt{2}}(|0\rangle + |1\rangle)\right) = |0\rangle.$$

One of the frequently used quantum logic gate is the quantum analog of XOR gate and is known as CNOT (controlled NOT) or CX gate. The matrix representation of CNOT is given by:

$$\begin{pmatrix} 1 & 0 & 0 & 0 \\ 0 & 1 & 0 & 0 \\ 0 & 0 & 0 & 1 \\ 0 & 0 & 1 & 0 \end{pmatrix} \quad (3.2)$$

and the truth table in this case can be written as:

$ A\rangle$	$ B\rangle$	$ A\rangle$	$ A \oplus B\rangle$
$ 0\rangle$	$ 0\rangle$	$ 0\rangle$	$ 0\rangle$
$ 0\rangle$	$ 1\rangle$	$ 0\rangle$	$ 1\rangle$
$ 1\rangle$	$ 0\rangle$	$ 1\rangle$	$ 1\rangle$
$ 1\rangle$	$ 1\rangle$	$ 1\rangle$	$ 0\rangle$

¹⁷Note that this is mathematically referred to as ‘Riemann sphere’ and is denoted as \mathbb{CP}^1 which is $\equiv SU(2)/U(1)$

This can also be written as:

$$\text{CNOT} = |0\rangle\langle 0| \otimes \mathbb{1} + |1\rangle\langle 1| \otimes \sigma_x, \quad (3.3)$$

where σ_x is one of the Pauli matrices. For this gate, we have two outputs (unlike classical XOR gate) and the first output is sometimes called ‘garbage output’ since it is just the first input. The second input ($|B\rangle$) is called the ‘target’ while the first is called the ‘control’ (or control line) for obvious reasons. The CNOT gate is a two-qubit operation, in which the first qubit is usually referred to as the control qubit and the second qubit as the target qubit. Now suppose an input

state is given by $|\psi\rangle = \begin{pmatrix} \alpha \\ \beta \\ 0 \\ 0 \end{pmatrix}$, it is easy to check that if we pass it through CNOT gate, it will

remain unchanged. We leave this simple exercise for the reader. There are many other important quantum gates such as the Pauli-X (simply X) which is a rotation through π radians around the x -axis and similar for other directions (y and z):

$$X = \sigma_x = \sigma_1 = \begin{pmatrix} 0 & 1 \\ 1 & 0 \end{pmatrix}$$

$$Y = \sigma_y = \sigma_2 = \begin{pmatrix} 0 & -i \\ i & 0 \end{pmatrix}$$

$$Z = \sigma_z = \sigma_3 = \begin{pmatrix} 1 & 0 \\ 0 & -1 \end{pmatrix}.$$

These three matrices also have corresponding rotation matrices, such as $R_X(\theta) = \exp(-iX\theta/2)$. X basis is also called Hadamard basis, since it can be generated from computational basis (Z) by acting by H . In Fig. 4, we denoted the state $|\psi\rangle = \cos(\theta/2) |0\rangle + e^{i\varphi} \sin(\theta/2) |1\rangle$. The outer product of this state is closely related to the dot product of the unit vector in spherical coordinates¹⁸ with Pauli matrices as:

¹⁸Recall that $(n_1, n_2, n_3) = (\cos \phi \sin \theta, \sin \phi \sin \theta, \cos \theta)$

$$\begin{aligned}
|\psi\rangle\langle\psi| &= \begin{pmatrix} \cos\frac{\theta}{2} \\ e^{i\phi}\sin\frac{\theta}{2} \end{pmatrix} \begin{pmatrix} \cos\frac{\theta}{2} & e^{-i\phi}\sin\frac{\theta}{2} \end{pmatrix} \\
&= \begin{pmatrix} \cos^2(\frac{\theta}{2}) & e^{-i\phi}\cos\frac{\theta}{2}\sin\frac{\theta}{2} \\ e^{i\phi}\cos\frac{\theta}{2}\sin\frac{\theta}{2} & \sin^2(\frac{\theta}{2}) \end{pmatrix} \\
&= \frac{1}{2} \begin{pmatrix} 1 + \cos\theta & e^{-i\phi}\sin\theta \\ e^{i\phi}\sin\theta & 1 - \cos\theta \end{pmatrix} \\
&= \frac{1}{2} \begin{pmatrix} 1 + \cos\theta & \cos\phi\sin\theta - i\sin\phi\sin\theta \\ \cos\phi\sin\theta + i\sin\phi\sin\theta & 1 - \cos\theta \end{pmatrix} \\
&= \frac{1}{2} \begin{pmatrix} 1 + n_3 & n_1 - in_2 \\ n_1 + in_2 & 1 - n_3 \end{pmatrix} \\
&= \frac{1}{2}(I + \hat{n} \cdot \vec{\sigma}). \tag{3.4}
\end{aligned}$$

The matrix $\hat{n} \cdot \vec{\sigma}$ is an involutory matrix (i.e., a matrix which is both unitary and hermitian and whose square is an identity matrix). It is straightforward to show that the eigenvalues of $\hat{n} \cdot \vec{\sigma}$ is ± 1 and denoting corresponding eigenvectors α and β , we can write: $\hat{n} \cdot \vec{\sigma} = |\alpha\rangle\langle\alpha| - |\beta\rangle\langle\beta|$ and $\exp(i\theta\hat{n} \cdot \vec{\sigma}) = \cos(\theta)\mathbb{1} + i\sin\theta\hat{n} \cdot \vec{\sigma}$.

EXAMPLE 2: Show that $\hat{n} \cdot \vec{\sigma} = \cos\theta|0\rangle\langle 0| + e^{-i\phi}\sin\theta|0\rangle\langle 1| + e^{i\phi}\sin\theta|1\rangle\langle 0| - \cos\theta|1\rangle\langle 1|$

Proof. We begin by noting that we have,

$$\hat{n} \cdot \vec{\sigma} = \begin{bmatrix} \cos\theta & \cos\phi\sin\theta - i\sin\phi\sin\theta \\ \cos\phi\sin\theta + i\sin\phi\sin\theta & -\cos\theta \end{bmatrix}.$$

Then using $e^{i\theta} = \cos\theta + i\sin\theta$ and matrix representations of $|00\rangle\langle 00|$, $|01\rangle\langle 01|$, $|10\rangle\langle 10|$, and $|11\rangle\langle 11|$, we obtain the required. \square

EXAMPLE 3: Show that any single qubit unitary can be written as:

$$U = \begin{bmatrix} e^{i(\alpha-\beta/2-\delta/2)}\cos(\theta) & e^{i(\alpha-\beta/2+\delta/2)}\sin(\theta) \\ e^{i(\alpha+\beta/2-\delta/2)}\sin(\theta) & e^{i(\alpha+\beta/2+\delta/2)}\cos(\theta) \end{bmatrix}. \tag{3.5}$$

Furthermore, show that $U = e^{i\alpha}R_z(\beta)R_y(\gamma)R_z(\delta)$.

Proof. We now give the proof of the above example. We can define general U as:

$$U = \begin{pmatrix} a & b \\ c & d \end{pmatrix}.$$

We have constraints: $|a|^2 + |c|^2 = 1$, $|b|^2 + |d|^2 = 1$, and $a^*b + c^*d = 0$. Then we have,

$$U = \begin{pmatrix} e^{\alpha_{11}} \cos \theta & e^{\alpha_{12}} \sin \theta \\ e^{\alpha_{21}} \sin \theta & e^{\alpha_{22}} \cos \theta \end{pmatrix}.$$

The last condition (orthogonal columns) gives: $e^{i(\alpha_{11}-\alpha_{12})} + e^{i(\alpha_{21}-\alpha_{22})} = 0$, where α_{11} is related to the other three by $\alpha_{11} = \alpha_{12} + \alpha_{21} - \alpha_{22} + \pi$. Now we can set $\theta = \gamma/2$, $\alpha_{12} = \alpha - \beta/2 + \delta/2 + \pi$, $\alpha_{21} = \alpha + \beta/2 - \delta/2$, and $\alpha_{22} = \alpha + \beta/2 + \delta/2$. \square

Another useful quantum gate which is an extension of CNOT gate is known as controlled-controlled NOT (CCNOT) gate or Toffoli gate. This is a three-qubit operation defined by:

$$\begin{pmatrix} 1 & 0 & 0 & 0 & 0 & 0 & 0 & 0 \\ 0 & 1 & 0 & 0 & 0 & 0 & 0 & 0 \\ 0 & 0 & 1 & 0 & 0 & 0 & 0 & 0 \\ 0 & 0 & 0 & 1 & 0 & 0 & 0 & 0 \\ 0 & 0 & 0 & 0 & 1 & 0 & 0 & 0 \\ 0 & 0 & 0 & 0 & 0 & 1 & 0 & 0 \\ 0 & 0 & 0 & 0 & 0 & 0 & 0 & 1 \\ 0 & 0 & 0 & 0 & 0 & 0 & 1 & 0 \end{pmatrix} \quad (3.6)$$

resulting in

$$\begin{aligned} |000\rangle &\rightarrow |000\rangle \\ |001\rangle &\rightarrow |001\rangle \\ |010\rangle &\rightarrow |010\rangle \\ |011\rangle &\rightarrow |011\rangle \\ |100\rangle &\rightarrow |100\rangle \\ |101\rangle &\rightarrow |101\rangle \\ |110\rangle &\rightarrow |111\rangle \\ |111\rangle &\rightarrow |110\rangle \end{aligned} \quad (3.7)$$

► QUESTION 1: Write the Z and P gate in the outer product notation and compute the action of P on a general qubit state.

In fact, Toffoli and any single qubit gate which does not preserve the computational basis (such as Hadamard) form a universal gate set [18] for quantum computation. But, Toffoli by itself is

$$-\boxed{H}- = \frac{1}{\sqrt{2}} \begin{bmatrix} 1 & 1 \\ 1 & -1 \end{bmatrix} , \quad |0\rangle \xrightarrow{-\boxed{H}-} |+\rangle$$

$$-\boxed{X}- = \begin{bmatrix} 0 & 1 \\ 1 & 0 \end{bmatrix} , \quad |0\rangle \xrightarrow{-\boxed{X}-} |1\rangle$$

$$-\boxed{Z}- = \begin{bmatrix} 1 & 0 \\ 0 & -1 \end{bmatrix} , \quad |1\rangle \xrightarrow{-\boxed{Z}-} -|1\rangle$$

$$-\boxed{Y}- = \begin{bmatrix} 0 & -i \\ i & 0 \end{bmatrix}$$

$$-\boxed{P}- = \begin{bmatrix} 1 & 0 \\ 0 & e^{i\phi} \end{bmatrix}$$

$$-\boxed{R_z(\theta)}- = \begin{bmatrix} e^{-i\theta/2} & 0 \\ 0 & e^{i\theta/2} \end{bmatrix}$$

$$-\boxed{S}- = \begin{bmatrix} 1 & 0 \\ 0 & i \end{bmatrix}$$

$$-\boxed{T}- = \begin{bmatrix} 1 & 0 \\ 0 & e^{i\pi/4} \end{bmatrix} = e^{\frac{i\pi}{8}} \begin{bmatrix} e^{\frac{-i\pi}{8}} & 0 \\ 0 & e^{\frac{i\pi}{8}} \end{bmatrix}$$

Figure 5. Definition of Hadamard (H), Paulis (X, Z, Y), Phase (P), Rotation around z-axis ($R_z(\theta)$), $\pi/2$ phase (S) and $\pi/8$ (T) single qubit gates and example of how some of them act on a single qubit.

universal for classical computation. Hence, it appears that one only needs to add the Hadamard gate to make a 'classical' set of gates quantum universal. And this is true and was proved in Ref. [19]. Another interesting fact about Toffoli which is often required is how can we efficiently decompose it into say two-qubit CNOT gates. In Ref. [20], it was shown that one needs at least $2n$ CNOT to implement any n -qubit Toffoli. For the standard case of $n = 3$, one needs at least 6 CNOTs. In some of the algorithms we discuss later in the notes, another important operation is

the swapping of qubits. This is represented by the matrix as:

$$\text{SWAP} = \begin{pmatrix} 1 & 0 & 0 & 0 \\ 0 & 0 & 1 & 0 \\ 0 & 1 & 0 & 0 \\ 0 & 0 & 0 & 1 \end{pmatrix}$$

The gate achieves $|a, b\rangle \rightarrow |b, a\rangle$ and can be written in terms of CNOT gates as: ¹⁹

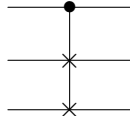
$$\begin{array}{c} |a\rangle \\ |b\rangle \end{array} \begin{array}{c} \times \\ \times \end{array} = \begin{array}{c} \bullet \oplus \bullet \\ \oplus \bullet \oplus \end{array} \quad (3.8)$$

A closely related version of this – which is often used to reorder or swap qubits with a control is the controlled SWAP (also known as ‘Fredkin gate’ ²⁰) is an important gate that can be implemented as: `qc.cswap(0,1,2)`. We can see how this gate can be decomposed in terms of CNOT gate in QISKIT as:

`qc.decompose().draw(output='mpl',style='iqx')`. The representation of the gate is given below:

$$\text{CSWAP} = |0\rangle\langle 0| \otimes \mathbb{1} \otimes \mathbb{1} + |1\rangle\langle 1| \otimes \text{SWAP} = \begin{pmatrix} 1 & 0 & 0 & 0 & 0 & 0 & 0 & 0 \\ 0 & 1 & 0 & 0 & 0 & 0 & 0 & 0 \\ 0 & 0 & 1 & 0 & 0 & 0 & 0 & 0 \\ 0 & 0 & 0 & 1 & 0 & 1 & 0 & 0 \\ 0 & 0 & 0 & 0 & 1 & 0 & 0 & 0 \\ 0 & 0 & 0 & 0 & 0 & 0 & 1 & 0 \\ 0 & 0 & 0 & 0 & 0 & 1 & 0 & 0 \\ 0 & 0 & 0 & 0 & 0 & 0 & 0 & 1 \end{pmatrix} \quad (3.9)$$

and is represented by the following symbol:



which means in our notation, $|0, a, b\rangle \rightarrow |0, a, b\rangle$, and $|1, a, b\rangle \rightarrow |1, b, a\rangle$ respectively. The use of control feature can be extended to any unitary gate. For example, consider the controlled RX gate where the transformation is defined by the matrix:

$$\text{RX} = \begin{pmatrix} \cos(\frac{\theta}{2}) & -i \sin(\frac{\theta}{2}) \\ -i \sin(\frac{\theta}{2}) & \cos(\frac{\theta}{2}) \end{pmatrix}.$$

¹⁹We can see this as follows: $|a, b\rangle \rightarrow |a, a \oplus b\rangle$ after application of first CNOT gate. Then the second CNOT (note with control now down and target on upper qubit) transforms $|a, a \oplus b\rangle \rightarrow |a \oplus (a \oplus b), a \oplus b\rangle = |b, a \oplus b\rangle$. Then the last CNOT transforms this to the desired $|b, a\rangle$

²⁰For a photonic based quantum computing implmentation of this gate, see Ref. [21]

If we want to build a controlled-RX gate then the matrix is given by a 4×4 matrix:

$$\text{CRX} = \begin{pmatrix} 1 & 0 & 0 & 0 \\ 0 & \cos(\frac{\theta}{2}) & 0 & -i \sin(\frac{\theta}{2}) \\ 0 & 0 & 1 & 0 \\ 0 & -i \sin(\frac{\theta}{2}) & 0 & \cos(\frac{\theta}{2}) \end{pmatrix}. \quad (3.10)$$

This gate is included in QISKIT like other gates we have discussed above. It can simply be called by doing `qc.crx($\pi/2, 0, 1$)` but double controlled RX gate is not included in usual gate library in QISKIT and we leave the design of this gate for the interested reader. In addition to the RX gate (which corresponds to rotation along x -axis), we can have RY or RZ gates. A general rotation gate is represented as:

$$\begin{aligned} R_{\vec{n}}(\theta) &= \exp \left[\frac{-i\theta}{2} (n_1 X + n_2 Y + n_3 Z) \right] \\ &= \begin{pmatrix} \cos(\theta/2) - in_3 \sin(\theta/2) & -n_2 \sin(\theta/2) - in_1 \sin(\theta/2) \\ n_2 \sin(\theta/2) - in_1 \sin(\theta/2) & \cos(\theta/2) + in_3 \sin(\theta/2) \end{pmatrix}. \end{aligned} \quad (3.11)$$

If we put $n_2 = n_3 = 0$ and $n_1 = 1$, we get back the RX gate²¹.

► QUESTION 2: Construct controlled-controlled-RX gate matrix and then implement it in QISKIT. Check that it has the correct behaviour by checking how $|110\rangle$ and $|000\rangle$ transform respectively.

► QUESTION 3: a) Show that the controlled-Hadamard (CH) gate given by:

$$\text{CH} = \begin{pmatrix} 1 & 0 & 0 & 0 \\ 0 & 1 & 0 & 0 \\ 0 & 0 & \frac{1}{\sqrt{2}} & \frac{1}{\sqrt{2}} \\ 0 & 0 & \frac{1}{\sqrt{2}} & -\frac{1}{\sqrt{2}} \end{pmatrix}, \quad (3.12)$$

can be written as $|00\rangle\langle 00| + |01\rangle\langle 01| + \frac{1}{\sqrt{2}}(|10\rangle\langle 10| + |10\rangle\langle 11| + |11\rangle\langle 10| - |11\rangle\langle 11|)$.

b) Suppose we act with $R_y(3\pi/4)$ on starting state $|0\rangle$. What is the probability that we measure the state we started with? Recall that $R_y(\theta)$ is defined as:

$$\begin{pmatrix} \cos(\theta/2) & -\sin(\theta/2) \\ \sin(\theta/2) & \cos(\theta/2) \end{pmatrix}. \quad (3.13)$$

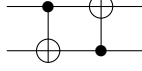
²¹Note that the matrices have θ rather than $\theta/2$. This is due to the fact that rotations on Bloch sphere by θ corresponds to $\theta/2$ for the $SU(2)$ unitary matrices due to double cover relation between $SO(3)$ and $SU(2)$

► QUESTION 4: Show that

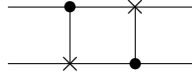
$$H \cdot S \cdot T \cdot H |0\rangle = \frac{1}{2} \left[\left(1 + e^{i3\pi/4}\right) |0\rangle + \left(1 - e^{i3\pi/4}\right) |1\rangle \right]$$

where H , S , and T are the usual gates defined in the text.

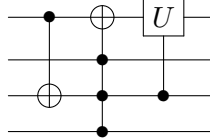
A simple circuit with two CNOT gates is given as:



Though we will use the modern notation for CNOT, the old notation used by Feynman [22] was instead:



Furthermore, a slightly more complicated circuit with multiple control lines and an arbitrary gate U can be drawn as:



It is easy for the reader to see that if we have two qubits and act with H on the first qubit and then apply CNOT gate, it results in an entangled state. For three qubits, this is more interesting. Three qubits can be entangled in two ways that are not related to each other. One of them is called the GHZ state and the other is known as W-state [23]. The GHZ state is fully separable, while the W state cannot be separated by any local operations and classical communication (LOCC). These are defined as follows:

$$\text{GHZ}_3 = \frac{1}{\sqrt{2}} (|000\rangle + |111\rangle),$$

$$\text{W}_3 = \frac{1}{\sqrt{3}} (|001\rangle + |010\rangle + |100\rangle).$$

It is straightforward to extend W state to its n -qubit version as:

$$|W\rangle = \frac{1}{\sqrt{n}} (|10 \dots 00\rangle + |01 \dots 00\rangle + \dots + |00 \dots 01\rangle). \quad (3.14)$$

We can also define something called the ‘generalized’ GHZ state defined as:

$$\text{GHZ}_n = \cos \theta |000 \dots 000\rangle + \sin \theta |111 \dots 111\rangle. \quad (3.15)$$

It is easy to implement these states in QISKIT and we leave that for the reader. Going beyond the discussion of single gates, for several purposes, some collection of quantum gates is often useful.

When these gates are collected together, they are referred to as a ‘set’. One of the examples is the stabilizer set, which is given by a group of three gates: $\{H, \text{CNOT}, P\}$ and the same as Clifford group. These gates are important for error-correcting codes but do not form a universal set as discussed later in the notes.

However, it was found that $\{\text{CNOT}, \text{single-qubit unitaries } (SU(2))\}$ form a universal set of gates but it is infinite. We would like this to be close to some finite gate set. A finite gate set can only produce a countable set of gates and one would think that every unitary cannot be obtained by this method. However, we do not need to get every unitary and this is where one of the most important theorems in quantum information/computation comes into play. Solovay-Kitaev (SK) theorem argues that if a single-qubit quantum gates generate a dense subset of $SU(2)$ then that set is guaranteed to fill $SU(2)$ quickly (means it is possible to obtain a decent approximation to any desired gate using gates from the generating set). We say that a subset \mathcal{S} of a topological space X is dense if every point $x \in X$ either belongs to \mathcal{S} or is a limit point of \mathcal{S} . The special unitary group $SU(N)$ is defined as the set of all $N \times N$ matrices with unit determinant. For example, the Pauli matrices are the three generators of $SU(2)$. There are two universal (approximately) gate sets: $\{H, \text{CNOT}, \pi/8\}$ as shown in Ref. [24] and $\{H, \text{CCNOT}, \pi/4\}$ as shown in Ref. [25] and CNOT plus all single-qubit gates [26]. Suppose we consider the gate set $\{H, \text{CNOT}, T(\pi/8)\}$ and ask how efficiently a given unitary transformation U can be implemented. This situation might arise due to the limitation of applying only single-qubit gate most prominently when one required fault-tolerant quantum computation where the features of fault-tolerance are available for selected gates in Clifford group and $\pi/8$ gate. We would like to have a polynomial (in precision and number of qubits) number of gates selected from this set. We ask this question because in general most unitary transformations cannot be approximated precisely. The SK theorem can be useful in this case. A direct consequence of this theorem is that a quantum circuit of N constant-qubit gates can be approximated to ϵ error (in operator norm) by a quantum circuit of $\mathcal{O}(N \log^c(N/\epsilon))$ gates from a desired finite universal gate set. Different proofs of the theorem give different values for c , in Ref. [27], it was shown to be ~ 3.97 . This theorem computes how many gates are needed to approximate a given operation for the specified accuracy ϵ and is polylogarithmic in $1/\epsilon$. We now write down the formal statement as below:

Solovay-Kitaev theorem: If \mathcal{S} is a finite set of 1-qubit gates which is universal and if for any gate $g \in \mathcal{S}$, the inverse g^{-1} can be achieved by finite sequence of gates in \mathcal{S} , then any 1-qubit gate and hence (any unitary transformation) can be approximated using $\mathcal{O}(\log^c(1/\epsilon))$ gates with $c < 4$. The basic algorithm is given below:

- **function** Solovay-Kitaev/SK (UnitaryGate U , depth n)
Read gate to be approximated and accuracy desired ($\epsilon \rightarrow 0$ as $n \rightarrow \infty$)
- **if** ($n = 0$), **return** basic approximation to U
The function is recursive, so that to obtain an n approximation to U , it will call itself

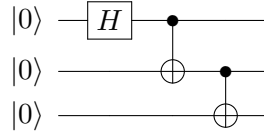
to obtain $n - 1$ -approximations to the unitary.

- **else set** $U_{n-1} = \text{SK}(U, n-1)$ **set** $V, W = \text{GC-Decompose}(UU^\dagger)$,
set $V_{n-1} = \text{SK}(V, n-1)$, **set** $W_{n-1} = \text{SK}(W, n-1)$, **return** $U_n = V_{n-1}W_{n-1}V^\dagger W_{n-1}^\dagger$

A single-gate set of universal quantum gates can also be formulated using the three-qubit Deutsch gate given by:

$$\mathbb{D} = \begin{pmatrix} 1 & 0 & 0 & 0 & 0 & 0 & 0 & 0 \\ 0 & 1 & 0 & 0 & 0 & 0 & 0 & 0 \\ 0 & 0 & 1 & 0 & 0 & 0 & 0 & 0 \\ 0 & 0 & 0 & 1 & 0 & 0 & 0 & 0 \\ 0 & 0 & 0 & 0 & 1 & 0 & 0 & 0 \\ 0 & 0 & 0 & 0 & 0 & 1 & 0 & 0 \\ 0 & 0 & 0 & 0 & 0 & 0 & i \cos(\theta) & \sin(\theta) \\ 0 & 0 & 0 & 0 & 0 & 0 & \sin(\theta) & i \cos(\theta) \end{pmatrix}. \quad (3.16)$$

► **QUESTION 5:** What does the following quantum circuit do? By what name do we know the final state known as?



► **QUESTION 6:** Check that CNOT results in the following transformations given below, i.e., $\text{CNOT}(X \otimes \mathbb{1}) \rightarrow (X \otimes X)\text{CNOT}$ or alternatively $\text{CNOT}(X \otimes \mathbb{1})\text{CNOT}^\dagger \rightarrow (X \otimes X)$ and so on.

- $X \otimes \mathbb{1} \rightarrow X \otimes X$
- $\mathbb{1} \otimes X \rightarrow \mathbb{1} \otimes X$
- $Z \otimes \mathbb{1} \rightarrow Z \otimes \mathbb{1}$
- $\mathbb{1} \otimes Z \rightarrow Z \otimes Z$

It is also known that this gate can be constructed from a sequence of two-qubit gates [28]. It can also be constructed from a two-qubit gate known as ‘Barenco gate’ [29] given by:

$$\mathbb{B} = \begin{pmatrix} 1 & 0 & 0 & 0 \\ 0 & 1 & 0 & 0 \\ 0 & 0 & e^{i\alpha} \cos(\theta) & -ie^{i(\alpha-\phi)} \sin(\theta) \\ 0 & 0 & -ie^{i(\alpha+\phi)} \sin(\theta) & e^{i\alpha} \cos(\theta) \end{pmatrix} \quad (3.17)$$

In fact, it was shown in Ref. [30] that the set $\{T, H\}$ is universal and was shown to be true by a short proof in Ref. [31]. The fact that T can perform all classical reversible computation makes it clear that H gate which is in fact a quantum Fourier transform (QFT) over \mathbb{Z}_2 is the real ‘quantum’ difference!

QUESTION 7: Show that H can be written for one-qubit as:

$$H = \frac{1}{\sqrt{2}} \left[(|0\rangle + |1\rangle) \langle 0| + (|0\rangle - |1\rangle) \langle 1| \right].$$

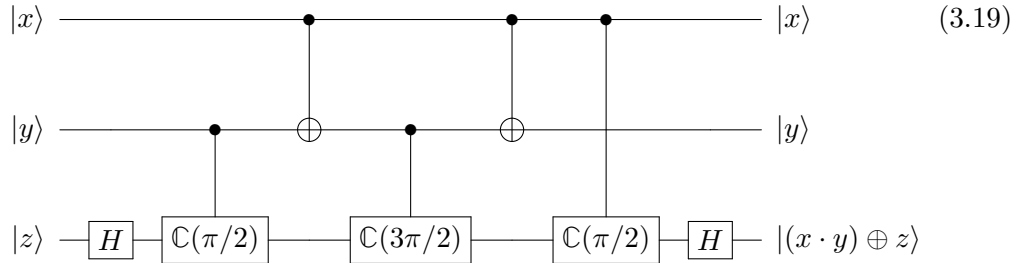
Show that this transform for n -qubits i.e., $H^{\otimes n}$ can be written as:

$$H^{\otimes n} = \frac{1}{2^{n/2}} \sum_{x,y} (-1)^{x \cdot y} |x\rangle \langle y|$$

► QUESTION 8: Consider a control line in a superposition state and target in $|0\rangle$. Pass this through the CNOT gate and write the result (a Bell state). Show that the circuit given below performs a measurement in the basis of Bell states. This exercise is reproduced from Exercise 4.33 of [11]. Find the measurement operators.



► QUESTION 9: Show that the circuit below is another way of implementing Toffoli gate. Find another decomposition of Toffoli gate?



We now discuss an important ingredient of the quantum circuit and it is related to the decomposition in terms of CNOT and single-qubit gates. It is a well-known result that we can decompose any $2^n \times 2^n$ unitary matrix in terms of single-qubit unitaries and CNOT gates. Every single-qubit unitary gate has 3 real parameters. So, for n qubits, we have $3n$ parameters. Once we add a CNOT gate, it appears that we can add twice one-qubit unitaries resulting in 6 real parameters. However,

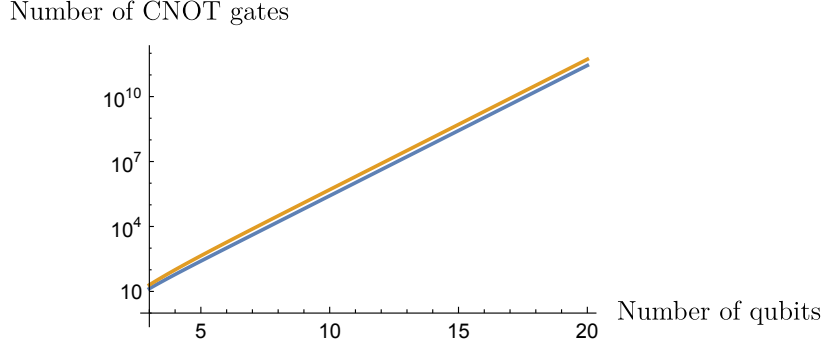


Figure 6. The theoretical lower bound on the number of CNOTs needed to approximate arbitrary unitary matrix. The upper bound is the cost attained using QSD in Ref. [32].

since the R_z gate commutes with the control line qubit and R_x commutes with the target qubit, we can pass them across and this reduces the number of effective parameters added by CNOT to 4. Suppose we need N CNOTs to approximate a $2^n \times 2^n$ matrix, then we have $3n + 4N \geq 4^n - 1$ which gives:

$$N \geq \frac{1}{4}(4^n - 3n - 1). \quad (3.20)$$

Using quantum Shannon decomposition (QSD), it was shown in Ref. [32] that one can get the cost down to:

$$N \geq \frac{23}{48}4^n - \frac{3}{2}2^n + \frac{4}{3}. \quad (3.21)$$

The difference between the lower bound and the implemented cost (about factor of 2) is shown in Fig. 6.

3.2 General quantum operations

Let us consider an orthonormal basis $|\phi_k\rangle$, we can write a state as $|\psi\rangle = \sum_k \alpha_k |\phi_k\rangle$. von Neumann (vN) measurement of $|\psi\rangle$ with respect to the ϕ basis is described by orthogonal projectors $\{|\phi_k\rangle, \langle\phi_k|\}$ and will have the output k with probability:

$$\text{Tr}(|\psi\rangle \langle\psi| |\phi_k\rangle \langle\phi_k|) = |\alpha_k|^2.$$

von Neumann (vN) measurements are a special kind of projective measurement (which is also known as Lüders measurement) which is complete. This is often used in quantum computing and communication. We give the circuit which can implement a vN measurement below.

In fact, the idea of projective measurements is related to identifying which state the system is in from the possible set of mutually exclusive states. Suppose, the atom is either in state $|a\rangle$ or $|b\rangle$, through projective measurement we can find out the state it is in. These are based on projection operators P which are Hermitian operators ($P = P^\dagger$, $P^2 = P$). We refer to two projection operators P_1 and P_2 as being orthogonal if $P_1 P_2 |\psi\rangle = 0$. The probability of obtaining

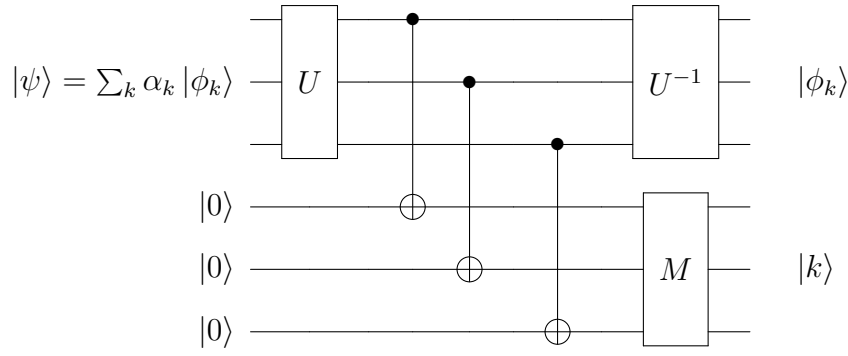


Figure 7. One way of implementing vN measurement through ancillary register. The measurement M measures $|k\rangle$ with probability, $|\alpha_k|^2$ while the map through U^{-1} gives the state $|\phi_k\rangle$ in the main register. One can also directly measure instead of introducing ancillary register. Note that U is a unitary transformation which implements basis change to the computational basis. The use of CNOT gate to copy to the ancillary register might seem illegal but note that we are just doing reversible transformation copying the computational basis states, we are not cloning/copying arbitrary superposition state.

output k (as discussed above) is $\text{Prob.}(k) = \langle \psi | P_k | \psi \rangle = \text{Tr}(P_k | \psi \rangle \langle \psi |)$. These measurements lead to the collapse of the wave function and the state after measurement ψ' is given by:

$$\psi' = \frac{P_k |\psi\rangle}{\sqrt{\langle \psi | P_k | \psi \rangle}}. \quad (3.22)$$

Projective measurements (of which von Neumann is a special case) can be generalized as well but we will not discuss it here and refer the reader to textbooks that discuss quantum measurements in depth.

EXAMPLE 4: What is the output of the quantum circuit given below? Assume U is some unitary gate.

$$\begin{array}{c} |0\rangle \text{ --- } [H] \text{ --- } \bullet \text{ --- } [H] \text{ ---} \\ | \psi_{\text{in}} \rangle \text{ --- } [U] \text{ ---} \end{array} \quad (3.23)$$

□ The initial state is given by: $|\psi_0\rangle = |0\rangle |\psi_{\text{in}}\rangle$. Once we apply the H gate it becomes, $|\psi_1\rangle$ which is given by:

$$|\psi_1\rangle = \frac{1}{\sqrt{2}} \left(|0\rangle |\psi_{\text{in}}\rangle + |1\rangle |\psi_{\text{in}}\rangle \right)$$

Then, if we act on this with the U as given in the Figure, we get:

$$|\psi_2\rangle = \frac{1}{\sqrt{2}} \left(|0\rangle |\psi_{\text{in}}\rangle + |1\rangle U |\psi_{\text{in}}\rangle \right)$$

and now we again act with the H gate,

$$|\psi_3\rangle = \frac{1}{2} \left((|0\rangle + |1\rangle) |\psi_{\text{in}}\rangle + (|0\rangle - |1\rangle) U |\psi_{\text{in}}\rangle \right)$$

and this is equal to:

$$= \frac{1}{2} \left(|0\rangle (\mathbb{1} + U) |\psi_{\text{in}}\rangle + |1\rangle (\mathbb{1} - U) |\psi_{\text{in}}\rangle \right)$$

□

3.3 Entanglement

One of the distinguishing features of quantum mechanics is ‘entanglement’²². Though there exist various definitions of entanglement of varying complexity, for our purposes, a simple one will suffice. We say that the state is entangled when it cannot be written as a product state. It is often useful to check whether a given state is separable (not entangled) or not. In order to show whether the state is entangled or not, it is easiest to compute the reduced density matrix and compute $\text{Tr} \rho_A^2$ and see if it is 1 or not (for normalized states). It is a separable state (not entangled) iff $\text{Tr} \rho_A^2 = 1$. Suppose we have a Bell state: $|\Psi\rangle = \frac{1}{\sqrt{2}}(|00\rangle + |11\rangle)$, then we have:

$$\rho_A = \text{Tr}_B(|\Psi\rangle\langle\Psi|) = \frac{1}{2} (|0\rangle\langle 0| + |1\rangle\langle 1|) = \frac{1}{2} \mathbb{1}$$

$\text{Tr}(\rho_A^2) = \frac{1}{4} \text{Tr}(\mathbb{1} \cdot \mathbb{1}) = \frac{1}{2}$. Hence, this is entangled. We have used the shorthand notation: $\text{Tr}_B(\rho_{AB}) = \rho_A$ above.

► QUESTION 10: Compute $\text{Tr}(\rho_A^2)$ and check if the state given below is separable?

$$|\psi\rangle = \frac{1}{2} (|00\rangle + |10\rangle - |01\rangle - |11\rangle). \quad (3.24)$$

Once you find it is separable, write it in terms of $|\pm\rangle = \frac{1}{\sqrt{2}}(|0\rangle \pm |1\rangle)$. Now consider a general state $|\psi\rangle = a|00\rangle + b|10\rangle + c|01\rangle + d|11\rangle$ and find the condition iff the state is to be a separable one. Now think of a measure using a, b, c, d of how we can quantify the extent of entanglement. Clearly for this case it should vanish. In later part of these notes, we will redo this exercise using QISKIT, see Question C.2. In the later part of the notes, we will encounter a name for the function which can be built out of a, b, c, d .

The above arguments can be systematically understood as follows. Consider a density matrix ρ written as:

$$\rho = \sum_i p_i |\psi_i\rangle\langle\psi_i|. \quad (3.25)$$

If the system is in a pure state then all the p_i , except one, is zero, and we get $\rho = |\psi\rangle\langle\psi|$. If the ρ is a pure state, then the following conditions are both sufficient and necessary to prove that it is in such a purity: $\rho = \rho^\dagger$, $\text{Tr} \rho = \text{Tr} \rho^2$. Usually one takes the ρ to be appropriately

²²This famously prompted Einstein to complain about spooky action at a distance (in German ‘spukhafte Fernwirkungen’)

normalized such that $\text{Tr}\rho = 1$ which is equivalent to saying that $\text{Tr}\rho = \text{Tr}\left(\sum_i p_i |\psi_i\rangle\langle\psi_i|\right) = 1$ or $\text{Tr}\rho = \sum_n \langle n|\rho|n\rangle = \sum_n \langle n|\psi\rangle\langle\psi|n\rangle = 1$ as per taste. It is straightforward to show that $\text{Tr}\rho = \text{Tr}\rho^2$. We will just show that $\rho = \rho^2$, which can be done by writing: $\rho^2 = |\psi\rangle\langle\psi|\psi\rangle\langle\psi| = \rho$, where the sums have been suppressed. Now consider a mixed state, and we will show that $\text{Tr}(\rho_{\text{mixed}})^2 < \text{Tr}\rho_{\text{mixed}}$. We also need to show that if $\rho^2 = \rho$, the state is pure. We first note that since ρ is Hermitian, the eigenvalues are real and the corresponding eigenvectors can be made orthonormal, the proof for this proceeds as follows,

$$\rho = \sum_i \lambda_i |\lambda_i\rangle\langle\lambda_i| \quad ; \text{ Spectral decomposition} \quad (3.26)$$

$$= \sum_i \lambda_i^2 |\lambda_i\rangle\langle\lambda_i| \quad ; (\because \rho = \rho^2) \quad (3.27)$$

This implies that the eigenvalues are either 0 or 1. Hence, $\lambda_i = 1$, for some $i = p$ and 0 for $i \neq p$. Hence, $\rho = \sum_i \lambda_i |\lambda_i\rangle\langle\lambda_i| = |\lambda_p\rangle\langle\lambda_p|$ which implies that ρ is pure. For mixed states, $\text{Tr}(\rho_{\text{mixed}})^2 < \text{Tr}(\rho_{\text{mixed}})$. The other properties still hold such as, $\rho = \rho^\dagger$, $\text{Tr}\rho = 1$ and $\rho \geq 0$ (positivity). The measure of $\text{Tr}\rho^2$ from 1 is a good measure of how mixed the state is. For a maximally mixed state, we have $\text{Tr}\rho^2 = 1/d$, where d is the dimension of the system. This is also called as a maximally mixed density matrix. A density matrix corresponding to a maximally mixed state also has the largest entropy as:

$$S_{\text{EE}} = -\text{Tr}_A(\rho \ln \rho) \quad (3.28)$$

$$= -d \frac{1}{d} \ln\left(\frac{1}{d}\right) = \ln d. \quad (3.29)$$

Any unitary transformation preserves the pureness of the state intact, i.e., a pure state remains pure.

$$\text{Tr}\left[(U\rho U^\dagger)^2\right] = \text{Tr}\left(U\rho \underbrace{U^\dagger U}_1 \rho U^\dagger\right) \quad (3.30)$$

$$= \text{Tr}\left(U\rho^2 U^\dagger\right) \quad (3.31)$$

$$= \text{Tr}\rho^2. \quad (3.32)$$

This definition of entropy (called entanglement entropy or von Neumann entropy) for pure states of a bipartite system is the most widely used measure to quantify entanglement. As the astute reader might have noticed before, we can also identify if the state is separable by computing the Schmidt number. Consider a state $|\psi\rangle \in \mathcal{H}_A \otimes \mathcal{H}_B$ to be a pure state. Then we have an expansion of the form:

$$|\psi\rangle = \sum_i \lambda_i |a_i\rangle |b_i\rangle,$$

where $|a_i\rangle$ and $|b_i\rangle$ are orthonormal states belonging to \mathcal{H}_A and \mathcal{H}_B respectively. The $\lambda_i \geq 0$ are Schmidt coefficients and satisfy $\lambda_i^2 = 1$. These are computed by constructing a matrix $\text{Tr}_B(|\psi\rangle\langle\psi|)$ whose eigenvalues are λ_i^2 . The Schmidt number is defined as the number of non-zero λ_i . The state is separable if this is 1 and entangled if it is greater than 1.

3.3.1 Partial trace method

In this subsection, we will discuss the idea which facilitates the computation of bipartite entropy. The partial trace, Tr_B is a map from the density matrix ρ_{AB} on some composite system with Hilbert space $\mathcal{H}_A \otimes \mathcal{H}_B$ onto density matrices ρ_A on \mathcal{H}_A . Let us assume that $\{|\alpha_i\rangle\}$ and $\{|\beta_i\rangle\}$ are the basis of \mathcal{H}_A and, \mathcal{H}_B respectively. Then a density matrix, ρ_{AB} can be decomposed as:

$$\rho_{AB} = \sum_{ijkl} c_{ijkl} |\alpha_i\rangle\langle\alpha_j| \otimes |\beta_k\rangle\langle\beta_l| \quad (3.33)$$

and the partial trace is given by²³:

$$\text{Tr}_B \rho_{AB} = \sum_{ijkl} c_{ijkl} |\alpha_i\rangle\langle\alpha_j| \langle\beta_l|\beta_k\rangle \quad (3.34)$$

$$\text{Tr}_B \begin{pmatrix} \rho_{11} & \rho_{12} & \rho_{13} & \rho_{14} \\ \rho_{21} & \rho_{22} & \rho_{23} & \rho_{24} \\ \rho_{31} & \rho_{32} & \rho_{33} & \rho_{34} \\ \rho_{41} & \rho_{42} & \rho_{43} & \rho_{44} \end{pmatrix} = \begin{pmatrix} \rho_{11} + \rho_{22} & \rho_{13} + \rho_{24} \\ \rho_{31} + \rho_{42} & \rho_{33} + \rho_{44} \end{pmatrix} \quad (3.35)$$

while the partial trace over A is given by:

$$\text{Tr}_A \begin{pmatrix} \rho_{11} & \rho_{12} & \rho_{13} & \rho_{14} \\ \rho_{21} & \rho_{22} & \rho_{23} & \rho_{24} \\ \rho_{31} & \rho_{32} & \rho_{33} & \rho_{34} \\ \rho_{41} & \rho_{42} & \rho_{43} & \rho_{44} \end{pmatrix} = \begin{pmatrix} \rho_{11} + \rho_{33} & \rho_{12} + \rho_{34} \\ \rho_{21} + \rho_{43} & \rho_{22} + \rho_{44} \end{pmatrix} \quad (3.36)$$

A two-qubit state can be expanded in the orthonormal basis $\{|00\rangle, |01\rangle, |10\rangle, |11\rangle\}$ given by:

$$\rho_{AB} = \rho_{11}|00\rangle\langle 00| + \rho_{12}|00\rangle\langle 01| + \dots + \rho_{44}|11\rangle\langle 11| \quad (3.37)$$

and the partial trace is given by 3.34:

$$\rho_A = (\rho_{11} + \rho_{22})|0\rangle\langle 0| + (\rho_{13} + \rho_{24})|0\rangle\langle 1| + (\rho_{31} + \rho_{42})|1\rangle\langle 0| + (\rho_{33} + \rho_{44})|1\rangle\langle 1| \quad (3.38)$$

One of the other ideas related is - purification. The fact that given mixed density matrix can always be thought of as being obtained from the partial trace of some bigger Hilbert space. This idea is closely related to the phrase – there exists a ‘church of bigger Hilbert space’ supposedly meaning that there always is a place where one can be purified. Suppose $|i\rangle \in \mathcal{H}_A$ such that:

$$\rho_A = \sum_i \lambda_i |i\rangle\langle i| \quad (3.39)$$

Extent $\mathcal{H}_A \rightarrow \mathcal{H}_A \otimes \mathcal{H}_B$, then we can write ρ_A as,

$$\rho_A = \text{Tr}_B |\psi\rangle_{AB} \langle\psi|_{AB} \quad (3.40)$$

which is a pure state where $|\Psi\rangle_{AB} = \sum_i \sqrt{\lambda_i} |i\rangle_A |i\rangle_B$ Suppose we have a density matrix, ρ_{123} , and we purify this state by adding a fourth Hilbert space, \mathcal{H}_4 . Then we have, $S_{1234} = 0$ and from this we get, $S_{123} = S_4$ and $S_{234} = S_1$ and $S_{12} = S_{34}$.

²³We note that $\text{Tr}|\beta_k\rangle\langle\beta_j| = \langle\beta_j|\beta_k\rangle$

► QUESTION 11: Consider the state given by:

$$|\psi\rangle = \cos(\alpha) |00\rangle + \sin(\alpha) |11\rangle, \quad 0 < \alpha < \pi/4 \quad (3.41)$$

Find the eigenvalues of ρ and ρ_2 and compute the von Neumann entropy.

In addition to von Neumann entropy, there is another notion of entropy often used. This is referred to as ‘relative entropy’. For two density operators ρ and σ , it is defined as:

$$S_b(\rho||\sigma) = \text{Tr}(\rho \log_b(\rho) - \rho \log_b(\sigma)) \quad (3.42)$$

3.3.2 Entangled mixed states

The von Neumann entropy is not a good measure when we deal with entanglement in mixed quantum states. We say a ‘mixed state’ is entangled if it cannot be represented by any mixture of pure states. Unlike the case for pure entangled case, there exists majorly three different definitions of entanglement. These are entanglement of formation (EOF), distillable entanglement (DE), and relative entropy of entanglement (REE)[33, 34]. For example, these definitions have distinguishing features. If we consider EOF of a density matrix, it is zero iff (if and only if) ρ can be written as a mixture of product states while DE can still be non-zero for this. We will consider only entanglement of formation in this article. The computation of entanglement of formation for a mixed bipartite state ($\rho_{AB} = \sum_j p_j |\Phi_j\rangle \langle \Phi_j|$) is given by:

$$E_f(\rho_{AB}) = \min. \sum_j p_j E(\Phi_j), \quad (3.43)$$

where the minimum is taken over all pure state decomposition of ρ_{AB} . In addition to EOF, there is another quantitative measure of entanglement known as ‘concurrence’. The entanglement of formation is closely related to another quantity, concurrence (C) through the following relation [35]:

$$E_f(C) = h\left(\frac{1 + \sqrt{1 - C^2}}{2}\right), \quad (3.44)$$

where h is defined as $-x \log_2(x) - (1 - x) \log_2(1 - x)$. In the appendix, we compute this quantity using QISKIT for the interested reader. These computations can also be done using MATHEMATICA and we give a brief sample code using [QI Mathematica package](#) in the Appendix. Alternatively, one can also use the [QuantumFramework](#) package from Wolfram.

► QUESTION 12: Using MATHEMATICA and the package mentioned above, answer the following:

- Pick two random density matrices and compute the relative entropy (as defined in 3.42) between them?

- Consider a density matrix given by:

$$\rho = \begin{pmatrix} 5/12 & 1/6 & 1/6 \\ 1/6 & 1/6 & 1/6 \\ 1/16 & 1/6 & 5/12 \end{pmatrix}. \quad (3.45)$$

Is this a pure or mixed state? Compute the von Neumann entropy.

- Create a random density matrix and compute the von Neumann entropy. Do this several times.

3.4 Quantum Fourier Transform (QFT)

The effectiveness of QFT²⁴ was emphasized in a 1994 paper [36] which eventually was used in Shor's factoring algorithm.

$$\begin{aligned} \text{QFT} |x\rangle &= \frac{1}{\sqrt{2}} \left(\sum_{y=0}^{N-1} e^{2\pi i x y / N} |y\rangle \right) \\ &= \frac{1}{\sqrt{2}} \left(e^{2\pi i x \cdot 0 / 2} |0\rangle + e^{2\pi i x \cdot 1 / 2} |1\rangle \right) \\ &= \frac{1}{\sqrt{2}} \left(|0\rangle + e^{i\pi x} |1\rangle \right). \end{aligned}$$

It is easy to check that $\text{QFT} |0\rangle = |+\rangle$ and $\text{QFT} |1\rangle = |-\rangle$. Hence, QFT on a single qubit is just like Hadamard gate. Now let us consider that $\{0, 1, \dots, N-1\}$ forms an orthonormal basis and let $|\alpha\rangle = \sum_{j=0}^{N-1} |j\rangle$ denote a state with $N = 2^n$ for n qubits. Then QFT transforms the state as:

$$|\alpha\rangle = \sum_{j=0}^{N-1} |j\rangle \rightarrow \sum_{j=0}^{N-1} \frac{1}{\sqrt{N}} \sum_{k=0}^{N-1} \gamma^{-jk} |k\rangle \quad (3.46)$$

where $\gamma = e^{-i2\pi/N}$. Therefore, we have a representation for the QFT as:

$$Q_N = \frac{1}{\sqrt{N}} \sum_{j,k} \gamma^{-jk} |k\rangle \langle j| \quad (3.47)$$

► QUESTION 13: Show that quantum Fourier transform defined by (3.47) is a unitary operation.

²⁴We understand that this acronym might be unsuited for field theorists

To see a more general working of QFT, let us assume that $|x\rangle = |x_1\rangle \otimes |x_2\rangle \otimes \cdots \otimes |x_N\rangle$, then if we perform quantum Fourier transformation on this, we get:

$$\begin{aligned}
\text{QFT } |x\rangle &= \frac{1}{\sqrt{N}} \sum_{y=0}^{N-1} e^{2\pi i x y / N} |y\rangle \\
&= \frac{1}{\sqrt{N}} \sum_{y=0}^{N-1} e^{2\pi i x \sum_{k=1}^n y_k / 2^k} \\
&= \frac{1}{\sqrt{N}} \sum_{y=0}^{N-1} \prod_{k=1}^n e^{\frac{2\pi i x y_k}{2^k}} |y_1 y_2 \dots y_n\rangle \\
&= \frac{1}{\sqrt{N}} \sum_{y_1=0}^1 \sum_{y_2=0}^1 \cdots \sum_{y_n=0}^1 \prod_{k=1}^n e^{\frac{2\pi i x y_k}{2^k}} |y_1 y_2 \dots y_n\rangle \\
&= \frac{1}{\sqrt{N}} \left(|0\rangle + e^{\frac{2\pi i x}{2^1}} |1\rangle \right) \otimes \left(|0\rangle + e^{\frac{2\pi i x}{2^2}} |1\rangle \right) \otimes \cdots \otimes \left(|0\rangle + e^{\frac{2\pi i x}{2^n}} |1\rangle \right) \quad (3.48)
\end{aligned}$$

We can see that at the qubit level, it maps each of them as: $|x_k\rangle \rightarrow \frac{1}{\sqrt{2}} \left(e^{\frac{2\pi i x \cdot 0}{2^k}} |0\rangle + e^{\frac{2\pi i x \cdot 1}{2^k}} |1\rangle \right) = \frac{1}{\sqrt{2}} \left(|0\rangle + e^{\frac{2\pi i x}{2^k}} |1\rangle \right)$. The complexity of QFT is $\mathcal{O}(n^2)$ where n is the number of qubits.

3.5 Quantum rules and limitations

Since quantum gates implement the principles of quantum mechanics, they are reversible and unitary. The fact that gates are reversible is clear by noting that they have the same number of inputs and outputs. This is not so in classical logic gates like AND, NOR, where there is a single output and the input cannot be created by examining the output. We will now mention several rules and ‘no-go’ theorems which are exclusively quantum in nature. These are important ingredients of the remainder of this article. There are several features of quantum computation that makes it much more interesting than classical counterpart. One of these is the property that arbitrary (unknown) quantum states cannot be cloned. This is known as ‘no-cloning’ theorem [37, 38] It is a simple theorem that has far-reaching consequences. In fact, there is also a reverse theorem known as ‘no-deleting theorem’ [39]. This is also a no-go theorem, which states that given two copies of some arbitrary quantum state, it is impossible to delete one of the copies. It is a time-reversed dual of the no-cloning theorem. These theorems follow from the linearity of quantum mechanics. The no-cloning theorem makes the theory of quantum error correction (discussed later) highly non-trivial since this means that to correct quantum errors due to computation, we cannot simply make backup copies of the quantum state we would like to preserve. Instead, we must protect the original from any likely error for as long as we can.

► **QUESTION 14:** The process of cloning means that there is a unitary transformation U such that $U |\psi\rangle |0\rangle \rightarrow |\psi\rangle |\psi\rangle$. Show that this is not possible for an arbitrary state.

The proof proceeds as follows. Lets take two cases where $|\psi\rangle = |0\rangle$ and $|\psi\rangle = |1\rangle$, then we have $U|10\rangle = |11\rangle$ and $U|00\rangle = |00\rangle$ respectively. By linearity we can write:

$$U\left(\frac{|00\rangle + |10\rangle}{\sqrt{2}}\right) = \frac{1}{\sqrt{2}}\left(|00\rangle + |11\rangle\right),$$

which is equivalent to:

$$U\left(\frac{|0\rangle + |1\rangle}{\sqrt{2}}\right)|0\rangle = \frac{1}{\sqrt{2}}\left(|00\rangle + |11\rangle\right), \quad (3.49)$$

but the left hand side of (3.49) is (by the definition of the U operator):

$$\left(\frac{|0\rangle + |1\rangle}{\sqrt{2}}\right)\left(\frac{|0\rangle + |1\rangle}{\sqrt{2}}\right)$$

and hence we have a contradiction, i.e.,

$$\left(\frac{|0\rangle + |1\rangle}{\sqrt{2}}\right)\left(\frac{|0\rangle + |1\rangle}{\sqrt{2}}\right) \neq \frac{1}{\sqrt{2}}\left(|00\rangle + |11\rangle\right). \quad (3.50)$$

Hence, there cannot be a general U operator which can clone an arbitrary state. Note that there are some cases where the theorem doesn't apply, which is often a source of confusion. The 'no-cloning' theorem does not apply in two cases. The first is if we have the knowledge of how the state was prepared and the second is with reference to classical information. Suppose we have states spanned by orthonormal basis (for example, using CNOT gate, we can do $|a\rangle \otimes |b\rangle \rightarrow |a\rangle \otimes |a \oplus b\rangle$ and setting $b = 0$ gives $|a\rangle \otimes |0\rangle \rightarrow |a\rangle \otimes |b\rangle$, so we can clone a bit alone.

Now we talk about another theorem which states that it is impossible to distinguish non-orthogonal quantum states. The 'non-distinguishable' theorem can be proved by contradiction as well. Let us suppose that there is a measurement operator M which has eigenvalues m_i and has projection operators P_i of some observable and that it allows us to distinguish between two non-orthogonal states $|\psi_1\rangle$ and $|\psi_2\rangle$ with $\langle\psi_1|\psi_2\rangle \neq 0$. Then we can write for some state $|\chi\rangle$ orthogonal to $|\psi_1\rangle$:

$$|\psi_2\rangle = \alpha|\psi_1\rangle + \beta|\chi\rangle \quad (3.51)$$

It is easy to show that $P_2|\psi_1\rangle = 0$ and,

$$1 = \langle\psi_2|P_2|\psi_2\rangle = \langle\psi_2|P_2P_2|\psi_2\rangle = |\beta|^2\langle\chi|P_2|\chi\rangle \leq |\beta|^2. \quad (3.52)$$

The last inequality follows from the completeness property. This implies $|\beta|^2 = 1$ which means that $\langle\psi_1|\psi_2\rangle = 0$ which is contradiction. So, it is impossible to unambiguously differentiate between non-orthogonal quantum states.

Towards Quantum algorithms

One major area of present research in quantum computing is building algorithms (quantum) that have substantial speedup²⁵ compared to its fastest known classical counterpart. This area of research is probably the most interesting and difficult. After close to three to four decades of effort, we only have a handful of algorithms that demonstrate a clear advantage over classical algorithms. By quantum algorithm, we mean a sequence of unitary steps that manipulate the initial state $|i\rangle$ such that a measurement of the final state $|f\rangle$ provides the desired solution. In this section, we will focus on some well-known algorithms and later show how they can be implemented in QISKIT. We will start with probably the simplest of algorithms and one we are well familiar with from an undergraduate course in conventional electronics, i.e., full-adder.

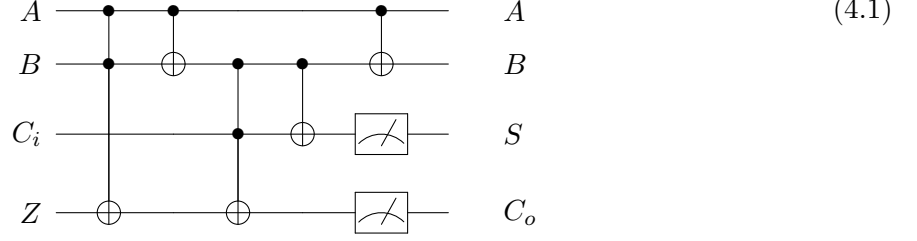
4.1 Full-adder

The addition of classical bits using adder circuits is one of the first things one learns in the undergraduate digital electronics course. We will not provide a recap here, but interested readers can refer to the classic textbook by Malvino and Leach [40]. The quantum full-adder is similar to the classical full-adder except that now we have an identical number of inputs and outputs because we need quantum circuits to be reversible. Therefore, we define a 4-qubit input, where the input qubits are A , B , C_i (Carry in) and null (Z). The output qubits are A , B , S (Sum) and C_o (Carry out). The table will be:

A	B	C_i	Z	C_o	S	A	B
0	0	0	0	0	0	0	0
0	0	1	0	0	1	0	0
0	1	0	0	0	1	0	1
0	1	1	0	1	0	0	1
1	0	0	0	0	1	1	0
1	0	1	0	1	0	1	0
1	1	0	0	1	0	1	1
1	1	1	0	1	1	1	1

²⁵In simple terms, the speedup depends on how much quantum mechanics is available.

Once we have prepared the inputs A and B it can be fed to the quantum circuit which will implement the full-adder. The circuit is given below:



The implementation of this circuit using QISKIT is given in the Appendix, and we test this for some input from the truth table mentioned above.

4.2 Phase kickback

One of the main ingredients for several quantum algorithms is the idea of - ‘phase kickback’. Consider the transformation: $U|\psi\rangle = e^{i2\pi\phi}|\psi\rangle$. For the case where U acts on more than one qubit, we might need more ancillas. We consider two qubits to convey this example. The three parts of this procedure can be summed as follows, 1) An extra qubit which is known as ancilla (control) qubit, 2) Performing Hadamard transform on control qubit(s), and 3) Perform controlled-unitary operation (c-U). It is straightforward to see that the final state will be:

$$\frac{1}{\sqrt{2}} \left(|0\rangle + e^{i\phi} |1\rangle \right) |1\rangle, \quad (4.2)$$

where we note that controlled-U acts like $U|u\rangle = e^{i2\pi\phi}|u\rangle$. The phase has been kicked back. This is what we set out to do, i.e., getting a phase rotation to our control qubit whereas the phase rotation gate was applied to the bottom qubit. This is different to the common belief that the control bit mostly remains the same and the controlled (target) bit transforms. This is the reason this procedure is called ‘phase kickback’. We can do higher powers of U to proceed in the same manner. So, if we instead do, U^{2^k} then we will obtain a phase of $e^{i2\pi 2^k \phi}$ kicked back. The QISKIT implementation of this algorithm is straightforward, and we do this in the Appendix for the interested reader. Note that sometimes we cannot obtain the exact answer. For example, if we implement the code in the Appendix for $\theta = 2\pi/3$, we expect to obtain ~ 0.3333 but indeed get output either to be 0.25 or 0.375. This is part of the algorithm, and it is known that any exact answer will only be obtained with some probability p . However, we can always increase the number of qubits to get a more precise answer.

4.3 Deutsch-Jozsa Algorithm

The first quantum algorithm which showed a speedup over classical algorithm was proposed by Deutsch and later generalized to n -qubits by Deutsch and Jozsa (DJ) in 1992 [41] and further improved by Cleve et al. [42]. We note that this doesn’t really solve a real problem but is just

an example of explicitly showing the quantum advantage. This algorithm makes use of Fourier transform like several other quantum algorithms such as Simon's algorithm (which we do not discuss in these notes) and several others. All these developments eventually led to Shor's algorithm - the most famous quantum algorithm today. We will first explain the Deutsch's algorithm and leave the generalization for the reader to explore from other excellent textbooks and notes available. In simple terms, the statement of the problem is: Suppose we have two boxes and each contains either a red or blue ball inside. We would like to know whether two boxes have the same colored ball. Mathematically, consider the Boolean function $f : \{0, 1\} \rightarrow \{0, 1\}$, then the problem is to find whether $f(0) = f(1)$ or $f(0) \neq f(1)$. We consider the oracle (or black box): $U_f |x, y\rangle = |x, y \oplus f(x)\rangle$ with $x, y \in \{0, 1\}$

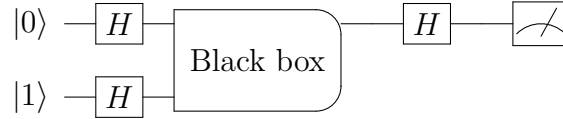


Figure 8. Circuit implementing the Deutsch algorithm.

In this case, the same color means that the function is constant while a different result implies it is balanced. So, $f(0) \oplus f(1) = 0$ if $f(0) = f(1)$ and 1 otherwise. The sequence of steps as given in the circuit diagram are summarized below:

$$|0, 1\rangle \xrightarrow{H \otimes H} |+, -\rangle = \frac{1}{\sqrt{2}}(|0\rangle + |1\rangle) \otimes |-\rangle, \quad (4.3)$$

$$\xrightarrow{U_f} \left[\frac{1}{\sqrt{2}}(-1)^{f(0)}|0\rangle + \frac{1}{\sqrt{2}}(-1)^{f(1)}|1\rangle \right] \otimes |-\rangle, \quad (4.4)$$

$$\xrightarrow{H \otimes \mathbb{1}} \frac{1}{2} \left[(-1)^{f(0)} + (-1)^{f(1)} \right] |0, -\rangle + \frac{1}{2} \left[(-1)^{f(0)} - (-1)^{f(1)} \right] |1, -\rangle. \quad (4.5)$$

Hence, if $f(0) = f(1)$, we will measure $\pm |0, -\rangle$ while if $f(0) \neq f(1)$ then we will measure $\pm |1, -\rangle$. Thus, one call to the oracle (i.e., U_f has been used only once above) solves the problem. If we ask how many queries to the oracle must be classically made to determine $f(0) \oplus f(1)$, it is simple to see that we must make two queries. This corresponds to opening both boxes and checking the color of the ball. This algorithm is capable of achieving a speedup to any classical algorithm. This becomes drastic with more qubits. This algorithm can be readily extended to n -qubit and to encourage the reader to generalize this algorithm, we give the circuit diagram as an appetizer below for the DJ algorithm in Fig. 9 below.

We might think what makes the single query to oracle possible? The reason is the parallelism achieved due to rules of quantum mechanics, which enables to perform multiple evaluations simultaneously.

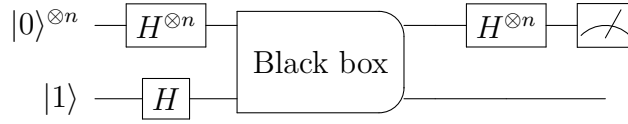


Figure 9. Circuit implementing the DJ algorithm on n -qubits.

► **QUESTION 15:** Apply the DJ algorithm to input $|0\rangle|0\rangle|1\rangle$ with $f(00) = f(01) = 0, f(10) = f(11) = 1$ and write down the output.

4.4 Bernstein-Vazirani algorithm

The Bernstein-Vazirani algorithm is sort of an extension of the Deutsch-Jozsa algorithm discussed above. Its main goal of the algorithm is to show that there can be advantages in using a quantum computer as a computational tool for far more complex problems than those covered by the Deutsch-Jozsa problem. The action of the oracle U_f is $|x\rangle \rightarrow (-1)^{f(x)}|x\rangle$ with $f(x) = x \cdot s$.

The main steps of the algorithm can be summarized below:

- Suppose the n qubit state is given by $|a\rangle$ usually initialized as $|00000 \dots 000\rangle$. We first start by applying $H^{\otimes n}$ i.e.,

$$|a\rangle \xrightarrow{H^{\otimes n}} \frac{1}{2^{n/2}} \sum_{x \in \{0,1\}^n} |x\rangle \quad (4.6)$$

- One now applies the oracle to get:

$$\frac{1}{2^{n/2}} \sum_{x \in \{0,1\}^n} |x\rangle \mapsto \frac{1}{2^{n/2}} \sum_{x \in \{0,1\}^n} (-1)^{f(x)} |x\rangle \quad (4.7)$$

- The second application of $H^{\otimes n}$ then returns:

$$\frac{1}{2^{n/2}} \sum_{x \in \{0,1\}^n} (-1)^{f(x)+x \cdot y} |x\rangle = |s\rangle \quad (4.8)$$

We leave the deduction of final step to get $|s\rangle$ for the interested reader. The similarity between DJ and BV algorithms are: 1) Takes in n qubits and outputs 0 or 1, 2) Use of H gate to examine all superposition states. The difference lies in the evaluation and the initial step. DJ determines whether the function is constant or balanced while BV determines the value of function (and search of string, s).

► **QUESTION 16:** Apply the BV algorithm for the three qubit case to find '011' using QISKIT.

4.5 Grover's algorithm

This quantum algorithm was proposed by Grover for structured searching [43, 44]. The goal of this algorithm is to find the solution to the search problem by making calls to the oracle. Suppose we have a list of $N = 10$ numbers arranged in increasing order from 0 to 9 and the goal is to find 5. On average, it will take $\mathcal{O}(N)$ calls to find this. It was shown by that quantum mechanics can help us solve this problem in $\mathcal{O}(\sqrt{N})$ attempts. This is a polynomial speedup over the classical case and works by a method called ‘amplitude amplification’. We will see later that Shor’s algorithm offers exponential speedup compared to the classical case. This quantum search algorithm consists of repeated application of Grover’s operator G . There are four steps involved in one iteration (applying G once). We list them below:

- Apply the oracle O
- Apply the Hadamard transformation on n qubits denoted by $H^{\otimes n}$
- Perform phase shift unitary operator where every state in computational basis receives a shift. This operator is given by $2|0\rangle\langle 0| - \mathbb{1}$
- Apply the Hadamard again, i.e., $H^{\otimes n}$

The Hadamard transform (where $N = 2^n$) puts the input state in an equal superposition state written as:

$$|\psi\rangle = \frac{1}{\sqrt{N}} \sum_{x=0}^{N-1} |x\rangle. \quad (4.9)$$

Using this, we can write the combined effect of all four steps as:

$$G = H^{\otimes n}(2|0\rangle\langle 0| - \mathbb{1})H^{\otimes n}O = (2|\psi\rangle\langle\psi| - \mathbb{1})O = D \cdot O. \quad (4.10)$$

In short, the oracle operation O reflects the state about $|\psi\rangle$ ²⁶ and then $2|\psi\rangle\langle\psi| - \mathbb{1}$ (also called ‘diffuser’ D) reflects it about $|\psi\rangle$. These are the product of two reflections, and the net result is a rotation. One step of Grover’s iteration can be diagrammatically represented by Fig. 10. We also note that $D = H^{\otimes n}(2|0\rangle\langle 0| - \mathbb{1})H^{\otimes n} = H^{\otimes n}X^{\otimes n}(\text{MCZ})X^{\otimes n}H^{\otimes n}$. Hence, this can be built from H gates, X gates, and single multi-controlled Z gate. We give the code to implement this algorithm using QISKIT in Sec. C.

4.6 Quantum phase estimation (QPE) algorithm

The QPE algorithm introduced by Kitaev is an important quantum computation algorithm. It plays a central role in several other algorithms. The goal of this algorithm is to estimate θ in $U|\psi\rangle = e^{i2\pi\theta}|\psi\rangle$ for a unitary operator U . Since the operator is unitary, all eigenvalues have a norm of unity. There are several steps involved in QPE which we describe below:

²⁶There is also an alternate way of achieving amplitude amplification when the state $|\psi\rangle$ is not known. This is called oblivious amplitude amplification (OAA)

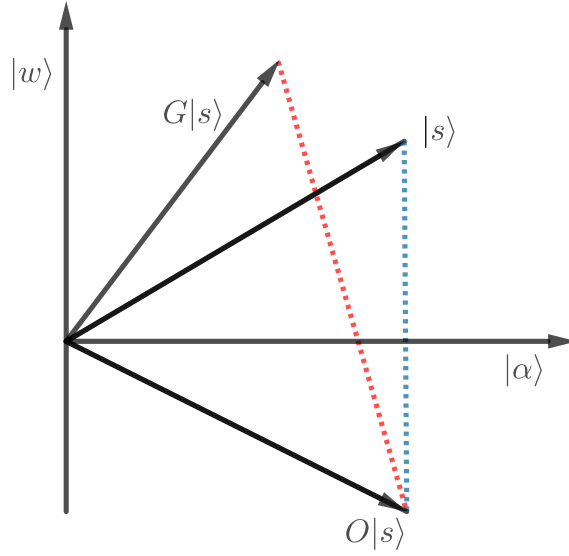


Figure 10. Diagrammatic representation of the Grover's algorithm.

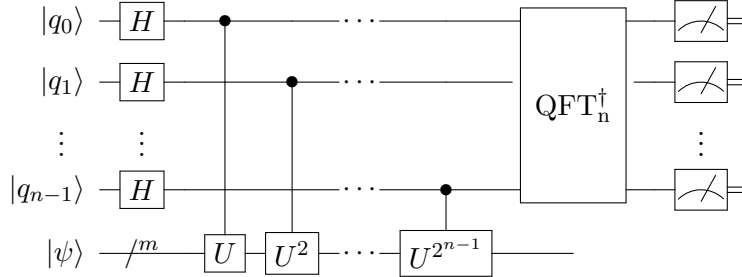
- $|\psi\rangle$ is one set of qubit registers (the one below in the figure) and the other set is n qubits counting (first) register. We have $|\psi_0\rangle = |0\rangle^{\otimes n} |\psi\rangle$
- Apply n -bit Hadamard gate on the first register to get $|\psi_1\rangle = \frac{1}{2^{n/2}}(|0\rangle + |1\rangle)^{\otimes n} |\psi\rangle$
- Apply controlled-U (CU) gate (or rather controlled phase with some θ)²⁷ to get

$$|\psi_2\rangle = \frac{1}{2^{n/2}} \left(|0\rangle + e^{2\pi i \theta 2^{n-1}} |1\rangle \right) \otimes \dots \otimes \left(|0\rangle + e^{2\pi i \theta 2^1} |1\rangle \right) \otimes \left(|0\rangle + e^{2\pi i \theta 2^0} |1\rangle \right) \otimes |\psi\rangle, \quad (4.11)$$

where we note that the rightmost qubit in the first register is $|q_0\rangle$ (see figure)

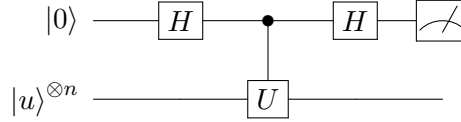
- Apply inverse quantum Fourier transform to get

$$|\psi_3\rangle = \frac{1}{2^{n/2}} \sum_{\alpha=0}^{2^n-1} e^{2\pi i \alpha \theta} |\alpha\rangle \otimes |\psi\rangle \xrightarrow{\text{QFT}_n^{-1}} \frac{1}{2^n} \sum_{x=0}^{2^n-1} \sum_{\alpha=0}^{2^n-1} e^{-\frac{2\pi i \alpha}{2^n} (x-2^n \theta)} |x\rangle \otimes |\psi\rangle \quad (4.12)$$



²⁷Note that this is what we discussed before in ‘phase kickback’

► QUESTION 17: Consider the following circuit (this is Problem 5.3 in Ref. [11]):



where $|u\rangle$ is an eigenstate of U with eigenvalue equal to $e^{i\theta}$. Show that the top qubit is measured to be 0 with probability equal to $\cos^2(\theta/2)$

4.7 Shor's factoring algorithm

One of the central goals of quantum computation is to identify a problem where the quantum offers a significant advantage over classical methods. In this regard, the pioneering work of Ref. [45] showed that it is possible to factor a number using a quantum computer in a polynomial time, unlike the requirement of exponential time with classical computers. This problem is much more interesting than it appears to be at first glance. It is a known fact that multiplying two numbers (say 13 and 73) is much easier than finding prime factors of 949 as it would take more time. This problem is very hard (and sometimes intractable) with large numbers. This was one of the first examples which explicitly showed that quantum algorithms can do exponentially better than classical ones. The factoring algorithm is the flagship result in quantum algorithms of the last three decades. The algorithm efficiently factors a given integer into two integers. For example, we can factor 1,624,637,792,837 into the primes 15,485,867 and 104,911 respectively faster than any classical algorithm. This is a very practical application because in today's world many modern cryptography systems, such as RSA protocol heavily rely upon the fact that factoring such large integers is computationally difficult for any given computer in a reasonable time. However, we are far from practical usage of this algorithm since one would ideally need several thousand qubits to perform such a task and is *well*-beyond the NISQ era. In 2001, it was shown how to successfully factor 15 via Shor's algorithm on a 7-qubit nuclear magnetic resonance (NMR) quantum computer [46]. In fact, a few years ago, it was argued in Ref. [47] that it would take about 8 hours to factor 2048-bit RSA integers using 20 million noisy qubits! We can summarize the algorithm in the following steps:

1. If N is even, return the factor 2 (of course this most likely won't happen!)
2. Check whether $N = a^b$ for integers a, b . Return a as a factor if it is true.
3. Pick a random integer p between 2 and N . If $\gcd(N, p) \neq 1$, we are done and can return the factor. If not, we continue to Step 4 (likely will always happen!).
4. Use an algorithm to find period r such that $a^r \bmod N = 1$
5. If r is even and $a^{r/2} \bmod N \neq -1$, then evaluate $\gcd(a^{r/2} \pm 1, N)$. If we find non-trivial factor, return that value as a factor otherwise we return to Step 3.

Note that Euclid’s algorithm can be used to find $\text{gcd}(\mathbf{a}, \mathbf{b})$ efficiently.²⁸ Let us clarify the step of period finding for the reader. Consider: $a^r = 1(\text{mod } N)$ where r is the smallest positive integer. Now suppose we have, $N = 15, a = 7$ then $r = 4$. This is well-defined only if N and a are co-prime or relatively prime (i.e., they have no common factor except 1). In MATHEMATICA, this can be evaluated by doing: `MultiplicativeOrder[7, 15]`. The fact that finding period can actually help us find prime factorization can be obtained from lemmas that follow from Fermat’s little theorem (1640) i.e., for every a and prime p , we have $a^p = a(\text{mod } p)$. An alternate statement of this theorem is also often mentioned: $a^{p-1} = 1(\text{mod } p)$ where p is prime and a is any integer not divisible by p .

SECTION 5

Variational Quantum Eigensolver (VQE)

One of the main motivations why quantum computing is required is the necessity to simulate complicated quantum many-body systems or solve large scale linear algebra problems. These are very challenging (and sometimes not possible) for classical computers due to the high computational cost involved. Even though quantum computers offer a promise to the solution, the error correction and feasibility are still not well understood. One of the major areas of research with respect to how algorithms can be developed is Variational Quantum Algorithms (VQAs). We refer the interested reader to Ref. [48] to start the reference trail. These algorithms make use of classical optimizer and along with quantum circuits are argued to have a role in wide-ranging areas where quantum computation might be useful in the future. But, in particular, the earliest and well-known of these VQAs is an algorithm that has drawn considerable interest in the last decade. This is known as VQE and makes use of the well-known variational principle to compute the ground state energy of a given Hamiltonian which is important for many problems in quantum chemistry, condensed matter physics, and quantum many-body systems. One of the main advertised advantages of this method is that it can be used to deal with complex wave functions of a wide class of systems in polynomial time when classical methods grow exponentially. Though this method has not yet truly outclassed the classical algorithms, it has incredible potential once we enter beyond NISQ era. This algorithm has well-known drawbacks since this is a non-linear optimization problem. We refer the interested reader to Ref. [49] for references. The Variational Quantum Eigensolver (VQE) was originally developed in Ref. [50] and is among the most promising examples of NISQ algorithms. It aims to compute an upper bound for the ground state energy of some given Hamiltonian. VQE is a hybrid (mixture of classical and quantum) algorithm which can be implemented on NISQ

²⁸In his book, ‘The Art of Computer Programming, Vol. 2: Seminumerical Algorithms’, Knuth comments that this algorithm is the granddaddy of all algorithms because it is the oldest nontrivial algorithm that has survived to the present day. It was written down by Euclid circa 300 B.C.

devices and used to obtain the ground state of the quantum many-body of given Hamiltonian \mathcal{H} using some ansatz. The basic steps of the algorithm are as follows:

1. Prepare an initial quantum state $|0\rangle$ on a quantum computer.
2. Generate a good ansatz quantum state $|\Psi(\Theta)\rangle$ by applying a suitable unitary transformation (quantum circuit composed of quantum gates) as $|\Psi(\Theta)\rangle = \hat{U}(\Theta) |0\rangle$
3. The energy expectation value is measured on a quantum computer as $E_\Theta = \langle \Psi(\Theta) | \mathcal{H} | \Psi(\Theta) \rangle$ by measuring each Pauli string separately and then summing the individual terms.
4. Update the parameters Θ to get smaller energy $E(\Theta)$ by using a classical optimizing algorithm.
5. Repeat steps 2-5 until desired convergence is attained.

Within VQE, the cost function is defined as the expectation value of the Hamiltonian computed in the trial state. The ground state of the target Hamiltonian is obtained by performing an iterative minimization of the cost function. The optimization is carried out by a classical optimizer, which leverages a quantum computer to evaluate the cost function and calculate its gradient at each optimization step. The local optimization within the vector space generated by ansatz can suffer due to the problem of vanishing gradients. This can often result in a phenomenon known as ‘barren plateaus’ [51] which are a well-known issue in VQE computations but there have been some proposed methods to overcome this issue [52]. A detailed discussion is beyond the scope of this article.

The choice of ansatz is usually determined by hardware availability (known as hardware-efficient ansatz) and efficiency of considering qubits as logical qubits.²⁹ We refer the interested reader to Ref. [53] for an elaborate discussion on hardware-efficient trial states. The VQE that accompanies QISKIT comes with some given choices such as RX, RYRZ, $SU(2)$ etc. with some user-defined number of repetitions. To measure the energy expectation value in the third step above, we must have a qubit Hamiltonian of size $2^n \times 2^n$. This is usually not an easy task, however, this can be simplified considerably by writing the original Hamiltonian in terms of the sum of Pauli operators (X,Y,Z, $\mathbb{1}$) and their tensor products. However, not all Hamiltonians (even though they are sparse) admit an efficient Pauli representation. For these kind of systems, alternate methods have also been proposed [54]. This can also be understood as the first step even before doing any computation and has to be done only once. The choice of the right optimization method is crucial for the problem. We can choose from a range of methods such as BFGS (Broyden–Fletcher–Goldfarb–Shanno) optimizer method, COBYLA³⁰(Constrained Optimization By Linear Approximation optimizer),

²⁹Usually when we have qubits, they are prone to errors and can make computation incorrect. We want qubits that are ideal or at least not prone to many errors, they are known as ‘logical qubits’. The problem is that usually for every logical qubit we need multiple physical qubits which can sometimes be hundreds of them.

³⁰Note that this is non-gradient based optimization, we do not need to know the derivative

SLSQP (Sequential Least Squares Programming optimizer), Nelder-Mead or any other depending on the requirement and efficiency required. For example, another example of a local optimizer in QISKIT is Powell method, which performs unconstrained optimization; it ignores bounds or constraints and is a conjugate direction method. More details can be found in Ref.[55]. Another interesting method to construct the ground state of an interacting Hamiltonian is the adiabatic state preparation (ASP) method. It works reasonably well when there is no level crossing (i.e., the excited state of the Hamiltonian do not cross each other and ground state). Recently, there have been some interesting work combining the ideas of VQE approach and ASP approach [56].

When we deal with physical systems, we can often express a given Hamiltonian as the linear combination of the tensor product of Pauli matrices σ_x , σ_y , and σ_z which we call ‘Pauli strings’ i.e., $\hat{P} = \otimes_{i=1}^n \hat{\Sigma}$ where $\hat{\Sigma} = \{\sigma_x, \sigma_y, \sigma_z, \mathbb{1}\}$. Note that as the Pauli strings form a complete basis, any Hamiltonian of size $2^N \times 2^N$ can be decomposed into a linear combination of Pauli strings. For example, let us consider the Hamiltonian of some system to be given by:

$$H = \begin{pmatrix} \frac{1}{2} & 0 & -\frac{i}{2} & 0 & 0 & 0 & 0 & -\frac{1}{2} - \frac{i}{2} \\ 0 & \frac{1}{2} & 0 & \frac{i}{2} & 0 & 0 & -\frac{1}{2} + \frac{i}{2} & 0 \\ \frac{i}{2} & 0 & \frac{1}{2} & 0 & 0 & -\frac{1}{2} + \frac{i}{2} & 0 & 0 \\ 0 & -\frac{i}{2} & 0 & \frac{1}{2} & -\frac{1}{2} - \frac{i}{2} & 0 & 0 & 0 \\ 0 & 0 & 0 & -\frac{1}{2} + \frac{i}{2} & \frac{1}{2} & 0 & \frac{i}{2} & 0 \\ 0 & 0 & -\frac{1}{2} - \frac{i}{2} & 0 & 0 & \frac{1}{2} & 0 & -\frac{i}{2} \\ 0 & -\frac{1}{2} - \frac{i}{2} & 0 & 0 & -\frac{i}{2} & 0 & \frac{1}{2} & 0 \\ -\frac{1}{2} + \frac{i}{2} & 0 & 0 & 0 & 0 & \frac{i}{2} & 0 & \frac{1}{2} \end{pmatrix}$$

which can be written in terms of Pauli operators as: $H = \frac{1}{2}(\sigma_z \otimes \sigma_y \otimes \sigma_z - \sigma_x \otimes \sigma_x \otimes \sigma_x - \sigma_y \otimes \sigma_y \otimes \sigma_y + \mathbb{1} \otimes \mathbb{1} \otimes \mathbb{1})$. The program to do this transformation can be found in the subroutine of the VQE program in Sec. C. One of the drawbacks for VQE are handling models for whose Hamiltonian there is no known efficient decomposition in terms of Pauli strings. In such a case, the advantage of VQE is reduced considerably. This is an important question and some work along this direction has already been done. We refer the reader to Ref. [57] for extended discussion.

One important issue with computations in the NISQ-era is the noise associated with the calculation. Strictly speaking, the theory of fault-tolerant quantum computing is still several decades away and hence there is need to understand and mitigate errors in calculations from current era. The quantum error mitigation (QEM) is a technique to understand the errors and reduce them such that we can still draw meaningful conclusions from the computations which otherwise seems just like noise and unphysical. There are several methods developed for QEM. We will mention few methods below and refer the reader to Ref. [58] for extended list.

- Zero noise extrapolation (ZNE): This technique mitigates errors in noisy quantum computations without using additional quantum resources. This is based on understanding how the noise scales and how we can extrapolate to zero noise. In ZNE, a quantum program is deliberately altered to run at different levels of noise from processors.

- **Randomized compilation (RC):** This is a protocol which is constructed to overcome this issue by converting coherent errors into stochastic noise. Randomized compiling makes use of twirling groups while preserving the overall unitarity of the circuit. Pauli twirling is a method which was introduced for the mapping of states into canonical form in entanglement purification studies in the quantum information literature. It was also used in reducing the exponential cost in quantum tomography. In QEM, it is used as a technique to improve the performance on NISQ devices. The nature of noise in quantum systems can be broadly classified as either coherent (unitary) or incoherent. The coherent noise are more dangerous since they accumulate quickly and can lead to worst-case error. One of the most effective methods of dealing with coherent noise/error is to convert them to Pauli errors. For this one often uses ‘Pauli twirling’. Pauli twirling convert error channels to Pauli channels for estimation of error threshold. Precisely, it converts the coherent noise into incoherent Pauli channels by suppressing the off-diagonal terms. In addition, if the twirling is performed with Clifford group, it is called Clifford twirling. This converts the error channels into depolarising channels. In general, any arbitrary channel can be converted to Pauli channel.
- **Learning based error mitigation:** This method was introduced in Ref. [59]. The basic idea of this method is to start with a noisy expectation value $E(\mathbf{P})$ for some primary circuit \mathbf{P} and achieve the noiseless value $E_0(\mathbf{P})$ passing through series of optimizations of the expectation value which depends on some set of parameters $\vec{\theta}$. The optimal choice of $\vec{\theta}$ when obtained through learning-based methods based on temporary circuit \mathbf{T} which is close enough to the primary circuit.

5.1 Quantum Anharmonic Oscillator

We will now discuss how to apply VQE to solve (i.e., find the ground state energy) quantum anharmonic oscillator. This example provides sufficient exposure to the basis working of VQE. This problem was also studied in [60] and we will follow their discussion closely. For the ansatz, we choose **EfficientSU2** circuit from QISKIT circuit library, which is a hardware-efficient, heuristic ansatz with alternating rotation and entanglement layers. Note that it is possible to calculate excited states of a Hamiltonian based on a technique known as variational quantum deflation (VQD) proposed recently in Ref. [61]. Let us write the Hamiltonian as:

$$\hat{H}' = \hat{H} - g\hat{X}^3 - h\hat{X}^4. \quad (5.1)$$

For the cubic oscillator, if we consider three qubits, \hat{H}' is a 8×8 matrix which for $g = 0.02$ is given by:

$$\begin{aligned} \hat{H}' = & 4\mathbb{1}_8 - 0.152956\mathbb{1}_4X - 0.5\mathbb{1}_4Z - 0.12289 * \mathbb{1}XX - 0.0629948\mathbb{1}YY - \mathbb{1}Z\mathbb{1} + 0.0237627\mathbb{1}ZX - 0.0280252X\mathbb{1}X \\ & - 0.0561195XXX + 0.0287333XYY + 0.0107047XZX - 0.0280252Y\mathbb{1}Y - 0.0287333YXY - 0.0561195YYX \\ & + 0.0107047YZY - 2Z\mathbb{1}_4 + 0.0872346Z\mathbb{1}X + 0.0842295ZXX + 0.041655ZYY + 0.0207442ZZX \end{aligned} \quad (5.2)$$

The energy levels for cubic anharmonic oscillator ($h = 0$) which we take as example is known to be:

$$E_n = -\frac{g^2}{8} (30n^2 + 30n + 11) + \mathcal{O}(g^4), \quad (5.3)$$

and the ground state energy level upto $\mathcal{O}(g^6)$ is given by (see Table (3.1) of Ref. [62])

$$E_0 = \frac{1}{2} - \frac{11}{8}g^2 - \frac{465}{32}g^4 - \frac{39709}{128}g^6 \quad (5.4)$$

We provide the code in QISKIT in the Appendix for the interested reader though admittedly it can definitely be improved and optimized of which we have not taken any care except checking that it works. We need to create H matrix for this system which can be done in MATHEMATICA as below³¹ which will be then converted to Pauli string and input to VQE to find E_0 :

```

1  SetDirectory[NotebookDirectory[]];
2  nbits = 3; (* number of qubits *)
3  n = 2^nbits;
4  lattice = Table[(2 a - n - 1)/2, {a, n}]; (* Lattice for position operator *)
5  X = DiagonalMatrix[Sqrt[(2 \[Pi])/n] lattice]; (* Position operator *)
6  F = (1/Sqrt[n]) Table[NExp[(-I 2 \[Pi] lattice[[j]] lattice[[k]])/n], {j, n}, {k, n}]; (*
   Discrete Fourier transform *)
7  P = Chop[F\[ConjugateTranspose] . X . F]; (* Momentum operator *)
8  A = Sqrt[0.5] (X + I P); (* Annihilation operator *)
9  A1 = Table[If[(j - i) == 1, i^.5, 0], {i, n}, {j, n}]; (* Annihilation operator in energy
   (E) basis *)
10 X1 = Sqrt[0.5] (A1\[ConjugateTranspose] + A1); (* Position operator in E basis *)
11 P1 = I Sqrt[0.5] (A1\[ConjugateTranspose] - A1); (* Momentum operator in E basis *)
12 g = 0.02;
13 h = 0.04;
14 H0[X_, P_] := .5 P . P + .5 X . X; (* Harmonic oscillator Hamiltonian *)
15 H1[X_, P_] := .5 P . P + .5 X . X - g MatrixPower[X, 3]; (* cubic anharmonic Hamiltonian *)
16 H2[X_, P_] := .5 P . P + .5 X . X + h MatrixPower[X, 4]; (* quartic anharmonic Hamiltonian *)
17 HOA[A_] := A\[ConjugateTranspose] . A + .5 IdentityMatrix[n]; (* Harmonic oscillator
   Hamiltonian in E basis *)
18 H1A[A_, X_] := HOA[A] - g MatrixPower[X, 3]; (* Cubic anharmonic Hamiltonian in E basis *)
19 H2A[A_, X_] := HOA[A] + h MatrixPower[X, 4]; (* Quartic anharmonic Hamiltonian in E basis *)
20 H = H1A[A1, X1]; (* Make Hamiltonian to export *)
21 hamName = "H0"; (* Set Hamiltonian name for file *)
22 Export["ham_" <> hamName <> ".txt", H, "Table"]; (* Export Hamiltonian to file which would be
   read by our QISKIT program! *)
23

```

In fact, an astute reader might ask: What is the point of doing this VQE computation when I can easily find the ground state energy of an 8×8 Hamiltonian in three lines by doing:

³¹Note that there are other ways to do this, but this is probably the cleanest

```

1 from numpy import linalg as LA
2 w, v = LA.eig(H)
3 print ("Ground state energy", w[0])
4

```

To address this, we note that the interest in VQE algorithms is because for a Hamiltonian of size $2^n \times 2^n$ where n is a large number and H is complicated enough that it is not very sparse like it is in this case, then it will take classical computing/exact diagonalization an exponentially longer time and a large amount of memory. This is often given the name ‘solution does not scale with system size’. However, if it is assisted through VQE (creating quantum state ansatz and optimizing classically) then the growth with n and sparseness of H will be much more efficient (at most polynomials!). It must be noted that VQE has already been able to substantially get close to some gold standard in quantum chemistry, however, the discussion of this lies beyond the scope of this article. We just point out one reference of the computation done in quantum chemistry that was for quantum simulation of the deuteron binding energy on quantum processors such as IBM QX5 (with 16 SC qubits) and Rigetti 19Q (19 SC qubits) [63] which can be used to start a reference trail.

5.2 $O(3)$ non-linear sigma model

We mention another toy model (familiar to most physicists), known as $O(3)$ non-linear sigma model in 1+1-dimensions. This was studied using VQE recently in the Ref. [64] on about 10 lattice sites in the weak and strong coupling limit with a topological $\theta = \pi$ term. The results obtained with two different choices of ansatz showed that VQE does not correctly reproduce the ground state energy for large β and works best for $\beta \ll 1$. The increase in number of parameters to be optimized did not allow the authors to explore VQE for $l_{\max.} > 1/2$. Note that the allowed values of l with $q = 1/2$ which corresponds to $O(3)$ model with $\theta = \pi$ are half-integer values. The eigenbasis is denoted by $|qlm\rangle$ rather than the usual $|lm\rangle$. If $q = \theta = 0$, the l takes integer values starting at 0.

Based on results from classical tensor network computations based on MPS, it is clear that to approach the asymptotic scaling regime where the continuum physics can be extracted, one needs $1.0 < \beta < 1.4$ and it is not possible without including higher charge representations. It would be interesting to study this system with improved hybrid methods like VQE for larger β and find agreement with tensor network results. In this subsection, we will not pursue any ‘quantum’ or hybrid calculations and just show that one can use exact diagonalization (ED)³² to compute the ground state energy for small number of sites in the strong and weak coupling limits. The Hamiltonian of the model is given by:

$$\hat{H} = \frac{1}{2\beta} \sum_i \mathbf{L}_i^2 - \beta \sum_{\langle i,j \rangle} \mathbf{n}_i \cdot \mathbf{n}_j, \quad (5.5)$$

³²We thank Kostas Orginos and Felix Ringer for some discussions related to this

where i and j are the nearest neighbour sites on a spatial line, \mathbf{n} is a unit 3-vector at site i , \mathbf{L} is the angular momentum and β is the coupling.

The dimension of the local on-site Hilbert space is given by $\sum_0^{l_{\max.}} (2l+1)$ which is $d=2$ with $l_{\max.} = 1/2$. Therefore, H will be a 16×16 matrix for $N=4$. We can exactly diagonalize (ED) the Hamiltonian by expressing (5.5) in terms of Pauli matrices and compare to the results from Ref. [64]. We find that for $\beta = 1/10$ and $N=4$, we get $E_0/N = 3.72778$ while for $\beta = 10$, we get $E_0/N = -2.1847$ at fixed truncation of $l_{\max.} = 1/2$ at each site. The result at large β is inaccurate (not close to convergence) since the truncation effects are important. One obtains $E_0/N = -5.62$ if $l_{\max.} = 3/2$ is used with $N=4$ sites with H given by a $6^4 \times 6^4$ matrix. For VQE, we would need to work with 11 qubits for which optimisation might not be straightforward. The code for implementing this with $l_{\max.} = 1/2$ is given below.

```

1  X = {{0, 1}, {1, 0}};
2  Y = {{0, -I}, {I, 0}};
3  Z = {{1, 0}, {0, -1}};
4  Nplus = (X + I Y) ;
5  Nminus = (X - I Y) ;
6  SITES = 4;
7  HH[\[Beta]_, N_] := N (3/(8 \[Beta] )) IdentityMatrix[16] + \[Beta] (KroneckerProduct[Nplus ,
    Nminus, IdentityMatrix[2], IdentityMatrix[2]] + KroneckerProduct[Nminus, Nplus,
    IdentityMatrix[2], IdentityMatrix[2]] + KroneckerProduct[Z , Z, IdentityMatrix[2],
    IdentityMatrix[2]]/9) + \[Beta] (KroneckerProduct[IdentityMatrix[2], Nplus , Nminus,
    IdentityMatrix[2]] + KroneckerProduct[IdentityMatrix[2], Nminus, Nplus,
    IdentityMatrix[2]] + KroneckerProduct[IdentityMatrix[2] , Z, Z, IdentityMatrix[2]]/9) +
    \[Beta] (KroneckerProduct[IdentityMatrix[2], IdentityMatrix[2], Nplus , Nminus ] +
    KroneckerProduct[IdentityMatrix[2], IdentityMatrix[2], Nminus, Nplus] +
    KroneckerProduct[IdentityMatrix[2] , IdentityMatrix[2], Z, Z ]/9) + \[Beta]
    (KroneckerProduct[Nminus, IdentityMatrix[2], IdentityMatrix[2], Nplus ] +
    KroneckerProduct[Nplus, IdentityMatrix[2], IdentityMatrix[2], Nminus] +
    KroneckerProduct[Z, IdentityMatrix[2] , IdentityMatrix[2], Z ]/9);
8  HH[0.1, SITES]/SITES // Eigenvalues // Min // N
9  (* Exercise: Write a general $$ site program. Try ED for 6 sites and compare.*)
10

```

Note that going beyond the $l_{\max.} = 1/2$ is non-trivial. The size of H with $l_{\max.} = 5/2$ will be $12^4 \times 12^4$ and we would need 14-15 qubits to represent it. If we take $\theta = 0$, then the allowed values of l will be $0, \dots, l_{\max.}$ with size of Hamiltonian given by $(l_{\max.} + 1)^{2N} \times (l_{\max.} + 1)^{2N}$ for N -sites.

There is an alternative view to think about quantum computation of this model. Rather than thinking about qubits, we can represent (5.5) in terms of two distinct harmonic oscillators (qumodes) at each site using the Schwinger representation. This representation is straightforward for the kinetic term (since it is just the number operator) but one can also express the nearest-

neighbor interaction term in oscillator basis. The schematic form of the Hamiltonian is:

$$H = \sum_{\langle ij \rangle} f(a_i^\dagger, b_i^\dagger, a_i, b_i) f(a_j^\dagger, b_j^\dagger, a_j, b_j) + \sum_i f(n_i), \quad (5.6)$$

where the two oscillators at each site are denoted by a, b and $n_i = a_i^\dagger a_i + b_i^\dagger b_i$. The Hamiltonian of this model has some similarity to the Bose-Hubbard for which mapping from bosonic infinite-dimensional Hilbert space to qubits have been developed [65, 66]. In addition to the 1+1-dimensional $O(3)$ model, the (hybrid) quantum algorithms have also been applied to other models (one spatial dimension) such as two-flavor Gross-Neveu model [67] and to Schwinger model [68]. It will be interesting to understand these models from the perspective of a continuous variable (bosonic) quantum computing methods and some work along these lines have already been done using Xanadu's simulator [69] where the ground state energy for scalar field theory was computed using the quantum imaginary time evolution (QITE) algorithm proposed with and without use of ansatzes in Refs. [70, 71].

SECTION 6

Quantum Error Correction (QEC)

Quantum computers often offer drastic speedup to solutions of certain types of problems by using principles of quantum mechanics such as: superposition and entanglement. However, the use of qubits in place of classical bits also makes the quantum computer susceptible to errors unlike anything we know in classical computers. The origin of these errors is primarily due to decoherence - a process in which the environment interacts with the qubits and changes the quantum states, which eventually leads to corrupted results. For example, the failure rate is about one error in 10^{17} operations for classical computers, which for quantum computers is much severe. This partly makes the theory of quantum error correction more subtle than classical counterpart, in addition to several reasons below:

- The act of measurement or observation in quantum mechanics destroys the quantum state and makes its recovery impossible. For example, if we have a superposition state, and we perform a measurement, we lose the superposition by choosing one outcome.
- No-cloning theorem prohibits the copying of any arbitrary quantum state, and this means that repetition code obtained by just duplicating the bit will not work.
- Unlike classical bit, qubit is continuous valued and hence we need infinite precision to locate the error exactly in order to correct it.

The goal of the quantum error-correcting (QEC) code is to protect some subspace of the entire Hilbert space \mathcal{H} from some errors. More precisely, suppose we want to preserve a k -dimensional

subspace (coding space) against some known errors. This is achieved by mapping the states into a larger, n -dimensional Hilbert space. In that case, we can refer to it as the (n, k) -quantum code. Sometimes, an alternate definition is also used, where by $[n, k, d]$ we denote a quantum error-correcting code that uses n qubits to encode k qubits with distance d . There is a well-known Knill-Laflamme theorem [72] for the conditions of quantum error correction. It is stated as follows: Let \mathcal{C} be a quantum-error correcting code defined as a subspace of the n -dimensional Hilbert space, $\mathcal{H}_2^{\otimes n}$, and let $\mathcal{E} \subset \mathfrak{C}^{2^n \times 2^n}$ be a set of errors. Then \mathcal{C} can correct \mathcal{E} if and only if

$$\langle \psi_i | E_a^\dagger E_b | \psi_j \rangle = c_{ab} \delta_{ij}, \quad (6.1)$$

where $|\psi_i\rangle$ is a base of the subspace that defines the code $\mathcal{C} \subset \mathcal{H}_2^{\otimes n}$ and $E_a, E_b \in \mathcal{E}$. Equivalently, we can also express the above statement as: Let C be a quantum code and let P be a projector onto C . Suppose a list of operation elements is represented by $\{E_i\}$. Then, a necessary and sufficient condition for the error-correcting scheme correcting error on C is:

$$PE_i^\dagger E_j P = \alpha_{ij} P, \quad (6.2)$$

for some Hermitian matrix α_{ij} . A quantum error-correcting code is a pair (C, R) consisting of a quantum code and a recovery operator. We will see one example (the Shor's nine-qubit code) for error correction toward the end of this section. In order to implement QEC, one would like to know which gate set are sufficient. The answer to this is given by the Rains-Solovay theorem.³³ It states that: The Clifford group (denoted below by C) together with any gate not in this group is universal for quantum computation. However, there are some combinations that are most frequently used and proven to be universal. Such examples are $\{C + \text{CCNOT}\}$, $\{C + \pi/8\}$, and $\{C + \text{controlled} - \pi/4\}$.

In 1995, Shor [73] discussed a way to reduce the rate of decoherence in quantum memory and hence paved the way for the practical usage of quantum computers. This work led to a lot of interesting developments in the field of 'quantum error correction'. This was a remarkable result since it implied that a quantum state even though it cannot be cloned due to the 'no-cloning' theorem can be protected in a noisy environment. One would at this point think - why do we need to correct errors at all? The error correction in quantum computers is more delicate than classical errors. This is partly because error correction is needed to protect the quantum superposition and entanglement, both of which are crucial ingredients of any quantum computation. In the original work, Shor proposed to store the quantum information not in a single qubit, but it was later shown that it can be reduced to five, which is the minimum required [74].

6.1 Bit-flip error

Bit flip is defined when we have $|0\rangle \rightarrow |1\rangle$ or vice versa. Suppose we are interested in sending out a single qubit $|\psi\rangle = \alpha|0\rangle + \beta|1\rangle$ through during which a flip i.e., $X|\psi\rangle = \beta|0\rangle + \alpha|1\rangle$ can

³³This theorem is not often referred to by this name, we call it this following the discussion at: <https://cstheory.stackexchange.com/questions/11308/universal-sets-of-gates-for-su3>

occur with some probability p . Such a process is referred to as ‘bit-flip’. One way to correct this is to do repetition as follows of the classical bit $|0\rangle_L \rightarrow |000\rangle$, where we mean logical qubit by subscript L . Assuming that the probability of bit-flip as p , we can show that the total probability of error persisting (i.e., remaining uncorrected or wrongly corrected) is $3p^2(1-p) + p^3 = 3p^2 - 2p^3$.

► QUESTION 18: Compute the minimum fidelity attained by the three-qubit bit flip?

The circuit to correct bit-flip is given by: For the example, we will take E_{bit} to be a X gate for

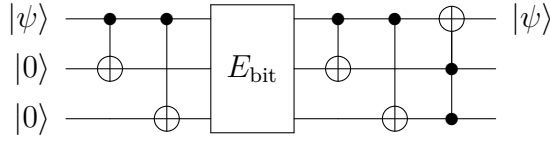


Figure 11. Bit flip circuit

now. We have $Z = |0\rangle\langle 0| - |1\rangle\langle 1|$

$$Z_1 Z_2 \mathbb{1} = \left(|00\rangle\langle 00| + |11\rangle\langle 11| \right) \otimes \mathbb{1} - \left(|01\rangle\langle 01| + |10\rangle\langle 10| \right) \otimes \mathbb{1} \quad (6.3)$$

If both first and second qubit are same, we get +1 or -1 if they are different. Similarly, we can compute $Z_2 Z_3$. Then assuming that there is a single bit flip, we can deduce the following table.

$Z_1 Z_2$	$Z_2 Z_3$	Which bit flipped?
+1	+1	None ($\mathbb{1}$)
+1	-1	Third (X_3)
-1	+1	First (X_1)
-1	-1	Second (X_2)

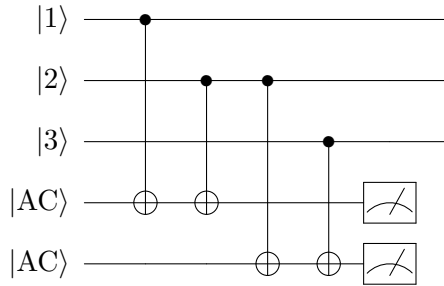


Figure 12. A circuit to identify the bit flip with two ancillary bits. This is the error-detection part of the bit flip code. This is followed by a recovery procedure.

This step detected the error. Now, in the recovery step, one simply applies X gate on the flipped bit to complete the error correction process. One important thing is that these measurements (ZZ) do not spoil the superposition of quantum states that we wish to preserve since they

never give any information about a, b (amplitudes). The bit flip code is similar in spirit to the classical error-correcting codes. One more advanced code is the ‘phase-flip’ code which has no classical counterpart and hence is more interesting as a quantum code. But note that there are ways to describe ‘phase-flip’ into ‘bit-flip’. We can always go from ‘quantum’ to ‘classical’ but not the other way around!

6.2 Phase-flip error

We now discuss another error that can occur. Instead of the operator X which was applied to the bit flip case, consider now the action of Z operator. Then the state $a|0\rangle + b|1\rangle$ is transformed to $a|0\rangle - b|1\rangle$. Now suppose we rather work in the basis $|\pm\rangle$, then $Z|+\rangle \rightarrow |-\rangle$. Hence, phase flip is like bit flip in a different basis! This presents itself that all the basic parts of the error correction i.e., encoding, error-detection, and recovery can be applied as bit flip code. The encoding circuit for bit flip will then be:

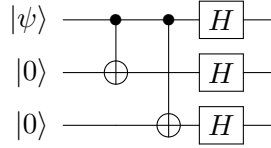


Figure 13. Circuit to encode the phase flip code.

6.3 Shor’s nine qubit code

Though it is nice to correct the bit and phase flip separately, one desires a code to correct any arbitrary error using a single code. The ability to correct arbitrary errors on a *single* qubit can be achieved by Shor’s nine-qubit code and is shown in Fig. 14. The basic step of Shor’s construction

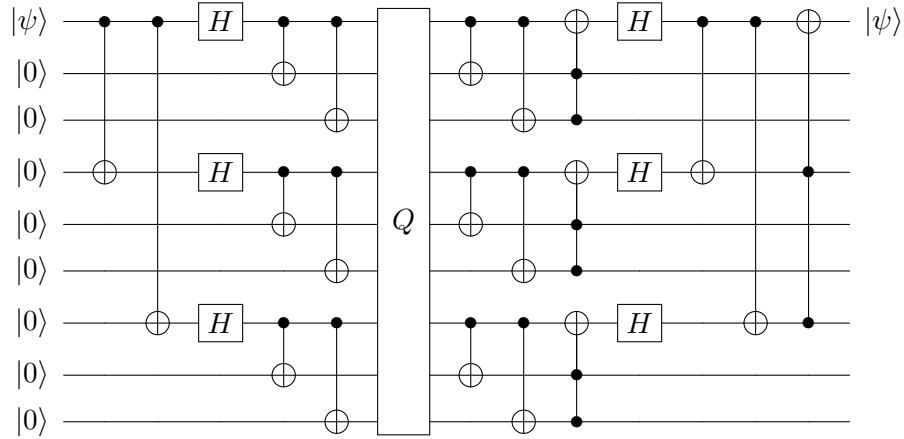


Figure 14. The circuit to implement Shor’s code where Q is a channel which can corrupt single qubit.

is to note that:

$$|0\rangle = |0\rangle_L = |+++ \rangle, \quad (6.4)$$

$$|1\rangle = |1\rangle_L = |-- - \rangle, \quad (6.5)$$

will control the phase errors, while,

$$|+\rangle = \frac{1}{\sqrt{2}}(|000\rangle + |111\rangle), \quad (6.6)$$

$$|-\rangle = \frac{1}{\sqrt{2}}(|000\rangle - |111\rangle), \quad (6.7)$$

will correct against the bit flip error. Combining these two, we can write:

$$|0\rangle \rightarrow \frac{1}{2\sqrt{2}}(|000\rangle + |111\rangle) \otimes (|000\rangle + |111\rangle) \otimes (|000\rangle + |111\rangle). \quad (6.8)$$

Suppose the error is modelled by a unitary transformation U such that:

$$U = c_0\mathbb{I} + c_1X + c_2Y + c_3Z \quad (6.9)$$

Now, if U is equal to \mathbb{I} , then no error has occurred. If $U = X$, then a bit flip occurs, if $U = Z$ then a phase flip occurs. Lastly, if $U = iY$ then both a bit flip error and a sign flip error occur.

► **QUESTION 19:** Show that if the probability of a single qubit being affected (either phase or bit flip or mixture of the two) is p , then the probability of having more than one qubit having an error in Shor's nine qubit code is $36p^2$.

The quantum error-correcting conditions are a set of equations which have to be satisfied by a quantum error-correcting code to protect against a particular type of noise. In the next paragraph, we will see what the stabilizer set is for Shor's code. But before this, we need to define the definition of a stabilizer of a state. We say that a unitary, U , stabilizes a pure state $|\psi\rangle$ if $U|\psi\rangle = |\psi\rangle$. Note that the phase is important and if we have $U|\psi\rangle = -|\psi\rangle$, then it does not stabilize.

► **QUESTION 20:** Show that $\{II, XX, -YY, ZZ\}$ forms a stabilizer group for the Bell state given by $(|00\rangle + |11\rangle)/\sqrt{2}$.

Now, we do a short example that will clarify this further. Suppose we are asked whether the three-qubit phase flip code $|0_L\rangle = |+++ \rangle$, $|1_L\rangle = |-- - \rangle$. satisfied the conditions for the set of error operators $\{I, Z_1, Z_2, Z_3\}$. The stabilizer set of Shor's code is³⁴:

$$\{Z_1Z_2, Z_2Z_3, Z_4Z_5, Z_5Z_6, Z_7Z_8, Z_8Z_9, X_1X_2X_3X_4X_5X_6, X_4X_5X_6X_7X_8X_9\} \quad (6.10)$$

³⁴Note that $Z_1Z_2 = ZZIIIIII$ or $Z \otimes Z \otimes I_{128}$

The Shor's code provides the window to the more complicated quantum error-correcting (QEC) codes. However, this code is not the most optimal and Steane 7-qubit code [75] is better. This code has six stabilizer generators compared to eight in Shor's code. These are given by:

$$\{IIIXXXX, IXXIIXX, XIXIXIX, IIIZZZZ, IZZIIZZ, ZIZIZIZ\} \quad (6.11)$$

All these QEC codes are best explained by the idea of stabilizer codes. For example, one famous example is the toric code, which is a topological quantum error correcting code and is an example of a stabilizer code/circuit ³⁵. It is defined on a two-dimensional spin-lattice and has \mathbb{Z}_2 topological order. It reduces to a \mathbb{Z}_2 lattice gauge theory well known for decades in an appropriate limit. In this code, the stabilizer operators are defined on the spins around each vertex and on the plaquette and are known as A and B operators defined as: $A_v = \prod_{i \in v} \sigma_i^x$ and $B_p = \prod_{i \in p} \sigma_i^z$ respectively. We often refer to a QEC code as $[[n, k, 2t + 1]]$ code ³⁶ and Shor's code is an example of $[[9, 1, 3]]$ stabilizer code. Sometimes, $2t + 1$ is also called 'distance', and code is referred to as $[[n, k, d]]$ code. Soon after nine-qubit code, Steane found a seven-qubit code that can correct the same error as Shor's code. In fact, both these codes are 'degenerate' which loosely means that it can be further improved. One of the ways we can optimize the code is to introduce the quantum Hamming bound [76]. If a given code uses n qubits, corrects error on up to t qubits and encodes k qubits, then the following inequality holds:

$$\left(\sum_{j=0}^t 3^j \binom{n}{j} \right) 2^k \leq 2^n. \quad (6.12)$$

It is easy to check that with $k = 1, t = 1$, the lower bound is saturated with $n = 5$ hence there exists a 5-qubit code which is $[[5, 1, 3]]$ which is nondegenerate. In general, it is clear that the stabilizer circuits/codes are very important for performing quantum error-correction and play an important role in fault-tolerant circuits. The idea of stabilizer circuits is also important for a theorem known as 'Gottesman-Knill' (GK) theorem [77]. The theorem implies that any stabilizer circuits can be perfectly simulated in polynomial time on a (probabilistic) classical computer. Hence, they offer no quantum advantage by themselves. This theorem originated in Ref. [77] where author refers to private communication with Knill. This result does not explain the reason why quantum computing can provide exponential speedup over classical computing, but it does tell us that quantum algorithms which make use of entanglement built using Hadamard and CNOT gates do not offer any advantage. This result is contrary to the natural expectation that no quantum gates can be simulated efficiently by classical computers since n -qubit quantum circuit operates in a 2^n -dimensional Hilbert space. But admittedly the situation is very different for non-Clifford gates which cannot be simulated efficiently. If it was shown someday that even non-Clifford gates can be

³⁵A stabilizer circuit is a quantum circuit in which every gate is selected from a stabilizer set i.e., $\{H, \text{CNOT}, P\}$ or a 1-qubit measurement gate

³⁶The two braces denote that is a quantum code unlike classical code such as Hamming code which uses single parentheses

simulated by classical computers, then it would imply a further (and significant) lack of usefulness of quantum computers.

However, even after different codes to perform quantum error correction, this has been not possible to do in practice. One of the issues is that encoding of a single logical qubit in N physical qubits also raises the possibility of error occurring by that factor. The apparatus which fixes the single-qubit error must therefore be reasonably fast to not incur other errors in one of those N qubits to reach a reasonable trade-off. This is not an easy experimental problem and hence there have been various other proposals to perform error corrections. One of the main alternatives is the use of ‘continuous variables’ degrees of freedom (quantum harmonic oscillator). In such a setting, the logical qubits will be photon (Fock) states that span a two-dimensional subspace from the potentially infinite harmonic oscillator states. Though, we have discussed the qubit-based quantum computing in this article, the quantum computation and information based on continuous variables (CV) are also extensively used in quantum teleportation, error correction, and cryptography. For the CV approach to quantum computation, the main role is played by Bose operators b_i^\dagger, b_i known as creation and annihilation operators satisfying following commutation relations (also known as ‘Heisenberg-Weyl algebra’):

$$[b_i^\dagger, b_j^\dagger] = 0, \quad [b_i, b_j] = 0, \quad [b_i, b_j^\dagger] = \delta_{ij} \mathbb{1}. \quad (6.13)$$

The inner product space must be of infinite dimension for (6.13) to hold. One defines the vacuum state of N qumodes (similar to N qubits) as $|0\rangle = |000 \cdots 0\rangle$. The normalized number state (or Fock state) can be written as:

$$\frac{1}{\sqrt{n_1! n_2! \cdots n_k!}} (b_{j_1}^\dagger)^{n_1} (b_{j_2}^\dagger)^{n_2} \cdots (b_{j_k}^\dagger)^{n_k} |0\rangle = |n_1, n_2, \cdots, n_k\rangle. \quad (6.14)$$

We refer the reader to Appendix A and excellent review [78] for more technical details and to start the reference trail.

SECTION 7

Looking at NISQ and beyond

One of the motivations for building the quantum computer, at least for physicists, is to solve the time evolution of some complicated quantum mechanical system. This was also the motivation given by Feynman around 1982. However, it was only in 1996 that an explicit quantum-inspired algorithm for simulating the time evolution of a quantum system with *local* Hamiltonian was given for the first time [79]. The algorithm made use of the Lie-Trotter formula to express the unitary time evolution as a sequence of exponentials and had a complexity of $\mathcal{O}(t||H||)^2$ where t is the time and $||H||$ is the spectral norm (also called two-norm) of the Hamiltonian.

However, it is clear that most of the physically interesting quantum models cannot be simulated on NISQ devices with just a few hundred/thousand noisy qubits. However, there is still a lot to

understand and this is an active area of research. It is already evident that even for non-relativistic quantum systems the size of Hilbert space is very large and adding the relativistic behavior when studying quantum field theories makes it worse. One has to understand the reduction of the degrees of freedom properly while keeping the symmetries (such as ‘gauge symmetry’) intact. There have been various proposals such as D -theory/quantum link models [80], dual variable using character expansions with sum over irreducible representations of the gauge group [81] which are then truncated, quantum groups such as $SU(2)_q$ approach, loop-string-hadron formalism [82], light front dynamics method, and truncating the continuous symmetry groups by discrete point symmetry such as in Ref. [83]. All these methods are based on finding smaller subspace of the vector space to be represented by qubits. There is also a method based on continuous variables (CVs) which plays an important role in analog quantum computing and has several advantages over the discrete methods. These schemes have their merits and drawbacks and the effectiveness in obtaining the continuum limit is still debatable. Some qubit regularization schemes also exists for $O(3)$ non-linear sigma model by exploiting equivalence to $SU(2)$ and associated truncation over irreducible representations but it is by no means a general method and works only for this specific group. We do not know of any work which attempts $O(N)$ models with $N \geq 4$. Even for scalar field theories such as ϕ^4 theory in 1+1-dimensions, the quantum simulation and extracting of real-time properties and correlators are still not fully understood. There are approaches based on field variables following JLP [84], harmonic oscillator basis [85], continuous variable approach [86], and single-particle basis [87] to name a few. Here, we will simply focus on some simple examples where one desires time evolution using some Hamiltonian with circuit depths ³⁷ that may be performed on the NISQ devices.

We can perceive any quantum circuit as a simulation of some Hamiltonian H . This follows from the standard observation that any (noiseless) the quantum circuit can be built up of pieces of unitary transformations whose product is also unitary. Once we have a given unitary transformation, we can find H such that $U = e^{-iHt}$ where t is some real parameter. The time evolution of any given state can be defined by this U .

In addition to the time evolution of a given quantum state with some H , this unitary evolution also plays an important role in the HHL algorithm [88, 89] which is a quantum algorithm to solve a linear system of equations i.e., $A\vec{x} = \vec{b}$ where A is a Hermitian $n \times n$ matrix which is d -sparse. HHL algorithm started a mini-revolution in various areas of research including quantum machine learning (QML). The reason was in the fact that it addresses one of the most important problems of linear algebra - solving linear systems. HHL is expected to have time complexity $\mathcal{O}(\log(n)d^2\kappa^2/\epsilon)$ and exponential speedup over the best known classical algorithm, conjugate gradient [90], with complexity $\mathcal{O}(nd\sqrt{\kappa}\log(1/\epsilon))$.

However, there are some conditions that must be satisfied for this to hold. These conditions

³⁷The depth of a circuit is the longest path between the data input and the output, where each intermediate gate counts as one. The circuit depth can be easily found in QISKIT using `qc.depth()` where `qc` is the quantum circuit.

related to loading \vec{b} quickly, applying e^{-iAt} with A being d -sparse³⁸, well-behaved condition number κ of matrix A , and the lack of obtaining all elements of \vec{x} [91]. It is clear that these might be difficult to satisfy all at once in practice and hence the speedup might be lost. And even if we satisfy all these conditions, we do not have full access to the \vec{b} like the classical case but only to $|A^{-1}b\rangle$. With the state in hand, we can make measurements to know the features of the output state. It might have deep implications in the future, but, in practice, HHL does not appear to be of much use in the NISQ era. Also, the HHL algorithm complexity severely depends (more than the best classical) on condition number and sparsity.

7.1 Hamiltonian Simulation

We now return to the main question of interest – how to implement $U = e^{-iHt}$ given some hermitian matrix H of size $N \times N$ which is d -sparse on a quantum initial state $|\psi\rangle$ i.e., how to do: $U|\psi\rangle \rightarrow |\psi(t)\rangle$. We say that we can efficiently simulate any N -qubit Hamiltonian H if we can approximate U for any t in $\text{poly}(N)$ using at most polynomial number of one- and two-qubit gates. It is widely believed that wide range of Hamiltonians cannot be simulated efficiently. However, if we are given that we can simulate some smaller Hamiltonians H_1, \dots, H_k , then their sum H can also be simulated using Lie-product formula which we discuss later in the section. In addition, if we can simulate H_1 and H_2 , then we can also simulate $[H_1, H_2]$ using the identity:

$$e^{-i[H_1, H_2]t} = \lim_{N \rightarrow \infty} \left(e^{-iH_1 t / \sqrt{N}} e^{-iH_2 t / \sqrt{N}} e^{iH_1 t / \sqrt{N}} e^{iH_2 t / \sqrt{N}} \right)^N. \quad (7.1)$$

Another important result is the unitary conjugation i.e., if we can simulate H and can perform (efficiently) the unitary operation U , then we can simulate UHU^\dagger . This is true because of the identity in (B.17).

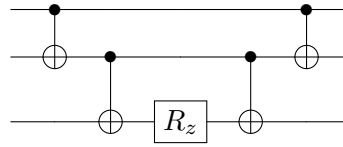
Let us consider a simple two-site model with $H = \sigma_z \otimes \sigma_z = Z_1 \otimes Z_2$. We could express this term: $\exp(i\sigma_z \otimes \sigma_z t)$ as $e^{i\sigma_z \otimes \sigma_z t} = \cos(t)\mathbb{1} + i\sin(t)\sigma_z \otimes \sigma_z$ ³⁹ which can be written by some manipulation (show this) as $\text{CNOT}(\mathbb{1} \otimes e^{i\sigma_z t})\text{CNOT}$ since $\text{CNOT} = |0\rangle\langle 0| \otimes \mathbb{1} + |1\rangle\langle 1| \otimes \sigma_x$. The circuit to implement [92] this term is given below:


(7.2)

where the argument of R_z gate is $-2t$. This is sometimes also written as: $\exp(itZ_j \otimes Z_k) = \text{CNOT}_{jk}(\mathbb{1}_j R_z(-2t)_k) \otimes \text{CNOT}_{jk}$ with j, k denoting the qubits on which the gates act. Similarly, we can construct a circuit for the three-qubit term, $\sigma_z \otimes \sigma_z \otimes \sigma_z$ as:

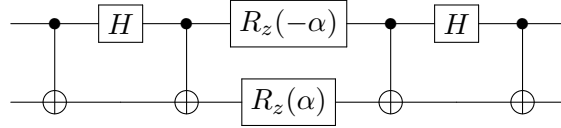
³⁸A matrix is d -sparse if it contains at most d nonzero entries per row/column for some $d \ll n$

³⁹Note that we have $\exp(\pm i\theta U) = \cos(\theta)\mathbb{1} \pm i\sin(\theta)U$ if $U^2 = \mathbb{1}$.



(7.3)

Sometimes, for brevity, we refer to the Pauli matrices just by X, Y, Z respectively. Now, suppose we have different Pauli matrices term in the Hamiltonian as: $(X \otimes X + Y \otimes Y)$. The corresponding circuit can be used to perform time evolution i.e., it is equivalent to $\exp[i(\alpha/2)(X \otimes X + Y \otimes Y)]$



(7.4)

It is easy to check this using MATHEMATICA code below which has been broken down for simplicity.

```

1  X = PauliMatrix[1];
2  Y = PauliMatrix[2];
3  Z = PauliMatrix[3];
4  XXplusYY = MatrixExp[I (KroneckerProduct[X, X] + KroneckerProduct[Y, Y]) \[Alpha]/2];
5  XtimesX = MatrixExp[I (KroneckerProduct[X, X]) \[Alpha]/2];
6  ZtimesZ = MatrixExp[I (KroneckerProduct[Z, Z]) \[Alpha]/2];
7  YtimesY = MatrixExp[I (KroneckerProduct[Y, Y]) \[Alpha]/2];
8  XtimesY = MatrixExp[I (KroneckerProduct[X, Y]) \[Alpha]/2];
9  CNOT = {{1, 0, 0, 0}, {0, 1, 0, 0}, {0, 0, 0, 1}, {0, 0, 1, 0}};
10 HAD = {{1/\[Sqrt]2, 1/\[Sqrt]2}, {1/\[Sqrt]2, -(1/\[Sqrt]2)}};
11 S = {{1, 0}, {0, I}};
12 S1 = KroneckerProduct[S, S];
13 HAD1 = KroneckerProduct[HAD, IdentityMatrix[2]];
14 HAD2 = KroneckerProduct[HAD, HAD];
15 RZ1 = KroneckerProduct[IdentityMatrix[2], MatrixExp[I (\[Alpha]/2) Z]];
16 RZ2 = KroneckerProduct[MatrixExp[I (\[Alpha]/2) Z], MatrixExp[I (-\[Alpha]/2) Z]];
17
18 (* Check! *)
19
20 XXYY = CNOT . HAD1 . CNOT . RZ2 . CNOT . HAD1 . CNOT // FullSimplify;
21 ZZ = CNOT . RZ1 . CNOT // FullSimplify;
22 XX = HAD2 . ZZ . HAD2 // FullSimplify;
23 YY = ConjugateTranspose[S1] . XX . S1 // FullSimplify;
24 XXplusYY == XXYY
25 ZtimesZ == ZZ
26 XtimesX == XX
27 YtimesY == YY
28 HY = {{1/\[Sqrt]2, -I/\[Sqrt]2}, {I/\[Sqrt]2, -(1/\[Sqrt]2)}};
29 HY . PauliMatrix[3] . HY == PauliMatrix[2] ; (* True *)
30 HAD . PauliMatrix[3] . HAD == PauliMatrix[1]; (* True *)

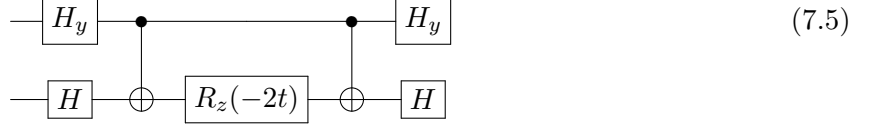
```

```

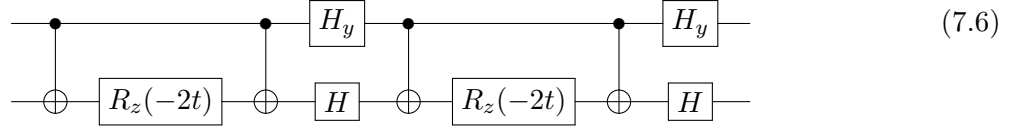
31 YYcir = KroneckerProduct[HY, HY] . ZZ . KroneckerProduct[HY, HY] // FullSimplify ;
32 YtimesY == YYcir;
33 XYcir = KroneckerProduct[HAD, HY] . ZZ . KroneckerProduct[HAD, HY] // FullSimplify ;
34 XtimesY = XYcir;

```

It is also useful to note that $e^{itI \otimes \mathcal{P} \otimes I} = I \otimes e^{it\mathcal{P}} \otimes I$, where \mathcal{P} is single Pauli matrix or a string because $e^{itI \otimes \mathcal{P} \otimes I} = \cos(t)I \otimes I \otimes I + i \sin(t)I \otimes \mathcal{P} \otimes I = I \otimes (\cos(t)I + i \sin(t)\mathcal{P}) \otimes I = I \otimes e^{i\mathcal{P}t} \otimes I$. Sometimes, it is possible that H has commuting terms. For example, consider $H = X \otimes Y + Z \otimes Z$. It is straightforward to see that the terms commute and therefore $\exp(-iHt) = \exp(-itX \otimes Y) \exp(-itZ \otimes Z)$. The circuit for the first term is:



where $H_y = \frac{1}{\sqrt{2}} \begin{pmatrix} 1 & -i \\ i & -1 \end{pmatrix}$ while the second term is given by (7.2). Combining, we get for one step,



consisting of four two-qubit gates and six one-qubit gates. But, this might not always be efficient. Consider the circuit in (7.4) for $H = (X \otimes X + Y \otimes Y)$. Since the terms commute, we can also use alternate circuit as given below in the MATHEMATICA code, however it requires many more gates.

```

1 CT = KroneckerProduct;
2 X = PauliMatrix[1];
3 Y = PauliMatrix[2];
4 Z = PauliMatrix[3];
5 CNOT = {{1, 0, 0, 0}, {0, 1, 0, 0}, {0, 0, 0, 1}, {0, 0, 1, 0}};
6 HAD = {{1/\[Sqrt]2, 1/\[Sqrt]2}, {1/\[Sqrt]2, -(1/\[Sqrt]2)}};
7 HY = {{1/\[Sqrt]2, -I/\[Sqrt]2}, {I/\[Sqrt]2, -(1/\[Sqrt]2)}};
8 XXYv1 = CNOT . CT[HAD, IdentityMatrix[2]] . CNOT . CT[MatrixExp[I (\[Alpha]/2) Z],
          MatrixExp[I (-\[Alpha]/2) Z]] . CNOT . CT[HAD, IdentityMatrix[2]] . CNOT // FullSimplify;
9 XXYv2 = (CT[HAD, HAD] . CNOT . CT[IdentityMatrix[2], MatrixExp[I (\[Alpha]/2) Z]] . CNOT .
          CT[HAD, HAD]) . (CT[HY, HY] . CNOT . CT[IdentityMatrix[2], MatrixExp[I (\[Alpha]/2) Z]] .
          CNOT . CT[HY, HY] ) // FullSimplify;
10 XXYv1 == XXYv2 == MatrixExp[I (KroneckerProduct[X, X] + KroneckerProduct[Y, Y]) \[Alpha]/2]

```

► QUESTION 21: Show that any Pauli string is 1-sparse.

► QUESTION 22: Consider the three-qubit Hamiltonian given by:

$$H = \sigma_y \otimes \sigma_y \otimes \sigma_x - \sigma_z \otimes \sigma_z \otimes \sigma_z - \sigma_z \otimes \mathbb{1} \otimes \mathbb{1}.$$

Construct the quantum circuit for the unitary operator ($\exp(iH)$) corresponding to it. It might be useful to remember that $X = H \cdot Z \cdot H$ and $Y = H_y \cdot Z \cdot H_y$ where $H_y = \frac{1}{\sqrt{2}} \begin{pmatrix} 1 & -i \\ i & -1 \end{pmatrix}$.

However, the method we just described in terms of Pauli strings is highly inefficient and in fact for most cases, as worse as classical methods. We will now consider some state-of-the-art Hamiltonian simulation techniques which are better suited for quantum computers. These are based on sparse representation rather than local representation in terms of Pauli operators.

We recall some useful definitions about norms of vectors and operators since they will appear later in the section. To measure the distance between two elements in an arbitrary vector space, we can use - Manhattan norm (also called ‘l1 norm’): $\|x\|_1 = \sum_{i=1}^n |x_i|$, or the Euclidean norm (also called ‘l2 norm’): $\|x\|_2 = \left(\sum_{i=1}^n x_i^2 \right)^{1/2}$ or the Supremum norm: $\|x\| = \max_i |x_i|$ where $x = (x_1, \dots, x_n) \in \mathbb{R}^n$. For matrices (operators), let us denote by $\sigma(A)$, the vector whose elements are singular values of positive operator $|A|$ which is defined as: $(A^\dagger \cdot A)^{1/2}$. Then the Schatten p -norm (where $1 \leq p < \infty$) is defined as:

$$\|A\|_p = \left(\sum_{i=1}^N \sigma_i^p \right)^{1/p}. \quad (7.7)$$

This norm is unitary invariant. When $p = 2$, it is called the Frobenius norm or the Hilbert–Schmidt norm. We also note that Frobenius norm is $\|A\|_F = \sqrt{\text{Tr} A^\dagger A} = \sum_{i,j} A_{ij}^2$. And that $\|UA\|_F^2 = \|A\|_F^2$. We can use this and the equivalent result $\|AV\|_F^2 = \|A\|_F^2$ for unitary matrices U, V to reduce it to the form of singular values. First we write SVD of A as USV^T . Then we have $\|A\|_F = \|USV^T\|_F = \|SV^T\|_F = \|S\|_F = \sqrt{\sum_{i=1}^N \sigma_i^2}$. The $p = \infty$ limit is called the spectral norm. In some cases, people also refer to the spectral or operator norm (Schatten ∞ -norm) by induced 2-norm which is square root of maximum eigenvalue of $(A^\dagger \cdot A)^{1/2}$.

In general, there are two most-used ways of decomposing the unitary operator (exponential of Hermitian matrix H): 1) Lie-product method, and 2) Taylor Series. We discuss them below.

- Lie-product decomposition approach: This is sometimes called divide and conquer method since the Hamiltonian is broken into small pieces as $H = \sum_{j=1}^m \alpha_j H_j$ which are then evolved. The unitary operator is given by:

$$\exp(-iHt) = \left(\prod_{j=1}^m \exp(-iH_j t/N) \right)^N + \mathcal{O} \left(\sum_{j,k} \left\| [H_j, H_k] \right\|^2 t^2 / N \right) \quad (7.8)$$

So, if we have all the terms in decomposition of H nearly-commuting, then the Trotter error is reduced greatly and vanishes if they commute. Therefore, one can improve on errors by making use of various commutative relations. Based on the structure of H , some Hamiltonian simulations might be very simple and some can be notoriously hard.

- Taylor Series: This approach proceeds following the standard decomposition:

$$U(t) = e^{-iHt} = \sum_{k=0}^{\infty} \frac{(-itH)^k}{k!}. \quad (7.9)$$

However for all practical purposes, we have to truncate this infinite sum at some order K as:

$$\begin{aligned} \hat{U}(t) &= \sum_{k=0}^K \frac{(-itH)^k}{k!} \\ &= \sum_{k=0}^K \sum_{l=1}^L \frac{t^k}{k!} \prod \alpha_l (-i)^k \prod H_l \end{aligned} \quad (7.10)$$

$$= \sum_{i=0}^N \tilde{\alpha}_i \tilde{H}_i. \quad (7.11)$$

where $\tilde{H} = (-i)^k \prod H$ and coefficients $\tilde{\alpha} = t^k/k! \prod \alpha$. The second sum in (7.10) comes from the decomposition⁴⁰ of H in terms of linear combination of unitaries (LCU). We have absorbed the negative imaginary number in the operator such that all α_l are positive. Similar to the product formula, we divide in r segments, such that:

$$\left\| \hat{U}(t/r) - U(t/r) \right\| \leq e^{\alpha t/r} \frac{(\alpha t/r)^{K+1}}{(K+1)!}, \quad (7.12)$$

where $\alpha = \sum \alpha_i$. If we want this upper bounded error to be ϵ , then we need to choose:

$$K = \mathcal{O}\left(\frac{\log(\alpha t/\epsilon)}{\log \log(\alpha t/\epsilon)}\right). \quad (7.13)$$

The proof of (7.12) proceeds as follows:

⁴⁰Recall that any complex matrix can be written as sum of unitary matrices. In this case, sum of L unitaries

Proof.

$$\begin{aligned}
\left\| \hat{U}(t) - \sum_{k=0}^{\infty} \frac{(-itH)^k}{k!} \right\| &= \left\| \sum_{k=K+1}^{\infty} \frac{(-itH)^k}{k!} \right\| \\
&\leq \sum_{k=K+1}^{\infty} \frac{(t \sum_l \alpha_l)^k}{k!} \\
&\leq \frac{(t \sum_l \alpha_l)^{K+1}}{(K+1)!} \left[\sum_{j=0}^{\infty} (t \sum_l \alpha_l)^j / j! \right] \\
&\leq e^{\alpha t/r} \frac{(\alpha t/r)^{K+1}}{(K+1)!}
\end{aligned} \tag{7.14}$$

□

Note that in the literature, the LCU followed by oblivious amplitude amplification [93] is referred to as ‘truncated Taylor series’ (TTS) algorithm [94].

The efficiency of the quantum simulation depends strongly on how the terms in Hamiltonian behave and how many qubits they act at a given time. In this regard, one defines the notion of k -local Hamiltonian. Suppose we have a Hamiltonian acting on n qubits, i.e., the operator is a $2^n \times 2^n$ matrix, $H = \sum_a H_a$, it is k -local in the sense that each H_a acts non-trivially on at most k qubits at a time. A k -local Hamiltonian can be read in polynomial time and is simpler to handle. If we want to determine the ground state energy of such a Hamiltonian, then it is called the k -local Hamiltonian problem. There is a very close relationship between complexity classes and k -local Hamiltonian problem. It was shown in several works that it is **QMA** complete for all $k \geq 2$ [95]. A detailed discussion of this lies beyond the scope of this article. In Table, we list all major Hamiltonian simulation algorithms and their complexity. However, note that no one algorithms fit all conditions. The choice is based on the nature of Hamiltonian (time-dependent or independent) and symmetries which can be exploited and how local the H is in general. In general, it is known that if the size of H is $2^n \times 2^n$, then there exists a decomposition of $H = \sum_{j=1}^m H_j$ where each H_j is 1-sparse, such that $m = \mathcal{O}(d^2)$ and each query to any H_j can be simulated⁴¹ by making $\mathcal{O}(\log^* n)$.

WE DENOTE THE SIZE OF HAMILTONIAN BY N , THE EVOLUTION TIME BY t , THE SPARSITY BY d AND THE MAXIMUM ALLOWED ERROR BY ϵ AND $1/2 > \delta > 0$.

⁴¹Note that $\log^* n$ implies the iterated algorithm. It is defined as:

$$\log^* n = \begin{cases} 0 & \text{if } n \leq 1 \\ 1 + \log^*(\log n) & \text{if } n > 1 \end{cases}$$

queries to H (which is very optimum!).

Algorithm	Complexity
Lie-trotter (only k -local H) [1996] [79]	$\mathcal{O}(\text{poly}(\log N)(\ H\ t)^2/\epsilon)$
Lie-trotter (simulatable H) [2007] [96]	$\mathcal{O}(d^4(\log^* N)\ H\ t)^{1+\delta}/\epsilon^\delta$
Lie-trotter (simulatable H) [2011] [97]	$\mathcal{O}(d^3(\log^* N)\ H\ t)^{1+\delta}/\epsilon^\delta$
Truncated Taylor Series with Trotter [2014] [94]	$\mathcal{O}(d^2\ H\ t)^{\frac{\log(d^2\ H\ t/\epsilon)}{\log \log(d^2\ H\ t/\epsilon)}}$
LCU+OAA with quantum walks [2015] [98]	$\mathcal{O}(d\ H\ t)^{\frac{\log(d\ H\ t/\epsilon)}{\log \log(d\ H\ t/\epsilon)}}$
Qubitization/Quantum Walks [99]	$\mathcal{O}(d\ H\ t + \log(1/\epsilon))$

One thing to note is that the Hamiltonian simulation algorithms based on Lie-Trotter product formulas do not admit error dependence that is $\text{polylog}(1/\epsilon)$ whereas starting with Ref. [94, 100]. However, for most applications in Physics, it seems like the use of Trotter method is preferred since for models with local interactions, the complexity of using non-Trotter is not worth the gain in errors. We are not aware of a systematic study of a lattice gauge theory model comparing different time evolution methods.

SECTION 8

Future

The challenges in making scalable quantum computers and performing interesting computations which could change the way we perceive the world is still decades away. We have come a long way since the first papers in the field were written about 45 years ago, however, lot remains to be done both on theoretical and experimental front. For the physically interesting problems physicists would really like to solve, it is expected that an order of million noisy qubits might be needed as shown in Fig. 15. The pursuit of this goal will definitely teach us new things about computation and more importantly about deep foundations of quantum mechanics. One must be hopeful to solve several if not all problems.

SECTION 9

Acknowledgements

The research was supported by the U.S. Department of Energy, Office of Science, National Quantum Information Science Research Centers, Co-design Center for Quantum Advantage under con-

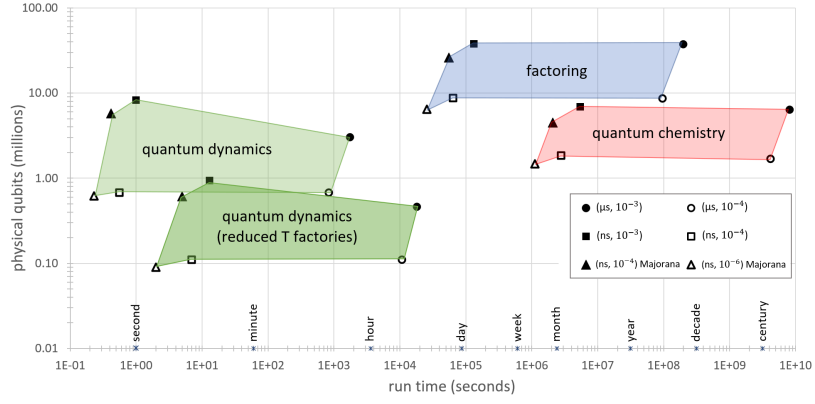


Figure 15. Estimate of the number of qubits needed to perform different types of computations. The inset mentions the effect of gate operation time on the estimate. The figure is taken from Ref. [101].

tract number DE-SC0012704. This material is based upon work supported by the U.S. Department of Energy, Office of Science, Office of Nuclear Physics under contract DE-AC05-06OR23177. Research at Perimeter Institute was supported by the Government of Canada through the Department of Innovation, Science and Economic Development Canada and by the Province of Ontario through the Ministry of Research, Innovation and Science. All the quantum circuits were made using `Qcircuit` introduced in Ref. [102].

SECTION A

Continuous variable quantum computing

In this article, we have focused only on the qubit-based quantum computing which utilize the two-state quantum system (qubits) to store and manipulate the information. However, not all quantum systems in nature are not restricted to this setup. For example, one can have qudit systems where the local Hilbert space is $d > 2$. In fact, one can go all the way to consider the $d \rightarrow \infty$ limit which are formally referred to as ‘qumodes’ and constitute the continuous variable (CV) formulation of quantum computing (CVQC). One can think of ‘qumodes’ as storing the state of a boson which lives in an infinite dimensional vector space. Therefore, a single qumode can be described by a quantum-mechanical harmonic oscillator. It is these states which one uses to encode the information similar to qubits where only $|0\rangle$ and $|1\rangle$ are used. In general, the state of the qumode is usually represented by two bases: 1) Phase-space basis where the CV gates or operators are written in terms of \hat{x}, \hat{p} , and 2) Fock space basis where operators are written in terms of \hat{a}, \hat{a}^\dagger . In the phase-space representation, the computational basis is in terms of strength of electric and magnetic fields which are related by Fourier transform. In the Fock basis, it is given in terms of measurement of the number of bosons (or photons) measured in the computational

basis represented by $|n\rangle$. In practice, one truncates the qumodes at some cutoff Λ to obtain a qudit system. We refer the interested reader to Ref. [103] for more detailed explanation.

This approach to quantum computing is formally related to the storing and manipulation in terms of quantum harmonic oscillators (QHO) and makes use of physical observables whose numerical values belong to continuous intervals (say the x and p quadrature operators). The CV formulation has a very natural experimental realisation in terms of photon and the protocols of quantum information can be implemented using the techniques of quantum optics. Every mode of the electromagnetic field is a single QHO with its own set of creation and annihilation operators which are related to the ‘quadratures’. It has been well-known now for decades that the theory of quantum information based on this alternate CV formalism provides an alternative ground for quantum computing [104, 105]. In particular, they have been shown to be useful towards long-term goal of fault-tolerant quantum computing [106, 107]. The CV quantum systems is also significant for quantum machine learning since it can provide an arena for realization of quantum neural networks [108]. There also have been extension of algorithms to continuous variables such as Grover’s algorithm [109], Deutsch-Jozsa [110] and analog of Shor’s code to correct an arbitrary single wavepacket errors using a 5-wavepacket code [111]. Before going into further details of CV states, gates, and how measurements are done, we present a quick summary of the QHO. A one-dimensional quantum harmonic oscillator is described by the following Hamiltonian:

$$\hat{H} = \frac{\hat{p}^2}{2} + \frac{\hat{x}^2}{2}. \quad (\text{A.1})$$

One can then define a complex operator \hat{a} as:

$$\hat{a} = \frac{1}{\sqrt{2}}(\hat{x} + i\hat{p}) \quad (\text{A.2})$$

and the complex conjugate of this as \hat{a}^\dagger . Using this, we can write \hat{x} and \hat{p} as:

$$\begin{aligned} \hat{x} &= \frac{1}{\sqrt{2}}(\hat{a} + \hat{a}^\dagger), \\ \hat{p} &= i\frac{1}{\sqrt{2}}(\hat{a} - \hat{a}^\dagger). \end{aligned} \quad (\text{A.3})$$

The operator \hat{a} is not Hermitian, since it is not equal to \hat{a}^\dagger . The action of these operators on the energy eigenstates $|n\rangle$ (also ‘Fock’ states) are given as:

$$\begin{aligned} \hat{a}^\dagger |n\rangle &= \sqrt{n+1} |n+1\rangle, \\ \hat{a} |n\rangle &= \sqrt{n} |n-1\rangle. \end{aligned} \quad (\text{A.4})$$

because of how it adds and removes quanta, these are also known as ‘creation’ and ‘annihilation’ operators. Using these relations, it is sometimes useful to define the number operator $N = \hat{a}^\dagger \hat{a}$ which acts as: $N |n\rangle = n |n\rangle$. Using this, we can write the QHO Hamiltonian as:

$$\hat{H} = \hbar\omega \left(N + \frac{1}{2} \right). \quad (\text{A.5})$$

We will first discuss some important gates in CVQC and then move to discuss the CV states and measurements.

A.1 CV gates

Just like the qubit based computation, we have CV gates in terms of creation and annihilation operators. We describe some Gaussian CV gates below:

- Displacement operator is defined as:

$$D(\alpha) = \exp(\alpha \hat{a}^\dagger - \bar{\alpha} \hat{a}) \quad (\text{A.6})$$

where $\alpha \in \mathbb{C}$ and \hat{a}^\dagger and \hat{a} are the creation and annihilation operators respectively. The set of all displacement operators form a Heisenberg-Weyl group which is the ‘qumodes’ generalization of Pauli group for qubits. This operator affects the position and momentum operators as $D^\dagger(\alpha) \hat{x} D(\alpha) = \hat{x} + \sqrt{2\hbar} \Re(\alpha) \mathbb{1}$ and $D^\dagger(\alpha) \hat{p} D(\alpha) = \hat{p} + \sqrt{2\hbar} \Im(\alpha) \mathbb{1}$

- Squeezing gate (operator) is given as:

$$S = \exp\left(\frac{1}{2}(z^* \hat{a}^2 - z \hat{a}^{\dagger 2})\right), \quad (\text{A.7})$$

where $z = r e^{i\phi}$ known as squeezing parameter. The operator transforms the position and momentum operators as: $S^\dagger(z) \hat{x} S(z) = e^{-r} \hat{x}$ and $S^\dagger(z) \hat{p} S(z) = e^r \hat{p}$

- Two-mode squeezing: The two-mode version of squeezing operator is given by:

$$S_2(z) = \exp\left(z \hat{a}_1^\dagger \hat{a}_2^\dagger - z^* \hat{a}_1 \hat{a}_2\right), \quad (\text{A.8})$$

where z is as defined above.

- Rotation:

$$R(\phi) = \exp(i\phi \hat{a}^\dagger \hat{a}) \quad (\text{A.9})$$

and action on x and p as:

$$\begin{aligned} R^\dagger(\phi) \hat{x} R(\phi) &= \hat{x} \cos \phi - \hat{p} \sin \phi, \\ R^\dagger(\phi) \hat{p} R(\phi) &= \hat{p} \cos \phi + \hat{x} \sin \phi. \end{aligned} \quad (\text{A.10})$$

- Beam-Splitter gate is defined as:

$$\text{BS}(\theta, \phi) = \exp(\theta(e^{i\phi} \hat{a}_i \hat{a}_j^\dagger - e^{-i\phi} \hat{a}_i^\dagger \hat{a}_j)) \quad (\text{A.11})$$

A 50-50 BS is the one when $\phi = 0, \pi$ and $\theta = \pi/4$.

- Controlled-X: The controlled-X gate (also known as sum/addition gate) is a controlled position displacement and is given by (in position basis):

$$\text{CX}(r) = \exp(-ir\hat{x}_1\hat{p}_2). \quad (\text{A.12})$$

It is called addition gate because $\text{CX}(r)|x_1, x_2\rangle = |x_1, x_2 + rx_1\rangle$. This gate can also be decomposed in terms of single-mode squeezing and beamsplitter gate. One can also define double-controlled version [112] of this gate i.e, $\text{CCX}(r) = \exp(-ir\hat{p}_3(\hat{x}_1 + \hat{x}_2))$. These gates have some interesting usage. For example, in the qubit formalism, to add, we use full-adder as discussed in Sec. 4.1 which makes use of single and double-controlled CNOT gates. An equivalent CV version would then make use of the gates discussed above.

There is another useful state known as ‘displaced squeezed’ state which is obtained $|\alpha, z\rangle = D(\alpha)|0, z\rangle = D(\alpha)S(z)|0\rangle$, with z being the squeezing parameter as above. In addition to these gates, there are also non-Gaussian gates such as ‘cubic’ and ‘Kerr’ gates given by $V(\gamma) = \exp(i\frac{\gamma}{3!}\hat{x}^3)$ and $K(\kappa) = \exp(i\kappa\hat{n}^2)$ respectively where κ is some real parameter and \hat{n} is the number operator.

EXAMPLE 5: Assume that we set $\phi = 0$ such that $\text{BS}(\theta) = \exp(\theta(\hat{a}\hat{b}^\dagger - \hat{a}^\dagger\hat{b}))$. Show that

$$\begin{aligned} B\hat{a}B^\dagger &= \hat{a}\cos\theta + \hat{b}\sin\theta, \\ B\hat{b}B^\dagger &= -\hat{a}\sin\theta + \hat{b}\cos\theta. \end{aligned} \quad (\text{A.13})$$

Proof. To show this, we have to use the BCH formula given by:

$$e^{\alpha X} A e^{-\alpha X} = \sum_{n=0}^{\infty} \frac{\alpha^n}{n!} C_n, \quad (\text{A.14})$$

where α is a complex number and A, C_n, X are operators. C_n is recursively defined as: $C_0 = A, C_1 = [A, C_0], C_2 = [A, C_1]$ and so on. For proving the first result, we note that $BaB^\dagger = e^{\theta X} a e^{-\theta X}$ where $X = ab^\dagger - a^\dagger b$. We have suppressed hat for convenience from the operators a, b . We find that $C_0 = a, C_1 = b, C_2 = a, C_3 = -b$ and so on. The general sum in (A.14) can be split in even and odd parts since $C_n = i^n a$ for even n and $C_n = -i^{n+1} b$ for odd n as:

$$\begin{aligned} BaB^\dagger &= \sum_{n, \text{even}} \frac{(i\theta)^n}{n!} a - i \sum_{n, \text{odd}} \frac{(i\theta)^n}{n!} b, \\ &= a \cos\theta + b \sin\theta. \end{aligned} \quad (\text{A.15})$$

□

We leave it for the reader to show the following for general ϕ ,

$$\begin{aligned} B^\dagger(\theta, \phi) a B(\theta, \phi) &= a \cos\theta - b e^{-i\phi} \sin\theta, \\ B^\dagger(\theta, \phi) b B(\theta, \phi) &= b \cos\theta + a e^{i\phi} \sin\theta. \end{aligned} \quad (\text{A.16})$$

A.2 CV states

The most basic CV state is the vacuum state (Gaussian) defined as:

$$|0\rangle = \frac{1}{\sqrt[4]{\pi}} \int dx e^{-x^2/(2)} |x\rangle, \quad (\text{A.17})$$

Following this, we can define other states by acting with some operator on $|0\rangle$ as:

- Coherent states: These are minimum uncertainty state and eigenstate of the annihilation operator ($\hat{a}|\alpha\rangle = \alpha|\alpha\rangle$) given by:

$$|\alpha\rangle = D(\alpha)|0\rangle = e^{-\frac{1}{2}|\alpha|^2} \sum_{n=0}^{\infty} \frac{\alpha^n}{\sqrt{n!}} |n\rangle \quad (\text{A.18})$$

in the Fock basis.

- Squeezed states: A squeezed state is a minimum uncertainty state with unequal quadrature variances unlike coherent states. They are obtained by the action of squeezing operator on vacuum i.e., $|z\rangle = S(z)|0\rangle$
- Displaced squeezed (or squeezed coherent) states: A displaced squeezed state is obtained by the action of squeezing operator on vacuum followed by a displacement operator i.e., $|\alpha, z\rangle = D(\alpha)S(z)|0\rangle$
- Cat states: These are superpositions of two coherent states (with opposite phases) $|\alpha\rangle$ and $|\alpha\rangle$ and are given by:

$$|\text{cat}\rangle = \mathcal{N} e^{-|\alpha|^2/2} (|\alpha\rangle + e^{i\phi} |\alpha\rangle), \quad (\text{A.19})$$

when $\phi = 0$, this is known as even cat state denoted by $|C_{\alpha}^{+}\rangle$ while an odd cat state which is $|\text{cat}\rangle \propto |\alpha\rangle - |\alpha\rangle$ is obtained with $\phi = \pi$. The normalization \mathcal{N} is equal to $(2 + 2e^{-2|\alpha|^2} \cos(\phi))^{-1/2} = (2 \pm 2e^{-2|\alpha|^2})^{-1/2}$ for even (odd) cat states i.e., $|C_{\alpha}^{\pm}\rangle$. These states are non-Gaussian in nature. The odd and even cat states are quasi-orthogonal: $\langle -\alpha|\alpha\rangle = e^{-2\alpha^2}$ and become orthogonal only as $\alpha \rightarrow \infty$.

A.3 Measurements

There are two classes of measurements in CVQC namely Gaussian and non-Gaussian. The Gaussian class consists of two types: homodyne and heterodyne measurements. The non-Gaussian measurement is photon counting.

Homodyne detection (ideal case) is a kind of projective measurement onto the eigenkets of the quadrature operator \hat{x} . While on the other hand, the heterodyne is a kind of projective measurement onto the eigenkets of both the quadrature operator \hat{x} and \hat{p} . Since they do not commute, they can only be measured with some uncertainty. They can also be thought of as projection onto the coherent states $|\alpha\rangle$. The lack of certainty stems from the fact that coherent states are not orthogonal.

The non-Gaussian photon counting measurement, also known as photon number resolving (PNR) detector, as the name suggests, counts the number of photons. This uses the particle like character of the quanta rather than wavelike from the above mentioned ‘dyne’-type measurements. This measurement projects onto the eigenkets of the number operator $|n\rangle$. The process of PNR detection on *single* mode of the multi-mode (large number of qumodes) Gaussian state changes the other modes to non-Gaussian. This is not the case for the ‘dyne’-type measurements which preserves the Gaussian character of the multimode state. In view of this, photon counting measurement is useful for implementing non-Gaussian gates like cubic gate discussed before.

Now, with some background behind us, let us implement these using some SDK. Similar to the use of QISKIT for qubit based QC, there is a photonic simulator using CVs developed by Xanadu known as STRAWBERRY FIELDS [113]. We refer to the reader to this reference for additional simulation details. We give a small code snippet below with this simulator.

```

1  import strawberryfields as sf
2  from strawberryfields.ops import *
3
4  with prog.context as q:
5
6      # Prepare the initial state
7      Fock(3) | q[0] # 3 photons in qumode 1
8      Fock(1) | q[1] # 1 photon in qumode 2
9
10     BSgate(theta, np.pi/2) | (q[0], q[1]) # Two-mode BS gate
11     Kgate(r) | q[0] # Kerr
12     Rgate(-r) | q[0]
13     Kgate(r) | q[1]
14     Rgate(-r) | q[1]
15     MeasureFock() | q[0]
16     # Photon counting measurement (also known as photon number resolving [PNR] detector)
17     # Measures a set of modes in the Fock basis.
18
19     # To export circuit in LaTeX format, use prog.draw_circuit()
20     # To print circuit, use prog.print()

```

SECTION B

Fun with commutator algebra

The fundamental commutation relation in quantum mechanics is between the position and momentum operator (we often suppress the hat over x and p and other operators):

$$[x, p] = i\hbar. \quad (\text{B.1})$$

This commutation relation is strictly obeyed only in infinite-dimensional Hilbert space. One way to see this is to obtain a ‘paradox’ by assuming that they belong to a finite vector space. Considering taking trace on both sides of (B.1). We find that left side is zero using cyclic nature of trace while the right side is non-zero. This is paradox arising because strictly speaking x, p are not trace-class operators. We can also consider commutation relation between powers of x, p as:

$$\begin{aligned}
[x, p^n] &= [x, pp^{n-1}] \\
&= p[x, p^{n-1}] + i\hbar p^{n-1} \\
&\dots \\
&= p^{n-1}[x, p] + (n-1)i\hbar p^{n-1} \\
&= i\hbar np^{n-1},
\end{aligned} \tag{B.2}$$

using $[A, BC] = [A, B]C + B[A, C]$ in the first step and repeating several intermediate steps $n-1$ times. We can also use the relation below to compute the above commutator:

$$[X^n, Y] = nX^{n-1}[X, Y] + X^n[Y, X], \tag{B.3}$$

and use it to show that

$$[x^n, p] = i\hbar nx^{n-1}, \tag{B.4}$$

and a more general form i.e., $[f(x), p] = i\hbar f'(x)$.

A widely studied physical system is the quantum harmonic oscillator. The reason is that it is quadratic in both x and p operators. We define the number operator $N = a^\dagger a$ satisfying following relations:

$$[N, a^\dagger] = [a^\dagger a, a^\dagger] = a^\dagger[a, a^\dagger] = a^\dagger \tag{B.5}$$

using $[AB, C] = A[B, C] + [A, C]B$ and $[a, a^\dagger] = 1$. Similarly, we can prove that $[N, a] = -a$. We also need to compute commutator such as $[a^n, a]$. For this, it is useful to note two relations when f is an analytic function.

$$\begin{aligned}
[a^\dagger, f(a)] &= -\frac{df(a)}{da}, \\
[a, f(a^\dagger)] &= \frac{df(a^\dagger)}{da^\dagger}.
\end{aligned} \tag{B.6}$$

This immediately leads to $[a, (a^\dagger)^n] = n(a^\dagger)^{n-1}$, and $[a^\dagger, a^n] = -na^{n-1}$. Using these we can then compute:

$$\begin{aligned}
[a^q, n] &= (a^q a^\dagger - a^\dagger a^q)a \\
&= -[a^\dagger, a^q]a \\
&= qa^q.
\end{aligned} \tag{B.7}$$

where q is some integer power. Similarly, we can show that $[(a^\dagger)^q, n] = -q(a^\dagger)^q$. Some other useful commutation relations which follows are: $[\hat{a}, e^{\alpha \hat{a}^\dagger}] = \alpha e^{\alpha \hat{a}^\dagger}$ and $[\hat{a}^\dagger, e^{\alpha \hat{a}}] = -\alpha e^{\alpha \hat{a}}$. When dealing with these operators, we should normal order them. The process of putting a product into normal order is called normal ordering, also known as Wick ordering. Doing this results in all creation operators being left of all annihilation operators in the product. It is denoted by the symbol $:$. For example, $:bb^\dagger := b^\dagger b$ and $:b^\dagger b := b^\dagger b$. We give a MATHEMATICA code to normal order the operators and simplify some commutation expressions discussed above.

```

1  Unprotect[NonCommutativeMultiply];
2  A_ ** (B_ + C_) := A ** B + A ** C
3  (B_ + C_) ** A_ := B ** A + C ** A
4  A_ ** c_?NumberQ := c A
5  c_?NumberQ ** A_ := c A
6  A_ ** (B_ c_?NumberQ) := c A ** B
7  (A_ c_?NumberQ) ** B_ := c A ** B
8  A_ ** (B_ c_Rational) := c A ** B
9  (A_ c_Rational) ** B_ := c A ** B
10 A_ ** (B_ c_Power) := c A ** B
11 (A_ c_Power) ** B_ := c A ** B
12
13 commutator[A_, B_] := A ** B - B ** A
14 fundamentalXP[expr_] := ExpandAll[expr //. p[i_] ** q[i_] :> q[i] ** p[i] - I h]
15 fundamentalH0[expr_] := ExpandAll[expr //. a ** SuperDagger[a] :> SuperDagger[a] ** a + 1 //.
    b ** SuperDagger[b] :> SuperDagger[b] ** b + 1]
16 h /: NumberQ[h] = True;
17 commutator[p[x], q[x] ** q[x] ** q[x]] // fundamentalXP (* [p,q^3] = -3 i \hbar q^2 *)
18 NCP[x___] := NonCommutativeMultiply[x];
19 NCP[0.50*SuperDagger[a] ** a + SuperDagger[b] ** b, 0.50 * SuperDagger[a] ** a +
    SuperDagger[b] ** b] // fundamentalH0

```

In dealing with continuous variable approach to quantum computation, one often has to manipulate the bosonic operators. We collect some results in this section for the convenience of the reader. The central result is the ‘BCH formula’. It is given by:

$$e^X e^Y = e^{X+Y+\frac{1}{2}[X,Y]+\frac{1}{12}([X,[X,Y]]+[Y,[Y,X]])+\dots} \quad (\text{B.8})$$

For example, using this we can write (A.6) as:

$$\begin{aligned}
D(\alpha) &= \exp(\alpha \hat{a}^\dagger - \bar{\alpha} \hat{a}) \\
&= \exp(-\frac{1}{2}|\alpha|^2) \exp(\alpha \hat{a}^\dagger) \exp(-\bar{\alpha} \hat{a})
\end{aligned} \quad (\text{B.9})$$

There is another very useful expression often called the dual of BCH formula first discussed in Sec. 4 of Ref. [114]. This is known as Zassenhaus formula.

$$e^{t(X+Y)} = e^{tX} \cdot e^{tY} \cdot e^{-\frac{t^2}{2}[X,Y]} \cdot e^{\frac{t^3}{6}(2[Y,[X,Y]]+[X,[X,Y]])} \dots \quad (\text{B.10})$$

In general, it is written as ($t = 1$):

$$e^{X+Y} = e^X e^Y \prod_{k=2}^{\infty} e^{C_k(X,Y)} \quad (\text{B.11})$$

where as written above, the first few terms are $C_2(X, Y) = -\frac{1}{2}[X, Y]$ and $C_3(X, Y) = \frac{1}{3}[Y, [X, Y]] + \frac{1}{6}[X, [X, Y]]$. Though this is not that well-known, the corollary of this formula is widely known as the Lie-product formula given as:

$$e^{t(A+B)} = \lim_{N \rightarrow \infty} \left(e^{\frac{At}{N}} e^{\frac{Bt}{N}} \right)^N \quad (\text{B.12})$$

, or equivalently:

$$e^{-it(A+B)} = e^{-itA} e^{-itB} + \mathcal{O}(t^2). \quad (\text{B.13})$$

The error with p -order product formula goes as $\mathcal{O}(t^{p+1})$. In fact, rather than exponential of just sum of two operators, we can consider the general case which is often the most useful in quantum simulation problems. In that case, we have the following result:

$$e^{-i \sum_{j=1}^m H_j t} = \prod_{j=1}^m e^{-i H_j t} + \mathcal{O}(m^2 t^2), \quad (\text{B.14})$$

with $t \ll 1$. This expansion would have been exact (i.e. no error) if it was just an ordinary exponential but the error is because H is an operator/matrix. What happens if our simulation time is $t \gg 1$. In that case, one just divides the entire evolution into r steps such that $t' = t/r \ll 1$,

$$e^{-i \sum_{j=1}^m H_j t} = \left(\prod_{j=1}^m e^{-i H_j t'} \right)^r + \mathcal{O}(m^2 t^2 / r). \quad (\text{B.15})$$

If we desire an error of ϵ , then we must take $r \sim m^2 t^2 / \epsilon$. One can also use second-order formula:

$$e^{-i \sum_{j=1}^m H_j t} = \left(\prod_{j=1}^m e^{-i H_j t / 2r} \prod_{j=m}^1 e^{-i H_j t / 2r} \right)^r + \mathcal{O}(m^3 t^3 / r^2). \quad (\text{B.16})$$

In this case, we need to scale r as $\sim m^{3/2} t^{3/2} / \sqrt{\epsilon}$. The gate costs, accuracy, and the structure of the Hamiltonian determines which choice is better.

Another frequently used identity is

$$U e^{-i H t} U^\dagger = e^{-i U H U^\dagger t}. \quad (\text{B.17})$$

To prove the identity, let's start with the left hand side and expand it:

$$U \left(\sum_{n=0}^{\infty} \frac{(-iHt)^n}{n!} \right) U^\dagger, \quad (\text{B.18})$$

since the operators U and U^\dagger commute with the scalar coefficients in the series, we can rearrange as:

$$\sum_{n=0}^{\infty} \frac{(-iUHU^\dagger t)^n}{n!} = e^{-iUHU^\dagger t} \quad (\text{B.19})$$

which proves the result. An expression often encountered in Hamiltonian evolution problem is of the form $U^\dagger A U$ where U is exponential of matrix. For this, we have the following result known as 'BCH lemma' given by:

$$e^B A e^{-B} = A + [B, A] + \frac{1}{2!} [B, [B, A]] + \frac{1}{3!} [B, [B, [B, A]]] + \dots \quad (\text{B.20})$$

Using (B.20), we can show that $e^{-i\theta a^\dagger a} a^\dagger e^{-i\theta a^\dagger a} = a^\dagger e^{i\theta}$. The proof proceeds as follows:

$$e^{-i\theta a^\dagger a} a^\dagger e^{-i\theta a^\dagger a} = a^\dagger + i\theta [a^\dagger a, a^\dagger] + \frac{(i\theta)^2}{2!} [a^\dagger a, [a^\dagger a, a^\dagger]] + \dots = a^\dagger (1 + i\theta + \frac{(i\theta)^2}{2!} + \dots) = a^\dagger e^{i\theta}. \quad (\text{B.21})$$

where we have used $N = a^\dagger a$ and $[N, a^\dagger] = a^\dagger$.

We can also show following results which we leave to the reader.

$$\hat{a} e^{-i\theta \hat{n}} = e^{-i\theta} e^{-i\theta \hat{n}} \hat{a}, \quad (\text{B.22})$$

$$\hat{a}^\dagger e^{-i\theta \hat{n}} = e^{i\theta} e^{-i\theta \hat{n}} \hat{a}^\dagger. \quad (\text{B.23})$$

Suppose now we have two set of oscillators (denoted by a and b respectively) with their own creation and annihilation operators. Let us define the following:

$$L_+ = a^\dagger b, L_- = b^\dagger a, K_+ = a^\dagger b^\dagger, K_- = ba \quad (\text{B.24})$$

Then we can compute:

$$[K_+, L_+] = a^\dagger b^\dagger a^\dagger b - a^\dagger b a^\dagger b^\dagger = a^\dagger a^\dagger b^\dagger b - a^\dagger a^\dagger b b^\dagger = -a^\dagger a^\dagger ([b, b^\dagger]) = -a^\dagger a^\dagger \quad (\text{B.25})$$

$$[K_-, L_+] = b a a^\dagger b - a^\dagger b b a = a a^\dagger b b - a^\dagger a b b = b b \quad (\text{B.26})$$

We can also compute the commutator of K_+ and K_- .

$$\begin{aligned} [K_+, K_-] &= a^\dagger b^\dagger b a - b a a^\dagger b^\dagger \\ &= a^\dagger b^\dagger b a - a a^\dagger b b^\dagger \\ &= a^\dagger b^\dagger b a - a^\dagger a b b^\dagger - b b^\dagger \\ &= a^\dagger a (b^\dagger b - b b^\dagger) - b b^\dagger \\ &= -a^\dagger a - 1 - b^\dagger b = -2K_3. \end{aligned} \quad (\text{B.27})$$

The operators K_+ , K_- , K_3 form a representation of the Lie algebra $\mathfrak{su}(1,1)$ and is the basis of Schwinger's work of rewriting the angular momentum in terms of oscillators.

$$e^A B e^{-A} = (I + A + \frac{1}{2!}A^2 + \frac{1}{3!}A^3 + \dots)(B - \frac{1}{1!}[A, B] + \frac{1}{2!}[A, [A, B]] - \frac{1}{3!}[A, [A, [A, B]]] + \dots) \quad (\text{B.28})$$

$$\begin{aligned} &= B + [A, B] + \frac{1}{2!}(A^2 B - AB^2 + [A, [A, B]]) + \frac{1}{3!}(A^3 B - A^2 B^2 + AB^3 - [A, [A, [A, B]]]) + \dots \\ &= B + \sum_{n=1}^{\infty} \frac{1}{n!} \sum_{k=0}^{n-1} (-1)^k A^k B \underbrace{A^{n-1-k}}_{(n-1-k) \text{ times}} - \sum_{n=1}^{\infty} \frac{1}{n!} \sum_{k=0}^{n-1} (-1)^k [A, [A, [\dots [A, B] \dots]]] \\ &= B + \sum_{n=1}^{\infty} \frac{1}{n!} \sum_{k=0}^{n-1} (-1)^k A^k B - \sum_{n=1}^{\infty} \frac{1}{n!} \sum_{k=0}^{n-1} (-1)^k [A, B_k] \\ &= B + \sum_{n=1}^{\infty} \frac{1}{n!} \sum_{k=0}^{n-1} [A, B_k]. \end{aligned}$$

where we have defined the nested commutator. There is another way to prove this using the idea of *parameter differentiation*. For this, consider $f(t)$ defined as $e^{tA} B e^{-tA}$ with $f(0) = B$. Then the derivatives are:

$$\begin{aligned} f'(t) &= e^{tA} A B e^{-tA} + e^{tA} B (-A) e^{-tA} = e^{tA} [A, B] e^{-tA}, \quad f'(0) = [A, B] \\ f''(t) &= e^{tA} [A, [A, B]] e^{-tA} \quad f''(0) = [A, [A, B]]. \end{aligned} \quad (\text{B.29})$$

Therefore, we can write:

$$f(t) = f(0) + t f'(0) + \frac{f''(0)}{2!} t^2 + \dots \quad (\text{B.30})$$

and setting $t = 1$, we get the desired expression. For $[A, B]$ central, i.e., commuting with both X and

Y i.e., $[A, [A, B]], [B, [A, B]] = 0$, we can also prove a general result. Let us denote $f(\epsilon) = e^{\epsilon A} e^{\epsilon B}$, then we have:

$$\begin{aligned} f'(\epsilon) &= A e^{\epsilon A} e^{\epsilon B} + e^{\epsilon A} e^{\epsilon B} B, \\ &= (A + e^{\epsilon A} B e^{-\epsilon A}) f(\epsilon), \\ &= (A + B + \epsilon [A, B]) f(\epsilon). \end{aligned} \quad (\text{B.31})$$

where we have used $e^{\epsilon A} B e^{-\epsilon A} = B + \epsilon [A, B]$. The solution of (B.31) is:

$$f(\epsilon) = \exp(\epsilon(A + B) + \frac{\epsilon^2}{2} [A, B]). \quad (\text{B.32})$$

Setting $\epsilon = 1$ above, the special case of BCH formula as:

$$e^A e^B = e^{A+B+\frac{1}{2}[X,Y]}. \quad (\text{B.33})$$

Another result that follows from BCH lemma is when the commutator of A and B is a c -number i.e., $[A, B] = c$ and $[A, [A, B]] = 0$. Then we get,

$$e^{\alpha A} B e^{-\alpha A} = B + \alpha c. \quad (\text{B.34})$$

If the nested first commutator is non-zero i.e., $[A, [A, B]] = \beta B$ then one can show that:

$$e^{\alpha A} B e^{-\alpha A} = B \cosh(\alpha \sqrt{\beta}) + [A, B] \frac{\sinh(\alpha \sqrt{\beta})}{\sqrt{\beta}}. \quad (\text{B.35})$$

Note that this reduces to former result since the $\beta \rightarrow 0$ limit of \sinh term is α . There is another useful theorem (often called similarity theorem):

$$e^{\alpha A} f(B) e^{-\alpha A} = f(e^{\alpha A} B e^{-\alpha A}) \quad (\text{B.36})$$

The proof is simple and proceeds as follows:

Proof. From the identity $[e^{\epsilon A} B e^{-\epsilon A}]^n = e^{\epsilon A} B^n e^{-\epsilon A}$, we find that the theorem follows if $f(B)$ can be expanded in power series. \square

Using this theorem, we can also obtain the following result:

$$\exp(-\alpha a^\dagger) f(a, a^\dagger) \exp(\alpha a^\dagger) = f(a + \alpha, a^\dagger) \quad (\text{B.37})$$

which also follows from (B.34) by setting $A = a^\dagger$ and $B = a$, and $c = -1$.

SECTION C

Sample programs using Qiskit

As mentioned before, QISKIT (pronounced kiss-kit) is a backend simulator created by IBM where we can build up a code which can then be sent to actual quantum hardware or quantum processing units (QPU) in use by companies like IBM, Amazon, Honeywell etc. This is like how commercial airline pilots train in a simulator when a new Boeing/Airbus aircraft is about to be launched⁴². Once we have sufficient practice, we can pass the quantum program to the real machines, but until we really need them for some problem, the simulator is good enough to learn and get acquainted with the fundamental working of the computation. We also note that the calculation of computation time and associated charges for quantum computing on real devices is not as straightforward as classical computers. For example, we will see below that to get reasonable output from the simulator, we have to perform a certain step number of times, which is referred to as ‘shot’ i.e., a

⁴²In fact, one of the reasons for the failure of 737 Max aircraft resulting in tragic accidents around 2019 is that even though some new systems were introduced, the pilots were never ordered to take the new simulator training because Boeing cited similarity with the ones they had already taken. It was however not true, and the cause of accidents (MCAS system) was indeed the crucial difference.

shot is a single execution of a quantum algorithm on a QPU. Depending on the quality of QPU, the per shot cost is determined. So, it might be that some quantum computing hardware company will charge 1 for 100 shots and some will charge the same for 1000 shots. The per-shot price is usually not affected by the number or type of gates used in a quantum circuit or the number of variables employed. The idea of shots is closely related to the errors in quantum computers, and it is to be expected that if there is a QPU with a well-defined error correcting procedure, then it will limit the number of shots needed considerably. Another part of the computation cost is based on number of ‘tasks’. A task is a sequence of successive shots using the same circuit design. QISKIT is made up of four elements, each of which has a specific functionality. These elements are Terra (Earth), Aer (Air), Ignis (Fire), and Aqua (Water). For example, the Aer provider contains a variety of high performance simulator backends for a variety of simulation methods. The available backends on the current system can be viewed using `Aer.backends()` in a Jupyter notebook.

This open-source software platform enables one to work with the quantum language Open Quantum Assembly Language (Open QASM), used in quantum computers in the IBM. We encourage the reader to read more about them if interested in Ref. [55]. Here, we will briefly summarize the different core modules of QISKIT for convenience. The Qiskit open-source development library is composed of four core modules:

- Qiskit Terra: This contains core elements to create quantum programs at the circuit/pulses level as well as to optimize these core elements by considering the particular physical quantum processor constraints.
- Qiskit Aer: This provides a C++ simulator framework and tools to develop noise models to conduct realistic simulations in the presence of noise and errors occurring during execution on real quantum devices.
- Qiskit Ignis: This provides a framework to understand the noise sources in the quantum circuits/devices as well as to develop different noise reduction procedures.
- Qiskit Aqua: This contains a library of cross-domain quantum algorithms suitable for application in the NISQ era.

The syntax of QISKIT consists of following high-level steps: 1. Building step in which we design a quantum circuit that represents the problem at hand, 2. The execution step in which we run experiments on different backends (including both actual quantum hardware and simulators), and the last is the analysis step where one summarizes the statistics and visualize the results. The SDK we will focus on in these notes deals with systems with finite local Hilbert space of $d = 2$ (qubits) or maybe some generalization to qudits too ($d > 2$) but they are often not the best way for bosonic states which have infinite sized vector space. For these models, it is often more practical to make use of what is called *qumodes* which are continuous-variable quantum modes. Very recently, an open-source software was introduced in Ref. [115] which extends QISKIT to admit bosonic degrees

of freedom. This enables the simulation of hybrid qubit and bosonic systems such as bosonic Hubbard models, Jaynes-Cummings etc. However, the support for parametrized circuits⁴³ is still in development phase. Another open-source project which is probably better suited for ground state energy computation of bosonic models is Xanadu’s **Strawberry Fields**, which is a full-stack Python library for designing, optimizing, and utilizing photonic quantum computers (analog computing). Using continuous variables (CV) instead of the more traditional qubits (digital) approach has both advantages and disadvantages. Some groups [69] have explored the use of QITE (quantum imaginary-time evolution) to study the ground state energy using CVs. This approach might also be useful in the future for other interesting models such as ϕ^4 -theory. Though the scope of this discussion lies beyond the scope of the current article, we will briefly mention some differences to qubit approach. The CV approach to quantum computing keeps the same computational power of the qubit model. This approach utilizes the infinite-dimensional bosonic mode called ‘qumodes’. While the qubits make use of discrete coefficients, the CV model makes use of bosonic harmonic oscillator, which is defined by the operators a and a^\dagger satisfying $[a, a^\dagger] = 1$ and where $|x\rangle$ are the eigenstates of x operator defined in terms of a, a^\dagger . In this approach, the information about input states are stored in terms of Gaussian states which are non-classical states with Gauss-Wigner quasi-probabilistic functions.

C.1 Installing package and quantum hello world

In this section, we will provide several codes related to sections in the main text. The easiest way is to visit Google’s Colab⁴⁴ and open a new Jupyter notebook. We can install QISKIT by doing: `!pip install qiskit ipywidgets`. A simple check that everything is installed properly is to write this short piece of code and run it.

```
1  from qiskit import *
2  qc = QuantumCircuit(2); # Circuit of two qubits
3  # This is equivalent to QuantumCircuit(2,0) i.e., 2 qubits and no classical bits
4  qc.h(0); # Apply Hadamard gate to the first qubit
5  qc.draw() # Draw the circuit
6
```

We then extend this to write our first ‘quantum’ code given below:

```
1  # Welcome to "Hello World" for quantum computing
2  from qiskit import *
3  from qiskit import QuantumCircuit, assemble, Aer
4  from qiskit.visualization import plot_bloch_multivector, plot_histogram
```

⁴³Parameterized quantum circuits consist of quantum gates defined through tunable parameters. They are fundamental building blocks of majority of near-term quantum machine learning algorithms

⁴⁴<https://research.google.com/colaboratory>

```

5  sim = Aer.get_backend('aer_simulator')
6
7  def x_measurement(qc, qubit, cbit):
8      qc.h(qubit) # Apply Hadamard to get superposition
9      qc.measure(qubit, cbit)
10     # Measure 'qubit' in the X-basis, and store the result in 'cbit'
11     return qc
12
13  qc = QuantumCircuit(1,1); # Initialize one quantum and one classical bit.
14  x_measurement(qc, 0, 0)
15  qobj = assemble(qc) # Assemble circuit to run
16  counts = sim.run(qobj).result().get_counts() # Do the simulation, returning the state vector
17  print (counts) # Count the occurrences
18  plot_histogram(counts) # Display the output as a histogram
19

```

C.2 Some basic operations using qubits and gates

Let us initialize two qubits in $|0\rangle$ each. We can apply Hadamard gate to the first qubit and then feed them through CNOT gate. It is easy to check that it generates the output as: $(1/\sqrt{2})(|00\rangle + |11\rangle)$. We provide the code below to compute this out state and check that it agrees with the expectations. We leave this to the reader.

```

1  from qiskit import *
2  from qiskit.quantum_info import Statevector
3  from qiskit.visualization import plot_bloch_multivector, plot_histogram, array_to_latex
4  qc = QuantumCircuit(2);
5  qc.h(0);
6  qc.draw()
7  q2 = qc.cx(0,1);
8  bell = Statevector.from_instruction(qc)
9  display(array_to_latex(bell, prefix="\\text{Statevector} = "))
10

```

It is easy to generate $d = 2^n$ -dimensional state vector using a short program and then view it on the Bloch sphere. Suppose we take $n = 2$ (two qubits) and generate a random state $|\psi\rangle$. It can be done as given below. Running this different times will move the arrow (on the Bloch sphere) corresponding to different random state. The reader is encouraged to check that they are appropriately normalized, i.e., $\langle\psi|\psi\rangle = 1$. The output on the Bloch sphere for a random state looks like that given in Fig. 16. Note that orthogonal states (such as $|0\rangle$ and $|1\rangle$) are antipodal on the Bloch sphere.

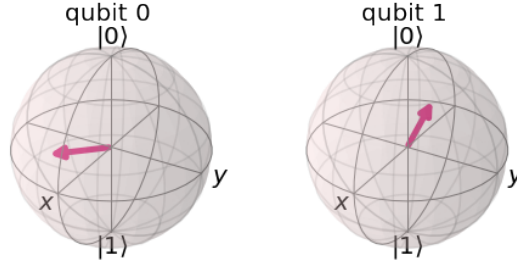


Figure 16. A random two-qubit state depicted on the sphere.

```

1 from qiskit.quantum_info import random_statevector, Statevector
2 from qiskit.visualization import plot_bloch_multivector
3
4 rand_sv = random_statevector(4).data
5 print(rand_sv)
6 plot_bloch_multivector(rand_sv)
7

```

Now, since we have a bipartite random state, we can compute EOF as discussed in Sec. 3.3.2. For example, if we compute this for Bell state mentioned above, it will be 1 (maximally entangled). We give the code below:

```

1 from qiskit import *
2 from qiskit.quantum_info import *
3
4 rand_sv = random_statevector(4).data
5 print("Entanglement of Formation = ", entanglement_of_formation(rand_sv))
6

```

► **QUESTION 21:** Set up a quantum circuit using QISKIT to create the state given by Eq. ?? and show that it is not entangled.

Let us now show the program to implement CSWAP gate as discussed in the text using QISKIT. Note that if we take $q_0 = |+\rangle$, $q_1 = |0\rangle$, and $q_2 = |1\rangle$, then the action of CSWAP looks like:

$$|1\rangle \otimes |0\rangle \otimes (1/\sqrt{2})(|0\rangle + |1\rangle) = \frac{1}{\sqrt{2}}(|100\rangle + |101\rangle) \xrightarrow{\text{CSWAP}} \frac{1}{\sqrt{2}}(|100\rangle + |011\rangle) \quad (\text{C.1})$$

```

1  from qiskit import *
2  from qiskit.quantum_info import *
3  from qiskit.visualization import *
4
5  qc = QuantumCircuit(3)
6  qc.h(0);
7  qc.x(2);
8  st = Statevector.from_instruction(qc)
9  display(array_to_latex(st, prefix="\text{In state} = "))
10 qc.cswap(0,1,2)
11 st = Statevector.from_instruction(qc)
12 display(array_to_latex(st, prefix="\text{Out state} = "))
13 qc.draw()
14

```

In the program above, we have used `qc.cswap(0,1,2)` to implement CSWAP. Suppose we do not have this three qubit gate and only have access to CNOT gate. We encourage the reader to write the equivalent program. We can also entangle n qubits (using GHZ state construction) as follows:

```

1  from qiskit import *
2  from qiskit.visualization import *
3  from qiskit.quantum_info import *
4
5  # We will now construct GHZ state
6  qn = 5 # five qubit GHZ
7
8  circ = QuantumCircuit(qn)
9  circ.h(0)
10 circ.cx(0, 1)
11 circ.cx(0, 2)
12 circ.cx(0, 3)
13 circ.cx(0, 4)
14 circ.draw()
15 ghz = Statevector.from_instruction(circ)
16 display(array_to_latex(ghz, prefix="\text{Statevector} = "))
17

```

Suppose we prepare some initial state and someone applies a quantum gate in our absence, is there a way in QISKIT to see what this transformation was? The way to do it, this is (apart from usual stuff):

```

1  job = execute(qc, Aer.get_backend('unitary_simulator'))
2  result = job.result()
3  print(result.get_unitary(qc, decimals=3))

```


4

We now turn to the computation of fidelity of two states which was discussed in the main text. Consider two-states given by:

$$|\psi\rangle = \frac{1}{2}(|001\rangle + |101\rangle - |011\rangle - |111\rangle),$$

and

$$\frac{1}{\sqrt{2}}(|000\rangle + |111\rangle).$$

Compute the fidelity between them using QISKIT.

```

1  from qiskit import *
2  from qiskit.quantum_info import *
3  from qiskit.visualization import *
4  from numpy import *
5
6  qc1 = QuantumCircuit(3)
7  qc1.h(0);
8  qc1.h(1);
9  qc1.x(2);
10 qc2 = QuantumCircuit(3)
11 qc2.h(0)
12 qc2.cx(0,1);
13 qc2.cx(0,2);
14
15 backend = Aer.get_backend('statevector_simulator')
16 sv1 = execute(qc1, backend).result().get_statevector(qc1)
17 sv2 = execute(qc2, backend).result().get_statevector(qc2)
18 print(state_fidelity(sv1, sv2))
19

```

C.3 Quantum full-adder

Similar to the classical logic gates where one can implement full-adder, we can do similar operation using quantum gates. The code is given below.

```

1  # Quantum full-adder program
2
3  from qiskit import *
4  from qiskit.visualization import *
5
6  qc = QuantumCircuit(4,2)
7
8  # Preparing inputs
9  # We do: A and B to a Bell state and CarryIn to a superposition state

```



```

13     for qubit in range(nqubits):
14         qc.h(qubit)
15
16     # Apply transformation  $|0 \dots 0\rangle \rightarrow |1 \dots 1\rangle$  (X-gates)
17     for qubit in range(nqubits):
18         qc.x(qubit)
19
20     # *****
21     # Do multi-controlled-Z gate
22     # by using Multi controlled Toffoli
23     # Recall that  $HXH = Z$ 
24     qc.h(nqubits-1)
25     qc.mct(list(range(nqubits-1)), nqubits-1) # Multi-controlled
26     qc.h(nqubits-1)
27     # *****
28
29     # Now X to all
30     # Apply transformation  $|1 \dots 1\rangle \rightarrow |0 \dots 0\rangle$ 
31     for qubit in range(nqubits):
32         qc.x(qubit)
33
34     # Apply transformation  $|0 \dots 0\rangle \rightarrow |s\rangle$ 
35     for qubit in range(nqubits):
36         qc.h(qubit)
37
38     # We will return the diffuser as a gate
39     U_s = qc.to_gate()
40     U_s.name = "Diffuser (D)"
41     return U_s
42
43
44 oracle = QuantumCircuit(n, name = 'Oracle (O)')
45
46 if n == 2:
47     oracle.cz(0,1)
48 if n == 3:
49     oracle.cz(1, 2)
50
51 oracle.to_gate()
52 # Oracle is CZ gate. This will change based on target state.
53 # We provide two example  $|11\rangle$  and  $|110\rangle$ 
54
55 backend = Aer.get_backend('statevector_simulator')
56 gro_circ = QuantumCircuit(n,n)
57 gro_circ.h(list(range(n)))
58 gro_circ.append(oracle,list(range(n)))

```

```

59
60 gro_circ.append(diffuser(n),list(range(n)))
61
62 backend = Aer.get_backend('qasm_simulator')
63 gro_circ.measure([0,1],[0,1])
64 job = execute(gro_circ,backend, shots=1)
65 result = job.result()
66 result.get_counts()

```

C.5 Implementing QFT

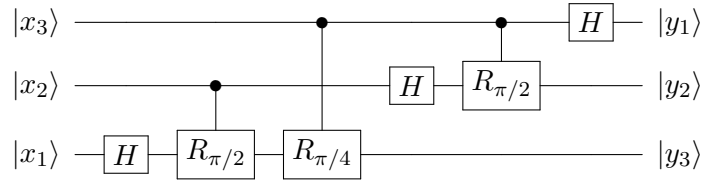
We now discuss the implementation of quantum Fourier transform in QISKIT. This makes use of two quantum gates, which we have already seen a lot of. The first is the Hadamard gate, the other is the controlled phase gate R . The matrix representation of these gates are given below:

$$H = \frac{1}{\sqrt{2}} \begin{bmatrix} 1 & 1 \\ 1 & -1 \end{bmatrix}, \quad (C.3)$$

while the rotation matrices are interchangeably defined as both:

$$R_k = \begin{bmatrix} 1 & 0 \\ 0 & \exp\left(\frac{2\pi i}{2^k}\right) \end{bmatrix}, \quad R_\theta = \begin{bmatrix} 1 & 0 \\ 0 & e^{i\theta} \end{bmatrix} \quad (C.4)$$

The simplified QFT circuit for three qubits is given below, while the program in QISKIT below is for general n -qubit case.



The code is given below:

```

1  # QuantumFourier program
2
3  from qiskit import *
4  from numpy import *
5  from qiskit.quantum_info import *
6  from qiskit.visualization import *
7
8
9  def qft_rotations(circuit, n):
10
11      if n == 0:
12          return circuit
13
14      n -= 1

```

```

15     circuit.h(n)
16
17     for qubit in range(n):
18         circuit.cp(pi/2**(n-qubit), qubit, n)
19
20     qft_rotations(circuit, n)
21
22
23 def swap_registers(circuit, n):
24
25     for qubit in range(n//2):
26         circuit.swap(qubit, n-qubit-1)
27     return circuit
28
29
30 def qft(circuit, n):
31
32     qft_rotations(circuit, n) # Goes in a circle until all done
33     swap_registers(circuit, n)
34     return circuit
35
36
37 nbits = 3 # number of qubits
38 N = 2**nbits
39 # So for this case it will be QFT_8
40
41 qc = QuantumCircuit(nbits)
42
43 # If done nothing, encodes 000 [i.e., all qubits set to 0 i.e., |000>]
44 # We will try encoding 5 i.e., |101>
45 qc.x(0)
46 qc.x(2)
47
48 sim = Aer.get_backend("aer_simulator")
49 qc_init = qc.copy()
50 qc_init.save_statevector()
51 statevector = sim.run(qc_init).result().get_statevector()
52 plot_bloch_multivector(statevector, title= "Before: |101> := |dud> ")
53
54 # Apply QFT
55
56 qft(qc,nbits)
57 #qc.draw()
58
59 psi_AB = Statevector.from_instruction(qc)
60 plot_bloch_multivector(psi_AB, title= "After: QFT_8|101>")

```

C.6 Bit-flip code, Phase kickback

```
1 # A simple example of how the bit flip of q0 can be corrected
2 # This version can be modified to do bit flip with probability 'p' < 1
3
4 from qiskit import *
5 from qiskit import Aer
6
7 backend = Aer.get_backend('qasm_simulator')
8 circuit = QuantumCircuit(3,1)
9
10 # Encode
11 circuit.cx(0,1)
12 circuit.cx(0,2)
13
14 # Noise
15 circuit.x(0) # Impose a bit flip error by Pauli X
16
17 # Decode
18 circuit.cx(0,1)
19 circuit.cx(0,2)
20 circuit.ccx(2,1,0)
21 circuit.measure(0,0)
22
23 job = execute(circuit, backend, shots=1024)
24 counts = job.result().get_counts()
25 print(counts)
```

Now we do phase kickback to reproduce the state mentioned in (4.2) with $\phi = \pi/4$.

```
1 # Phase kickback
2
3 from qiskit import *
4 from numpy import *
5 from qiskit.quantum_info import Statevector
6 from qiskit.visualization import plot_bloch_multivector, plot_histogram, array_to_latex
7
8 def phase_kickback():
9     qreg = QuantumRegister(2, 'q')
10     qc1 = QuantumCircuit(qreg)
11     qc1.x(qreg[1])
12     qc1.h(qreg[0])
13     qc1.cp(pi/4, 0, 1) # Controlled T
14     return qc1
15
16 qc = phase_kickback()
```

```

17 qc.draw()
18 co = Statevector.from_instruction(qc)
19 plot_bloch_multivector(co)
20 # We can see the qubit 0 has been rotated by pi/4 around
21 # the Z-axis of the Bloch sphere as expected.

```

C.7 VQE solution to anharmonic quantum oscillator for three qubits

In this section, we provide code which accompanies Sec. 5.1. We first decompose the Hamiltonian in terms of Paulis operators and then use it as input to VQE solver by defining some appropriate ansatz.

```

1  #!pip install qiskit ipywidgets
2  import numpy as np
3  import math
4  import time
5  import warnings
6  import itertools
7  from qiskit import Aer
8  from qiskit.algorithms import VQE
9  from qiskit.opflow import MatrixOp
10 from qiskit.opflow import X, Y, Z, I
11 from qiskit.algorithms.optimizers import SLSQP
12 from qiskit.algorithms.optimizers import COBYLA
13 from qiskit.circuit.library import EfficientSU2
14 from qiskit.utils import algorithm_globals, QuantumInstance
15 from qiskit.visualization.array import array_to_latex
16
17 def decompose(H):
18
19     def dagger(a):
20         return np.transpose(a).conj()
21
22     def HS(M1, M2):
23         # Hilbert-Schmidt prod. of two matrices
24         return np.trace(dagger(M1) @ M2)
25
26     def c2s(c):
27         if c == 0.0:
28             return "0"
29         if c.imag == 0:
30             return "%g" % c.real
31         elif c.real == 0:
32             return "%gj" % c.imag
33         else:
34             return "%g+%gj" % (c.real, c.imag)

```

```

35
36 sx = np.array([[0, 1], [ 1, 0]], dtype=np.complex128)
37 sy = np.array([[0, -1j], [1j, 0]], dtype=np.complex128)
38 sz = np.array([[1, 0], [0, -1]], dtype=np.complex128)
39 id = np.array([[1, 0], [ 0, 1]], dtype=np.complex128)
40 S = [id, sx, sy, sz]
41 labels = ['I', "X", "Y", "Z"]
42 final = ""
43
44 if nbits == 2:
45     for i, j in itertools.product(range(4), range(4)):
46         a = (1/2**nbits) * HS(np.kron(S[i], S[j]), H)
47         # Formula: (1/2^2) (Si otimes Sj) dot H
48         if a != 0.0:
49             term = c2s(a), '*', labels[i], '^', labels[j]
50             t2 = str(term).replace(',', ', ')
51             t2 = str(t2).replace("'", "")
52
53             if final == "":
54                 final = "".join((final, t2))
55             else:
56                 final = "+".join((final, t2))
57
58 if nbits == 3:
59     for i, j, k in itertools.product(range(4), range(4), range(4)):
60         a = (1/2**nbits) * HS(np.kron(np.kron(S[i], S[j]), S[k]), H)
61
62         if a != 0.0:
63             term = c2s(a), '*', labels[i], '^', labels[j], '^', labels[k]
64             t2 = str(term).replace(',', ', ')
65             t2 = str(t2).replace("'", "")
66
67             if final == "":
68                 final = "".join((final, t2))
69             else:
70                 final = "+".join((final, t2))
71
72     return final
73
74
75 # Alternative way
76
77 def numberToBase(n, b, n_qubits):
78     if n == 0:
79         return np.zeros(n_qubits, dtype=int)
80     digits = np.zeros(n_qubits, dtype=int)

```



```

81     counter = 0
82     while n:
83         digits[counter] = int(n % b)
84         n //= b
85         counter += 1
86     return digits[::-1]
87
88 def decomposePauli(H):
89
90     sx = np.array([[0, 1], [1, 0]], dtype=np.complex128)
91     sy = np.array([[0, -1j], [1j, 0]], dtype=np.complex128)
92     sz = np.array([[1, 0], [0, -1]], dtype=np.complex128)
93     id = np.array([[1, 0], [0, 1]], dtype=np.complex128)
94     S = [id, sx, sy, sz]
95     dim_matrix=np.shape(H)[0]
96     n_qubits=int(np.log2(dim_matrix))
97     if(dim_matrix != 2**n_qubits):
98         raise NameError("Matrix is not power of 2!")
99     hilbertspace = 2**n_qubits
100     n_paulis = 4**n_qubits
101     pauli_list = np.zeros([n_paulis,n_qubits],dtype=int)
102     for k in range(n_paulis):
103         pauli_list[k,:] = numberToBase(k,4,n_qubits)
104     weights = np.zeros(n_paulis,dtype=np.complex128)
105     for k in range(n_paulis):
106         pauli=S[pauli_list[k][0]]
107
108         for n in range(1,n_qubits):
109             pauli = np.kron(pauli,S[pauli_list[k][n]])
110         weights[k] = 1/hilbertspace* np.dot(pauli,H).trace()
111
112     nnz = [i for i, e in enumerate(weights) if e != 0]
113     for i in nnz:
114         print (weights[i],pauli_list[i])
115
116
117 # Yet another way
118 def decompose_ham_to_pauli(H):
119
120     n = int(np.log2(len(H)))
121     N = 2 ** n
122     # Basic checks!
123
124     if H.shape != (N, N):
125         raise ValueError("The Hamiltonian should have shape (2**n, 2**n), for any qubit
        number n>=1")

```

```

126
127     if not np.allclose(H, H.conj().T):
128         raise ValueError("The Hamiltonian is not Hermitian")
129
130     sI = np.eye(2, 2, dtype=complex)
131     sX = np.array([[0, 1], [1, 0]], dtype=complex)
132     sZ = np.array([[1, 0], [0, -1]], dtype=complex)
133     sY = complex(0, -1)*np.matmul(sZ, sX)
134     paulis = [sI, sX, sY, sZ]
135     paulis_label = ['I', 'X', 'Y', 'Z']
136     obs = []
137     coeffs = []
138     matrix = []
139
140     for term in itertools.product(paulis, repeat=n):
141         matrices = [pauli for pauli in term]
142         coeff = np.trace(ft.reduce(np.kron, matrices) @ H) / N
143         coeff = np.real_if_close(coeff).item()
144
145         if not np.allclose(coeff, 0):
146             coeffs.append(coeff)
147             obs.append(''.join([paulis_label[[i for i, x in enumerate(paulis)
148                 if np.all(x == t)]] [0]] + str(idx) for idx, t in enumerate(reversed(term))))
149             matrix.append(ft.reduce(np.kron, matrices))
150
151     return obs, coeffs, matrix
152
153
154 g = 0.02 # Coupling used to create ham_H0.txt as input to this code
155 H = np.loadtxt("ham_H0.txt", dtype='f', delimiter='\t')
156 nbits = math.log2(np.shape(H)[0])
157
158 # Two options until nbits=3.
159
160 qubitOp = MatrixOp(primitive=H)
161 Hps = decompose(H)
162 print (Hps)
163
164 Hps = (4 * I ^ I ^ I) + (-0.152955 * I ^ I ^ X) + (-0.5 * I ^ I ^ Z) + (-0.12289 * I ^ X ^
    X) + (-0.0629948 * I ^ Y ^ Y) + (-1 * I ^ Z ^ I) + (0.0237627 * I ^ Z ^ X) + (-0.0280252 * X ^ I
    ^ X) + (-0.0561195 * X ^ X ^ X) + (0.0287333 * X ^ Y ^ Y) + (0.0107047 * X ^ Z ^ X) + (-0.0280252
    * Y ^ I ^ Y) + (-0.0287333 * Y ^ X ^ Y) + (-0.0561195 * Y ^ Y ^ X) + (0.0107047 * Y ^ Z ^
    Y) + (-2 * Z ^ I ^ I) + (0.0872346 * Z ^ I ^ X) + (0.0842295 * Z ^ X ^ X) + (0.041655 * Z ^ Y ^
    Y) + (0.0207442 * Z ^ Z ^ X)
165 # Nice formatting using LaTeX
166 # H_matrix = H.to_matrix()

```

```

167 # array_to_latex(H_matrix)
168
169 start_time = time.time()
170 var_form = EfficientSU2(qubitOp.num_qubits, su2_gates=['ry'], entanglement="full", reps=1)
171
172 rngseed = 5
173 warnings.filterwarnings("ignore")
174 backend = Aer.get_backend("statevector_simulator", max_parallel_threads=1,
175                             max_parallel_experiments=0)
176 q_instance = QuantumInstance(backend, seed_transpiler=rngseed, seed_simulator=rngseed)
177 #optimizer = SLSQP(maxiter=600)
178 optimizer = COBYLA(maxiter=600)
179 # COBYLA works little better!
180
181 # Run the VQE
182 vqe = VQE(ansatz=var_form, optimizer=optimizer, quantum_instance=q_instance)
183 ret = vqe.compute_minimum_eigenvalue(Hps)
184 vqe_result = np.real(ret.eigenvalue)
185 print("VQE Result:", vqe_result)
186 exact = 0.5 - (11/8)*g*g - (465/32)*g*g*g*g
187 print ("Exact result for cubic oscillator upto 0(g^4) is", exact)
188 print ("Error is", np.round(abs((exact-vqe_result)/exact)*100,10), "percent")
189 end_time = time.time()
190 runtime = end_time-start_time
191 print('Program runtime: ',runtime, "seconds")
192
193 # WCUBIC[n_, g_] := (n + 0.5) - ( 45 g^2)/12 (n^2 + n + 11/30);

```

It returns an output given below:

VQE Result: 0.4994476532684504

Exact result for cubic oscillator upto 0(g⁴) is 0.499447675

Error is 4.3511e-06 percent

Program runtime: 2.118819236755371 seconds

C.8 Phase estimation

We provide in this subsection the code to estimate the phase as discussed in the main text.

```

1 from qiskit import *
2 from qiskit.quantum_info import *
3 from qiskit.visualization import *
4 from numpy import *
5 import sys
6
7 qbits=4
8 cbits=3

```

```

9  theta= 2*pi*(1/4) # Actually \theta is without 2*pi but abuse notation!
10 qc = QuantumCircuit(qbits, cbits)
11
12 def qft_dagger(qc, n):
13
14     # Swap is crucial. Remove this to see change in result
15     for qubit in range(n//2):
16         qc.swap(qubit, n-qubit-1)
17         for j in range(n):
18             for m in range(j):
19                 qc.cp(-pi/float(2**(j-m)), m, j)
20             qc.h(j)
21
22     for qubit in range(3):
23         qc.h(qubit)
24
25     qc.x(qbits-1) # Initialize |psi> to |1>
26
27     sheets = 1
28     for qubit_first_reg in range(qbits-1):
29         for i in range(sheets):
30             qc.cp(theta, qubit_first_reg, qbits-1); # Target is last qubit (i.e. first qubit of
31                 second register)
32             sheets *= 2
33
34     # Apply inverse QFT
35     qft_dagger(qc, qbits-1)
36     # Measure
37     qc.barrier()
38     for n in range(3):
39         qc.measure(n,n)
40
41     # Get results and plot
42
43     backend = Aer.get_backend('aer_simulator')
44     job = execute(qc,backend,shots=2048)
45     result = job.result()
46     count = result.get_counts()
47     plot_histogram(count)

```

C.9 Decomposing any unitary in single-qubit and CNOT gates

In this subsection, we provide the code which reproduces the gate count of the shown in Fig. 6.

```

1  import numpy as np
2  from qiskit import QuantumCircuit, QuantumRegister

```

```

3 from qiskit.quantum_info.synthesis import two_qubit_decompose
4 from qiskit.compiler import transpile
5
6
7
8 def random_unitary_matrix(n):
9     # Generate a random complex matrix
10    mat = np.random.randn(n, n) + 1j * np.random.randn(n, n)
11    # Compute the QR decomposition
12    q, r = np.linalg.qr(mat)
13    # Return the unitary matrix
14    return q
15
16
17 def quantum_shannon_decomposition(circuit, unitary_matrix, qubits):
18     # Create a temporary circuit with the desired number of qubits
19     temp_qubits = QuantumRegister(len(qubits))
20     temp_circuit = QuantumCircuit(temp_qubits)
21
22     # Apply the unitary operator to the temporary circuit
23     temp_circuit.unitary(unitary_matrix, qubits)
24
25
26     # Decompose each two-qubit gate in the temporary circuit
27     decomposed_circuit = transpile(temp_circuit, basis_gates=['ry', 'rx', 'cx'],
28     optimization_level = 2)
29     # 3 is highest optimization in QISKIT or ibmq
30
31     # Apply the decomposed gates to the original circuit
32     circuit.compose(decomposed_circuit, qubits, inplace=True)
33
34 # Example usage
35 qubits=3
36 qubits = [i for i in range(0, qubits)]
37
38 # Create a quantum circuit
39 circuit = QuantumCircuit(qubits)
40 # Apply the Quantum Shannon Decomposition
41 unitary_matrix = random_unitary_matrix(2**qubits)
42 quantum_shannon_decomposition(circuit, unitary_matrix, qubits)
43
44 print(dict(circuit.count_ops()))

```

C.10 Sample Mathematica code for to compute vN entropy

We need to install the appropriate package (as discussed in Sec. 3.3.2) and then execute the commands below.

```

1  ent = Sqrt[1/2]*(KetV[0,2] \[CircleTimes] KetV[0,2]+ KetV[1,2] \[CircleTimes] KetV[1,2])
2  rho12 = DM[ent];
3  rhonew = {{5/12, 1/6, 1/6}, {1/6, 1/6, 1/6}, {1/6, 1/6, 5/12}};
4  vNEntropy[rhonew, {1}, {3}]*Log[2] // N
5  rho1 = PickRandomRho[4];
6  rho2 = PickRandomRho[4];
7  Chop[RelEnt[rho1, rho2]]
8  rstate = PickRandomRho[4]
9  vNEntropy[rstate, {1}, {4}] * Log[2]
10

```

References

- [1] R. Landauer, “Information is physical,” *Physics Today* **44** no. 5, (May, 1991) 23–29. <https://doi.org/10.1063%2F1.881299>.
- [2] R. Landauer, “The physical nature of information,” *Physics Letters A* **217** no. 4-5, (Jul, 1996) 188–193. <https://doi.org/10.1016%2F0375-9601%2896%2900453-7>.
- [3] J. Preskill, “Quantum information and physics: some future directions,” *J. Mod. Opt.* **47** (2000) 127–137, [arXiv:quant-ph/9904022](https://arxiv.org/abs/quant-ph/9904022).
- [4] R. Landauer, “Irreversibility and heat generation in the computing process,” *IBM Journal of Research and Development* **5** no. 3, (Jul, 1961) 183–191. <https://doi.org/10.1147%2Frd.53.0183>.
- [5] C. H. Bennett, “The thermodynamics of computation—a review,” *International Journal of Theoretical Physics* **21** no. 12, (Dec, 1982) 905–940. <https://doi.org/10.1007%2Fbfb02084158>.
- [6] P. Benioff, “The computer as a physical system: A microscopic quantum mechanical hamiltonian model of computers as represented by turing machines,” *Journal of Statistical Physics* **22** no. 5, (May, 1980) 563–591. <https://doi.org/10.1007%2Fbfb01011339>.
- [7] P. Benioff, “Quantum mechanical hamiltonian models of turing machines,” *Journal of Statistical Physics* **29** no. 3, (Nov., 1982) 515–546.
- [8] C. H. Bennett, “Logical reversibility of computation,” *IBM Journal of Research and Development* **17** no. 6, (Nov, 1973) 525–532. <https://doi.org/10.1147%2Frd.176.0525>.
- [9] Y. Manin, “Computable and Uncomputable (in Russian),” 1980.
- [10] R. P. Feynman, “Simulating physics with computers,” *International Journal of Theoretical Physics* **21** no. 6, (1982) 467–488.
- [11] M. A. Nielsen and I. L. Chuang, *Quantum Computation and Quantum Information: 10th Anniversary Edition*. Cambridge University Press, USA, 10th ed., 2011.
- [12] P. W. Shor, “Introduction to Quantum Algorithms,” *arXiv e-prints* (Apr., 2000) quant-ph/0005003, [arXiv:quant-ph/0005003](https://arxiv.org/abs/quant-ph/0005003) [quant-ph].
- [13] D. P. DiVincenzo, “The physical implementation of quantum computation,” *Fortschritte der Physik* **48** no. 9-11, (Sep, 2000) 771–783. <https://doi.org/10.1002%2F1521-3978%28200009%2948%3A9%2F11%3C771%3A%3Aaid-prop771%3E3.0.co%3B2-e>.
- [14] S. P. Jordan, H. Krovi, K. S. M. Lee, and J. Preskill, “BQP-completeness of Scattering in Scalar Quantum Field Theory,” *Quantum* **2** (2018) 44, [arXiv:1703.00454](https://arxiv.org/abs/1703.00454) [quant-ph].
- [15] S. Aaronson and L. Chen, “Complexity-theoretic foundations of quantum supremacy experiments,” 2016. <https://arxiv.org/abs/1612.05903>.
- [16] <https://ai.googleblog.com/2019/10/quantum-supremacy-using-programmable.html>.
- [17] P. A. M. Dirac, “A new notation for quantum mechanics,” *Mathematical Proceedings of the Cambridge Philosophical Society* **35** no. 3, (Jul, 1939) 416–418. <https://doi.org/10.1017%2Fs0305004100021162>.

- [18] Y. Shi, “Both toffoli and controlled-not need little help to do universal quantum computation,” *arXiv preprint quant-ph/0205115* (2002) .
- [19] D. Aharonov, “A simple proof that toffoli and hadamard are quantum universal,” *arXiv preprint quant-ph/0301040* (2003) .
- [20] V. V. Shende and I. L. Markov, “On the CNOT-cost of TOFFOLI gates,” *arXiv e-prints* (Mar., 2008) arXiv:0803.2316, arXiv:0803.2316 [quant-ph] .
- [21] G. J. Milburn, “Quantum optical fredkin gate,” *Phys. Rev. Lett.* **62** (May, 1989) 2124–2127. <https://link.aps.org/doi/10.1103/PhysRevLett.62.2124>.
- [22] R. P. Feynman, “Quantum mechanical computers,” *Foundations of Physics* **16** no. 6, (1986) 507–531.
- [23] W. Dür, G. Vidal, and J. I. Cirac, “Three qubits can be entangled in two inequivalent ways,” *Physical Review A* **62** no. 6, (Nov, 2000) . <https://doi.org/10.1103/PhysRevA.62.062314>.
- [24] P. Boykin, T. Mor, M. Pulver, V. Roychowdhury, and F. Vatan, “A new universal and fault-tolerant quantum basis,” *Information Processing Letters* **75** no. 3, (Aug, 2000) 101–107. [https://doi.org/10.1016/S0020-0190\(2000\)0084-3](https://doi.org/10.1016/S0020-0190(2000)0084-3).
- [25] A. Y. Kitaev, “Quantum computations: algorithms and error correction,” *Russian Mathematical Surveys* **52** no. 6, (Dec, 1997) 1191–1249. <https://doi.org/10.1070/2Frm1997v052n06abeh002155>.
- [26] A. Barenco, C. H. Bennett, R. Cleve, D. P. DiVincenzo, N. Margolus, P. Shor, T. Sleator, J. A. Smolin, and H. Weinfurter, “Elementary gates for quantum computation,” *Phys. Rev. A* **52** (Nov, 1995) 3457–3467. <https://link.aps.org/doi/10.1103/PhysRevA.52.3457>.
- [27] C. M. Dawson and M. A. Nielsen, “The solovay-kitaev algorithm,” 2005. <https://arxiv.org/abs/quant-ph/0505030>.
- [28] D. P. DiVincenzo and J. Smolin, “Results on two-bit gate design for quantum computers,” *arXiv e-prints* (Sept., 1994) cond-mat/9409111, arXiv:cond-mat/9409111 [cond-mat] .
- [29] A. Barenco, “A Universal two bit gate for quantum computation,” *Proc. Roy. Soc. Lond. A* **449** (1995) 679, arXiv:quant-ph/9505016.
- [30] Y. Shi, “Both Toffoli and Controlled-NOT need little help to do universal quantum computation,” *arXiv e-prints* (May, 2002) quant-ph/0205115, arXiv:quant-ph/0205115 [quant-ph] .
- [31] D. Aharonov, “A Simple Proof that Toffoli and Hadamard are Quantum Universal,” *arXiv e-prints* (Jan., 2003) quant-ph/0301040, arXiv:quant-ph/0301040 [quant-ph] .
- [32] V. Shende, S. Bullock, and I. Markov, “Synthesis of quantum-logic circuits,” *IEEE Transactions on Computer-Aided Design of Integrated Circuits and Systems* **25** no. 6, (June, 2006) 1000–1010. <https://doi.org/10.1109/tcad.2005.855930>.
- [33] S. Hill and W. K. Wootters, “Entanglement of a pair of quantum bits,” *Physical Review Letters* **78** no. 26, (Jun, 1997) 5022–5025. <https://doi.org/10.1103/PhysRevLett.78.5022>.
- [34] W. K. Wootters, “Entanglement of formation of an arbitrary state of two qubits,” *Physical Review Letters* **80** no. 10, (Mar, 1998) 2245–2248. <https://doi.org/10.1103/PhysRevLett.80.2245>.

- [35] W. K. Wootters, “Entanglement of formation and concurrence,” *Quantum Info. Comput.* **1** no. 1, (Jan, 2001) 27–44.
- [36] D. Coppersmith, “An approximate fourier transform useful in quantum factoring,”
<https://arxiv.org/abs/quant-ph/0201067>.
- [37] W. K. Wootters and W. H. Zurek, “A single quantum cannot be cloned,” *Nature* **299** no. 5886, (Oct, 1982) 802–803. <https://doi.org/10.1038%2F299802a0>.
- [38] D. Dieks, “Communication by EPR devices,” *Physics Letters A* **92** no. 6, (Nov, 1982) 271–272.
- [39] A. K. Pati and S. L. Braunstein *Nature* **404** no. 6774, (Mar, 2000) 164–165.
<https://doi.org/10.1038%2F35004532>.
- [40] D. Leach and A. Malvino, “Digital principles and applications,”.
- [41] D. Deutsch and R. Jozsa, “Rapid solution of problems by quantum computation,” *Proceedings of the Royal Society of London. Series A: Mathematical and Physical Sciences* **439** no. 1907, (Dec, 1992) 553–558. <https://doi.org/10.1098%2Frsph.1992.0167>.
- [42] R. Cleve, A. Ekert, C. Macchiavello, and M. Mosca, “Quantum algorithms revisited,” *Proceedings of the Royal Society of London. Series A: Mathematical, Physical and Engineering Sciences* **454** no. 1969, (Jan, 1998) 339–354. <https://doi.org/10.1098%2Frsph.1998.0164>.
- [43] L. K. Grover, “A fast quantum mechanical algorithm for database search,” *arXiv e-prints* (May, 1996) quant-ph/9605043, [arXiv:quant-ph/9605043](https://arxiv.org/abs/quant-ph/9605043) [quant-ph].
- [44] L. K. Grover, “Quantum mechanics helps in searching for a needle in a haystack,” *Physical Review Letters* **79** no. 2, (Jul, 1997) 325–328. <https://doi.org/10.1103%2Fphysrevlett.79.325>.
- [45] P. W. Shor, “Polynomial time algorithms for prime factorization and discrete logarithms on a quantum computer,” *SIAM J. Sci. Statist. Comput.* **26** (1997) 1484, [arXiv:quant-ph/9508027](https://arxiv.org/abs/quant-ph/9508027).
- [46] L. M. K. Vandersypen, M. Steffen, G. Breyta, C. S. Yannoni, M. H. Sherwood, and I. L. Chuang, “Experimental realization of shor's quantum factoring algorithm using nuclear magnetic resonance,” *Nature* **414** no. 6866, (Dec, 2001) 883–887. <https://doi.org/10.1038%2F414883a>.
- [47] C. Gidney and M. Ekerå, “How to factor 2048 bit RSA integers in 8 hours using 20 million noisy qubits,” *arXiv e-prints* (May, 2019) arXiv:1905.09749, [arXiv:1905.09749](https://arxiv.org/abs/1905.09749) [quant-ph].
- [48] M. Cerezo, A. Arrasmith, R. Babbush, S. Benjamin, S. Endo, K. Fujii, J. McClean, K. Mitarai, X. Yuan, L. Cincio, and P. J. Coles, “Variational quantum algorithms,” *nature reviews physics* (2020) .
- [49] J. Tilly *et al.*, “The Variational Quantum Eigensolver: a review of methods and best practices,” [arXiv:2111.05176](https://arxiv.org/abs/2111.05176) [quant-ph].
- [50] A. Peruzzo, J. McClean, P. Shadbolt, M.-H. Yung, X.-Q. Zhou, P. J. Love, A. Aspuru-Guzik, and J. L. O’Brien, “A variational eigenvalue solver on a photonic quantum processor,” *Nature Communications* **5** no. 1, (Jul, 2014) . <https://doi.org/10.1038%2Fncoms5213>.
- [51] J. R. McClean, S. Boixo, V. N. Smelyanskiy, R. Babbush, and H. Neven, “Barren plateaus in quantum neural network training landscapes,” *Nature Communications* **9** no. 1, (Nov., 2018) . <https://doi.org/10.1038/s41467-018-07090-4>.

- [52] R. Wiersema, C. Zhou, Y. de Sereville, J. F. Carrasquilla, Y. B. Kim, and H. Yuen, “Exploring entanglement and optimization within the hamiltonian variational ansatz,” *PRX Quantum* **1** (Dec, 2020) 020319. <https://link.aps.org/doi/10.1103/PRXQuantum.1.020319>.
- [53] A. Kandala, A. Mezzacapo, K. Temme, M. Takita, M. Brink, J. M. Chow, and J. M. Gambetta, “Hardware-efficient variational quantum eigensolver for small molecules and quantum magnets,” [arXiv:1704.05018](https://arxiv.org/abs/1704.05018) [quant-ph].
- [54] W. M. Kirby and P. J. Love, “Variational quantum eigensolvers for sparse hamiltonians,” *Physical Review Letters* **127** no. 11, (Sept., 2021) . <https://doi.org/10.1103/physrevlett.127.110503>.
- [55] <https://qiskit.org/textbook/preface.html>.
- [56] B. F. Schiffer, J. Tura, and J. I. Cirac, “Adiabatic Spectroscopy and a Variational Quantum Adiabatic Algorithm,” *PRX Quantum* **3** no. 2, (2022) 020347, [arXiv:2103.01226](https://arxiv.org/abs/2103.01226) [quant-ph].
- [57] W. M. Kirby and P. J. Love, “Variational Quantum Eigensolvers for Sparse Hamiltonians,” *PRL* **127** no. 11, (Sept., 2021) 110503, [arXiv:2012.07171](https://arxiv.org/abs/2012.07171) [quant-ph].
- [58] Z. Cai, R. Babbush, S. C. Benjamin, S. Endo, W. J. Huggins, Y. Li, J. R. McClean, and T. E. O’Brien, “Quantum Error Mitigation,” *arXiv e-prints* (Oct., 2022) [arXiv:2210.00921](https://arxiv.org/abs/2210.00921), [arXiv:2210.00921](https://arxiv.org/abs/2210.00921) [quant-ph].
- [59] A. Strikis, D. Qin, Y. Chen, S. C. Benjamin, and Y. Li, “Learning-Based Quantum Error Mitigation,” *PRX Quantum* **2** no. 4, (Nov., 2021) 040330, [arXiv:2005.07601](https://arxiv.org/abs/2005.07601) [quant-ph].
- [60] Raffaele Miceli and Michael McGuigan, “Quantum Computation and Visualization of Hamiltonians using Discrete Quantum Mechanics and IBM QISKIT,” [quant-ph/1812.01044](https://arxiv.org/abs/1812.01044).
- [61] O. Higgott, D. Wang, and S. Brierley, “Variational quantum computation of excited states,” *Quantum* **3** (Jul, 2019) 156. <https://doi.org/10.22331/q-2019-07-01-156>.
- [62] H. Kleinert, “Path Integrals in Quantum Mechanics, Statistics, Polymer Physics, and Financial Markets,”.
- [63] E. Dumitrescu, A. McCaskey, G. Hagen, G. Jansen, T. Morris, T. Papenbrock, R. Pooser, D. Dean, and P. Lougovski, “Cloud quantum computing of an atomic nucleus,” *physical review letters* (2018) .
- [64] J. Y. Araz, S. Schenk, and M. Spannowsky, “Towards a Quantum Simulation of Nonlinear Sigma Models with a Topological Term,” [arXiv:2210.03679](https://arxiv.org/abs/2210.03679) [quant-ph].
- [65] R. Somma, G. Ortiz, E. Knill, and J. Gubernatis, “Quantum simulations of physics problems,” [arXiv:quant-ph/0304063](https://arxiv.org/abs/quant-ph/0304063).
- [66] N. P. D. Sawaya, T. Menke, T. H. Kyaw, S. Johri, A. Aspuru-Guzik, and G. G. Guerreschi, “Resource-efficient digital quantum simulation of d -level systems for photonic, vibrational, and spin- s hamiltonians,” [arXiv:1909.12847](https://arxiv.org/abs/1909.12847).
- [67] M. Asaduzzaman, S. Catterall, G. C. Toga, Y. Meurice, and R. Sakai, “Quantum Simulation of the N flavor Gross-Neveu Model,” [arXiv:2208.05906](https://arxiv.org/abs/2208.05906) [hep-lat].
- [68] A. F. Shaw, P. Lougovski, J. R. Stryker, and N. Wiebe, “Quantum Algorithms for Simulating the Lattice Schwinger Model,” *Quantum* **4** (2020) 306, [arXiv:2002.11146](https://arxiv.org/abs/2002.11146) [quant-ph].

- [69] K. Yeter-Aydeniz, E. Moschandreou, and G. Siopsis, “Quantum imaginary-time evolution algorithm for quantum field theories with continuous variables,” *Phys. Rev. A* **105** no. 1, (2022) 012412, [arXiv:2107.00791 \[quant-ph\]](#).
- [70] S. McArdle, T. Jones, S. Endo, Y. Li, S. C. Benjamin, and X. Yuan, “Variational ansatz-based quantum simulation of imaginary time evolution,” *npj Quantum Information* **5** (Sept., 2019) 75, [arXiv:1804.03023 \[quant-ph\]](#).
- [71] M. Motta, C. Sun, A. T. K. Tan, M. J. O’Rourke, E. Ye, A. J. Minnich, F. G. S. L. Brandão, and G. K.-L. Chan, “Determining eigenstates and thermal states on a quantum computer using quantum imaginary time evolution,” *Nature Physics* **16** no. 2, (Jan., 2020) 205–210, [arXiv:1901.07653 \[quant-ph\]](#).
- [72] E. Knill and R. Laflamme, “A Theory of quantum error correcting codes,” *Phys. Rev. Lett.* **84** (2000) 2525–2528, [arXiv:quant-ph/9604034](#).
- [73] P. W. Shor, “Scheme for reducing decoherence in quantum computer memory,” *Phys. Rev. A* **52** (Oct, 1995) R2493–R2496. <https://link.aps.org/doi/10.1103/PhysRevA.52.R2493>.
- [74] R. Laflamme, C. Miquel, J. P. Paz, and W. H. Zurek, “Perfect quantum error correction code,” [arXiv:quant-ph/9602019](#).
- [75] A. Steane, “Multiple particle interference and quantum error correction,” *Proc. Roy. Soc. Lond. A* **452** (1996) 2551, [arXiv:quant-ph/9601029](#).
- [76] D. Gottesman, “An Introduction to Quantum Error Correction and Fault-Tolerant Quantum Computation,” *arXiv e-prints* (Apr., 2009) arXiv:0904.2557, [arXiv:0904.2557 \[quant-ph\]](#).
- [77] D. Gottesman, “The Heisenberg representation of quantum computers,” in *22nd International Colloquium on Group Theoretical Methods in Physics*, pp. 32–43. 7, 1998. [arXiv:quant-ph/9807006](#).
- [78] S. L. Braunstein and P. van Loock, “Quantum information with continuous variables,” *Rev. Mod. Phys.* **77** (2005) 513–577, [arXiv:quant-ph/0410100](#).
- [79] S. Lloyd, “Universal quantum simulators,” *Science* **273** no. 5278, (Aug., 1996) 1073–1078. <https://doi.org/10.1126/science.273.5278.1073>.
- [80] S. Chandrasekharan and U. J. Wiese, “Quantum link models: A Discrete approach to gauge theories,” *Nucl. Phys. B* **492** (1997) 455–474, [arXiv:hep-lat/9609042](#).
- [81] A. Bazavov, S. Catterall, R. G. Jha, and J. Unmuth-Yockey, “Tensor renormalization group study of the non-Abelian Higgs model in two dimensions,” *Phys. Rev. D* **99** no. 11, (2019) 114507, [arXiv:1901.11443 \[hep-lat\]](#).
- [82] I. Raychowdhury and J. R. Stryker, “Loop, string, and hadron dynamics in SU(2) Hamiltonian lattice gauge theories,” *Phys. Rev. D* **101** no. 11, (2020) 114502, [arXiv:1912.06133 \[hep-lat\]](#).
- [83] A. Alexandru, P. F. Bedaque, R. Brett, and H. Lamm, “Spectrum of digitized QCD: Glueballs in a S(1080) gauge theory,” *Phys. Rev. D* **105** no. 11, (2022) 114508, [arXiv:2112.08482 \[hep-lat\]](#).
- [84] S. P. Jordan, K. S. M. Lee, and J. Preskill, “Quantum Computation of Scattering in Scalar Quantum Field Theories,” *Quant. Inf. Comput.* **14** (2014) 1014–1080, [arXiv:1112.4833 \[hep-th\]](#).

- [85] N. Klco and M. J. Savage, “Digitization of scalar fields for quantum computing,” *Phys. Rev. A* **99** no. 5, (2019) 052335, [arXiv:1808.10378 \[quant-ph\]](#).
- [86] K. Marshall, R. Pooser, G. Siopsis, and C. Weedbrook, “Quantum simulation of quantum field theory using continuous variables,” *Phys. Rev. A* **92** no. 6, (2015) 063825, [arXiv:1503.08121 \[quant-ph\]](#).
- [87] J. Barata, N. Mueller, A. Tarasov, and R. Venugopalan, “Single-particle digitization strategy for quantum computation of a ϕ^4 scalar field theory,” *Phys. Rev. A* **103** no. 4, (2021) 042410, [arXiv:2012.00020 \[hep-th\]](#).
- [88] A. W. Harrow, A. Hassidim, and S. Lloyd, “Quantum algorithm for linear systems of equations,” *Phys. Rev. Lett.* **103** (Oct, 2009) 150502.
<https://link.aps.org/doi/10.1103/PhysRevLett.103.150502>.
- [89] J. Morrell, Hector Jose, A. Zaman, and H. Y. Wong, “Step-by-Step HHL Algorithm Walkthrough to Enhance the Understanding of Critical Quantum Computing Concepts,” *arXiv e-prints* (Aug., 2021) [arXiv:2108.09004](#), [arXiv:2108.09004 \[quant-ph\]](#).
- [90] M. Hestenes and E. Stiefel, “Methods of conjugate gradients for solving linear systems,” *Journal of Research of the National Bureau of Standards* **49** no. 6, (Dec., 1952) 409.
<https://doi.org/10.6028/jres.049.044>.
- [91] S. Aaronson, “Read the fine print,” *Nature Physics* **11** no. 4, (Apr., 2015) 291–293.
<https://doi.org/10.1038/nphys3272>.
- [92] J. D. Whitfield, J. Biamonte, and A. Aspuru-Guzik, “Simulation of electronic structure hamiltonians using quantum computers,” *Molecular Physics* **109** no. 5, (Mar, 2011) 735–750.
<https://doi.org/10.1080%2F00268976.2011.552441>.
- [93] D. W. Berry, A. M. Childs, R. Cleve, R. Kothari, and R. D. Somma, “Exponential improvement in precision for simulating sparse Hamiltonians,” *arXiv e-prints* (Dec., 2013) [arXiv:1312.1414](#), [arXiv:1312.1414 \[quant-ph\]](#).
- [94] D. W. Berry, A. M. Childs, R. Cleve, R. Kothari, and R. D. Somma, “Simulating Hamiltonian Dynamics with a Truncated Taylor Series,” *PRL* **114** no. 9, (Mar., 2015) 090502, [arXiv:1412.4687 \[quant-ph\]](#).
- [95] J. Kempe, A. Kitaev, and O. Regev, “The complexity of the local hamiltonian problem,” [arXiv:quant-ph/0406180](#).
- [96] D. W. Berry, G. Ahokas, R. Cleve, and B. C. Sanders, “Efficient quantum algorithms for simulating sparse hamiltonians,” *Communications in Mathematical Physics* **270** no. 2, (Dec., 2006) 359–371.
<https://doi.org/10.1007/s00220-006-0150-x>.
- [97] A. M. Childs and R. Kothari, “Simulating sparse hamiltonians with star decompositions,”
https://doi.org/10.1007/978-3-642-18073-6_8.
- [98] D. W. Berry, A. M. Childs, and R. Kothari, “Hamiltonian simulation with nearly optimal dependence on all parameters,” *arXiv e-prints* (Jan., 2015) [arXiv:1501.01715](#), [arXiv:1501.01715 \[quant-ph\]](#).

- [99] G. Hao Low and I. L. Chuang, “Hamiltonian Simulation by Qubitization,” *arXiv e-prints* (Oct., 2016) [arXiv:1610.06546](#), [arXiv:1610.06546 \[quant-ph\]](#).
- [100] D. W. Berry, A. M. Childs, R. Cleve, R. Kothari, and R. D. Somma, “Exponential improvement in precision for simulating sparse Hamiltonians,” *arXiv e-prints* (Dec., 2013) [arXiv:1312.1414](#), [arXiv:1312.1414 \[quant-ph\]](#).
- [101] M. E. Beverland, P. Murali, M. Troyer, K. M. Svore, T. Hoeffler, V. Kliuchnikov, G. Hao Low, M. Soeken, A. Sundaram, and A. Vashchillo, “Assessing requirements to scale to practical quantum advantage,” *arXiv e-prints* (Nov., 2022) [arXiv:2211.07629](#), [arXiv:2211.07629 \[quant-ph\]](#).
- [102] B. Eastin and S. T. Flammia, “Q-circuit tutorial,” [arXiv:quant-ph/0406003 \[quant-ph\]](#).
- [103] A. Serafini, “Quantum Continuous Variables: A Primer of Theoretical Methods,” *CRC Press* (2017) .
- [104] S. L. Braunstein and P. van Loock, “Quantum information with continuous variables,” *Reviews of Modern Physics* **77** no. 2, (Apr., 2005) 513–577, [arXiv:quant-ph/0410100 \[quant-ph\]](#).
- [105] C. Weedbrook, S. Pirandola, R. García-Patrón, N. J. Cerf, T. C. Ralph, J. H. Shapiro, and S. Lloyd, “Gaussian quantum information,” *Reviews of Modern Physics* **84** no. 2, (Apr., 2012) 621–669, [arXiv:1110.3234 \[quant-ph\]](#).
- [106] D. Gottesman, A. Kitaev, and J. Preskill, “Encoding a qubit in an oscillator,” [arXiv:quant-ph/0008040 \[quant-ph\]](#).
- [107] M. Mirrahimi, Z. Leghtas, V. V. Albert, S. Touzard, R. J. Schoelkopf, L. Jiang, and M. H. Devoret, “Dynamically protected cat-qubits: a new paradigm for universal quantum computation,” *New Journal of Physics* **16** no. 4, (Apr., 2014) 045014, [arXiv:1312.2017 \[quant-ph\]](#).
- [108] N. Killoran, T. R. Bromley, J. M. Arrazola, M. Schuld, N. Quesada, and S. Lloyd, “Continuous-variable quantum neural networks,” *Physical Review Research* **1** no. 3, (Oct., 2019) 033063, [arXiv:1806.06871 \[quant-ph\]](#).
- [109] A. K. Pati, S. L. Braunstein, and S. Lloyd, “Quantum searching with continuous variables,” *arXiv preprint quant-ph/0002082* (2000) .
- [110] A. K. Pati and S. L. Braunstein, “Deutsch-jozsa algorithm for continuous variables,” *Quantum Information with Continuous Variables* (2003) 31–36.
- [111] S. L. Braunstein, “Error correction for continuous quantum variables,” *Phys. Rev. Lett.* **80** (1998) 4084–4087, [arXiv:quant-ph/9711049](#).
- [112] X. Wang, “Continuous-variable and hybrid quantum gates,” *Journal of Physics A: Mathematical and General* **34** no. 44, (Oct., 2001) 9577–9584. <https://doi.org/10.1088/0305-4470/34/44/316>.
- [113] N. Killoran, J. Izaac, N. Quesada, V. Bergholm, M. Amy, and C. Weedbrook, “Strawberry Fields: A Software Platform for Photonic Quantum Computing,” *Quantum* **3** (Mar., 2019) 129, [arXiv:1804.03159 \[quant-ph\]](#).
- [114] W. Magnus, “On the exponential solution of differential equations for a linear operator,” *Commun. Pure Appl. Math.* **7** (1954) 649–673.

- [115] T. J. Stavenger, E. Crane, K. Smith, C. T. Kang, S. M. Girvin, and N. Wiebe, “Bosonic Qiskit,” [arXiv:2209.11153 \[quant-ph\]](#).